# Feshbach resonances in ultracold gases

Cheng Chin

*Department of Physics and James Franck Institute, University of Chicago, Chicago, Illinois 60637, USA*

Rudolf Grimm

*Center for Quantum Physics and Institute of Experimental Physics, University of Innsbruck, Technikerstraße 25, 6020 Innsbruck, Austria and Institute for Quantum Optics and Quantum Information, Austrian Academy of Sciences, Otto-Hittmair-Platz 1, 6020 Innsbruck, Austria*

Paul Julienne and Eite Tiesinga

*Joint Quantum Institute, National Institute of Standards and Technology and University of Maryland, 100 Bureau Drive, Gaithersburg, Maryland 20899-8423, USA*

(Published 29 April 2010)

Feshbach resonances are the essential tool to control the interaction between atoms in ultracold quantum gases. They have found numerous experimental applications, opening up the way to important breakthroughs. This review broadly covers the phenomenon of Feshbach resonances in ultracold gases and their main applications. This includes the theoretical background and models for the description of Feshbach resonances, the experimental methods to find and characterize the resonances, a discussion of the main properties of resonances in various atomic species and mixed atomic species systems, and an overview of key experiments with atomic Bose-Einstein condensates, degenerate Fermi gases, and ultracold molecules.

DOI: 10.1103/RevModPhys.82.1225 PACS number(s): 03.75.−b, 34.50.Cx, 67.85.−d

**CONTENTS**



0034-6861/2010/82(2)/1225(62)  

## I. INTRODUCTION

### A. Ultracold gases and Feshbach resonances: Scope of the review

The impact of ultracold atomic and molecular quantum gases on present-day physics is linked to the extraordinary degree of control that such systems offer to investigate the fundamental behavior of quantum matter under various conditions. The interest goes beyond atomic and molecular physics, reaching far into other fields, such as condensed matter and few- and many-body physics. In all these applications, Feshbach resonances represent the essential tool to control the interaction between the atoms, which has been the key to many breakthroughs.

Ultracold gases are generally produced by laser cooling (Metcalf and van der Straten, 1999) and subsequent evaporative cooling (Ketterle and van Druten, 1997). At temperatures in the nanokelvin range and typical number densities somewhere between $10^{12}$ and $10^{15}$ cm$^{-3}$, quantum-degenerate states of matter are formed when the atomic de Broglie wavelength exceeds the typical interparticle distance and quantum statistics governs the behavior of the system. The attainment of Bose-Einstein condensation (BEC) in dilute ultracold gases marked the starting point of a new era in physics (Anderson *et al.*, 1995; Bradley *et al.*, 1995; Davis *et al.*, 1995), and degenerate atomic Fermi gases entered the stage a few years later (DeMarco *et al.*, 1999; Schreck *et al.*, 2001; Truscott *et al.*, 2001). The developments of the techniques to cool and trap atoms by laser light were recognized with the 1997 Nobel prize in physics (Chu, 1998; Cohen-Tannoudji, 1998; Phillips, 1998). Only four years later, the achievement of BEC in dilute gases of alkali atoms and early fundamental studies of the properties of the condensates led to the 2001 Nobel prize (Cornell and Wieman, 2002; Ketterle, 2002).[1]

In this review, we give a broad coverage of Feshbach resonances in view of the manifold applications they have found in ultracold gases. Regarding theory, we focus on the underlying two-body physics and on models to describe Feshbach resonances. In the experimental part, we include applications to few- and many-body physics; we discuss typical or representative results instead of the impossible attempt to exhaustively review all developments in this rapidly growing field. Several aspects of Feshbach resonances and related topics have already been reviewed elsewhere. An early review on Feshbach resonance theory was given by Timmermans *et al.* (1999). In another theoretical review, Duine and Stoof (2004) focused on atom-molecule coherence. Hutson and Soldán (2006) and Köhler *et al.* (2006) reviewed the formation of ultracold molecules near Feshbach resonances. The closely related topic of photoassociation was reviewed by Jones *et al.* (2006).

In Sec. II, we start with a presentation of the theoretical background. Then, in Sec. III, we present the various experimental methods to identify and characterize Feshbach resonances. There we also discuss the specific interaction properties of different atomic species, which can exhibit vastly different behaviors. In Sec. IV, we present important applications of interaction control in experiments on atomic Bose and Fermi gases. In Sec. V, we discuss properties and applications of ultracold molecules created via Feshbach association. Finally, in Sec. VI, we discuss some related topics, such as optical Feshbach resonances, interaction control in optical lattices, few-body physics, and the relation to molecular scattering resonances and cold chemistry.

### B. Basic physics of a Feshbach resonance

The physical origin and the elementary properties of a Feshbach resonance can be understood from a simple picture. Here we outline the basic ideas, whereas in Sec. II we provide a more detailed theoretical discussion.

We consider two molecular potential curves $V_{\rm bg}(R)$ and $V_c(R)$, as shown in Fig. 1. For large internuclear distances $R$, the background potential $V_{\rm bg}(R)$ asymptotically connects to two free atoms in the ultracold gas. For a collision process, having small energy $E$, this potential represents the energetically open channel, in the follow-

[1]For overviews on laser cooling and trapping, BEC, and ultracold Fermi gases see the proceedings of the Varenna summer schools in 1991, 1998, and 2006 (Arimondo *et al.*, 1992; Inguscio *et al.*, 1999, 2008). For reviews on the theory of degenerate quantum gases of bosons and fermions see Dalfovo *et al.* (1999) and Giorgini *et al.* (2008), respectively, and Stringari and Pitaevskii (2003) and Pethick and Smith (2008).

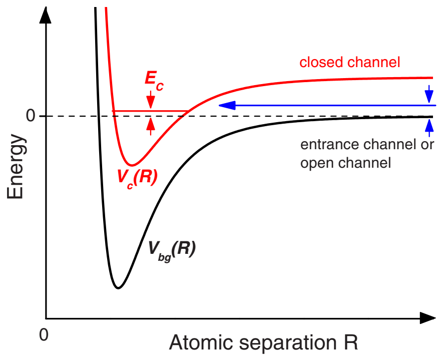


FIG. 1. (Color online) Basic two-channel model for a Feshbach resonance. The phenomenon occurs when two atoms colliding at energy $E$ in the entrance channel resonantly couple to a molecular bound state with energy $E_c$ supported by the closed channel potential. In the ultracold domain, collisions take place near zero energy, $E \rightarrow 0$. Resonant coupling is then conveniently realized by magnetically tuning $E_c$ near 0 if the magnetic moments of the closed and open channels differ.

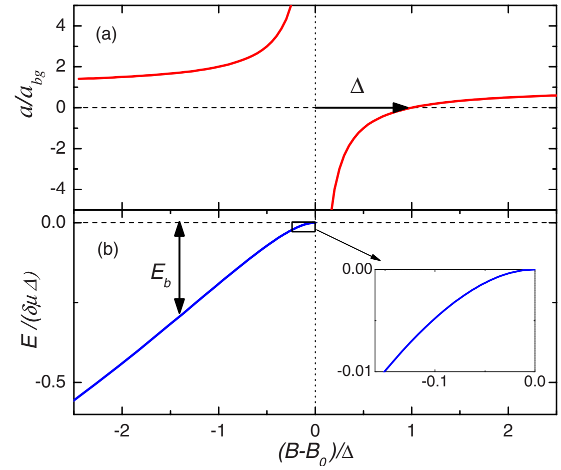


FIG. 2. (Color online) Feshbach resonance properties. (a) Scattering length $a$ and (b) molecular state energy $E$ near a magnetically tuned Feshbach resonance. The binding energy is defined to be positive, $E_b=-E$. The inset shows the universal regime near the point of resonance where $a$ is very large and positive.

ing referred to as the entrance channel. The other potential $V_c(R)$, representing the closed channel, is important as it can support bound molecular states near the threshold of the open channel.

A Feshbach resonance occurs when the bound molecular state in the closed channel energetically approaches the scattering state in the open channel. Then even weak coupling can lead to strong mixing between the two channels. The energy difference can be controlled via a magnetic field when the corresponding magnetic moments are different. This leads to a magnetically tuned Feshbach resonance. The magnetic tuning method is the common way to achieve resonant coupling and it has found numerous applications, as discussed in this review. Alternatively, resonant coupling can be achieved by optical methods, leading to optical Feshbach resonances with many conceptual similarities to the magnetically tuned case (see Sec. VI.A). Such resonances are promising for cases where magnetically tunable resonances are absent.

A magnetically tuned Feshbach resonance can be described by a simple expression,[2] introduced by Moerdijk *et al.* (1995), for the $s$-wave scattering length $a$ as a function of the magnetic field $B$,

$$a(B) = a_{\text{bg}}\left(1 - \frac{\Delta}{B - B_0}\right). \tag{1}$$

Figure 2(a) shows this resonance expression. The background scattering length $a_{\text{bg}}$, which is the scattering length associated with $V_{\text{bg}}(R)$, represents the off-resonant value. It is directly related to the energy of the last-bound vibrational level of $V_{\text{bg}}(R)$. The parameter $B_0$ denotes the resonance position, where the scattering length diverges ($a \rightarrow \pm\infty$), and the parameter $\Delta$ is the resonance width. Note that both $a_{\text{bg}}$ and $\Delta$ can be positive or negative. An important point is the zero crossing of the scattering length associated with a Feshbach resonance; it occurs at a magnetic field $B=B_0+\Delta$. Note also that we use G as the magnetic field unit in this paper because of its near-universal usage among groups working in this field, 1 G$=10^{-4}$ T.

The energy of the weakly bound molecular state near the resonance position $B_0$ is shown in Fig. 2(b) relative to the threshold of two free atoms with zero kinetic energy. The energy approaches threshold at $E=0$ on the side of the resonance where $a$ is large and positive. Away from resonance, the energy varies linearly with $B$ with a slope given by $\delta\mu$, the difference in magnetic moments of the open and closed channels. Near resonance the coupling between the two channels mixes in entrance-channel contributions and strongly bends the molecular state.

In the vicinity of the resonance position at $B_0$, where the two channels are strongly coupled, the scattering length is very large. For large positive values of $a$, a "dressed" molecular state exists with a binding energy given by

$$E_b = \hbar^2/2\mu a^2, \tag{2}$$

where $\mu$ is the reduced mass of the atom pair. In this limit $E_b$ depends quadratically on the magnetic detuning $B-B_0$ and results in the bend shown in the inset of Fig. 2. This region is of particular interest because of its universal properties; here the state can be described in terms of a single effective molecular potential having scattering length $a$. In this case, the wave function for the relative atomic motion is a quantum halo state which extends to a large size on the order of $a$; the molecule is then called a halo dimer (see Sec. V.B.2).

[2]This simple expression applies to resonances without inelastic two-body channels. Some Feshbach resonances, especially the optical ones, feature two-body decay. For a more general discussion including inelastic decay see Sec. II.A.3.

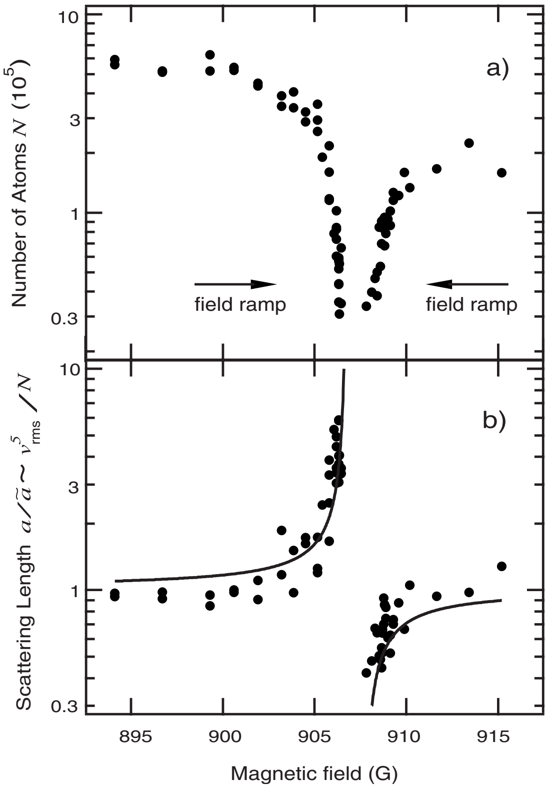


FIG. 3. Observation of a magnetically tuned Feshbach resonance in an optically trapped BEC of Na atoms. The upper panel shows a strong loss of atoms near the resonance, which is due to enhanced three-body recombination. The lower panel shows the dispersive shape of the scattering length $a$ near the resonance, as determined from measurements of the mean-field interaction by expansion of the condensate after release from the trap; here $a$ is normalized to the background value $a_{bg}$. From Inouye *et al.*, 1998.

A useful distinction can be made between resonances that exist in various systems (see Sec. II.B.2). For narrow resonances with a width $\Delta$ typically well below 1 G (see the Appendix) the universal range persists only for a very small fraction of the width. In contrast, broad resonances with a width typically much larger than 1 G tend to have a large universal range extending over a considerable fraction of the width. The first class of resonances is referred to as closed-channel dominated resonances, whereas the second class is called entrance-channel dominated resonances. For the distinction between both classes, the width $\Delta$ is not the only relevant parameter. Also the background scattering length $a_{bg}$ and the differential magnetic moment $\delta\mu$ need to be taken into account. Section II.B.2 discusses this important distinction in terms of a dimensionless resonance strength.

Figure 3 shows the observation of a Feshbach resonance as reported by Inouye *et al.* (1998) for an optically trapped BEC of Na atoms. This early example highlights the two most striking features of a Feshbach resonance, the tunability of the scattering length according to Eq. (1) and the fast loss of atoms in the resonance region. The latter can be attributed to strongly enhanced three-body recombination and molecule formation near a Feshbach resonance (see Sec. III.A.2).

A Feshbach resonance in an ultracold atomic gas can serve as a gateway into the molecular world and is thus strongly connected to the field of ultracold molecules (see Sec. V). Various techniques have been developed to associate molecules near Feshbach resonances. Ultracold molecules produced in this way are commonly referred to as *Feshbach molecules*. The meaning of this term is not precisely defined, as Feshbach molecules can be transferred to many other states near threshold or to much more deeply bound states, thus being converted to more conventional molecules. We use the term Feshbach molecule for any molecule that exists near the threshold in an energy range set by the quantum of energy for near-threshold vibrations. The universal halo state is a special very weakly bound case of a Feshbach molecule.

### C. Historical remarks

Early investigations on phenomena arising from the coupling of a bound state to the continuum go back to the 1930s. Rice (1933) considered how a bound state predissociates into a continuum, Fano (1935) and Fano *et al.* (2005) described asymmetric line shapes occurring in such a situation as a result of quantum interference, and Beutler (1935) reported on the observation of highly asymmetric line shapes in rare gas photoionization spectra. Nuclear physicists considered basically the same situation, having nuclear scattering experiments in mind instead of atomic physics. Breit and Wigner (1936) considered the situation in the limit when the bound state plays a dominant role and the asymmetry disappears. Later interference and line-shape asymmetry were taken into account by several authors (Blatt and Weisskopf, 1952).

Feshbach (1917–2000) and Fano (1912–2001) developed their thorough treatments of the resonance phenomena that arise from the coupling of a discrete state to the continuum. Their work was carried out independently using different theoretical approaches. While Feshbach's work originated in the context of nuclear physics (Feshbach, 1958, 1962), Fano approached the problem on the background of atomic physics (Fano, 1961). reformulating and extending his earlier work (Fano, 1935; Fano *et al.*, 2005). Nowadays, the term "Feshbach resonance" is most widely used in the literature for the resonance phenomenon itself, but sometimes also the term "Fano-Feshbach resonance" appears. As a curiosity Feshbach himself considered his name being attached to a well-known resonance phenomenon as a mere atomic physics jargon (Kleppner, 2004; Rau, 2005). Fano's name is usually associated with the asymmetric line shape of such a resonance, well known in atomic physics as a "Fano profile."

A prominent example for the observation of a Feshbach resonance in atomic physics is the experiment of Bryant *et al.* (1977) on photodetachment by the negative ion of hydrogen. Near a photon energy of 11 eV two

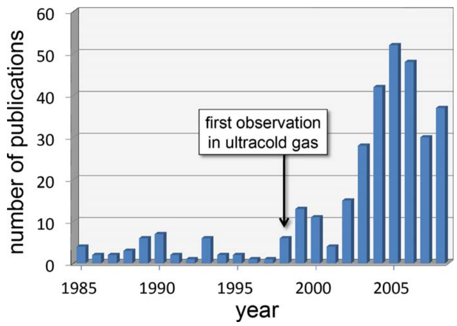


FIG. 4. (Color online) Number of publications per year (from 1985 to 2008) with Feshbach resonances appearing in the title. Data from ISI Web of Science.

prominent resonances were seen, one of them being a Feshbach resonance and the other one a "shape resonance" (see Sec. II.A.3). Many more situations where Feshbach resonances play an important role can be found in atomic, molecular, and chemical physics [see Spence and Noguchi (1975), Gauyacq and Herzenberg (1982), MacArthur *et al.* (1985), Nieh and Valentini (1990), and Weber *et al.* (1999) for a few examples]. In such experiments, the resonances occur when the scattering energy is varied. This is in contrast to the experiments on ultracold gases, where scattering takes place in the zero-energy limit and the resonances occur when an external field tunes bound states near threshold.

In the context of quantum gases, Feshbach resonances were first considered by Stwalley (1976), who suggested the existence of magnetically induced Feshbach resonances in the scattering of spin-polarized hydrogen and deuterium atoms (H+D and D+D). He pointed to enhanced inelastic decay near these resonances and suggested that they should be avoided to maintain stable spin-polarized hydrogen gases. A related loss resonance in hydrogen was observed by Reynolds *et al.* (1986). The positive aspect of such resonances was first pointed out by Tiesinga *et al.* (1993), who showed that they can be used to change the sign and strength of the interaction between ultracold atoms. In 1998, the possibility of interaction tuning via Feshbach resonances was demonstrated by Inouye *et al.* (1998) for a $^{23}$Na BEC, as already discussed in the preceding section. In the same year, Courteille *et al.* (1998) demonstrated a Feshbach resonance in a trapped sample of $^{85}$Rb atoms through the enhancement of photoassociative loss induced by a probe laser.

The important role of Feshbach resonances in present-day quantum gas experiments can be highlighted by looking at the number of publications per year with Feshbach resonances in the title (see Fig. 4). Before 1998, one finds just a few publications with the majority not related to ultracold atoms. Then, after 1998, a substantial increase is observed as a result of the first successful experiments with Feshbach resonances in ultracold gases. It then took a few years until Feshbach resonances had become a fully established tool and opened up many new applications in the field. This is reflected in the steep increase of the publication rate in the period from 2002 to 2004.

## II. THEORETICAL BACKGROUND

This review primarily concentrates on magnetically tunable resonances, described in the next sections, while Sec. VI.A discusses optical changes in scattering lengths. Here we describe the two-body physics of collision resonances, not the few- or many-body aspects. Properties of a number of magnetic Feshbach resonances are tabulated in the Appendix.

### A. Basic collision physics

The theory for describing two-body collisions is described in a number of textbooks (Mott and Massey, 1965; Messiah, 1966; Taylor, 1972). First consider the collision of two structureless atoms, labeled 1 and 2 with masses $m_1$ and $m_2$ interacting under the influence of the potential $V(\mathbf{R})$, where $\mathbf{R}$ is the vector between the positions of the two atoms with magnitude $R$. The separated atoms are prepared in a plane wave with relative kinetic energy $E=\hbar^2k^2/(2\mu)$ and relative momentum $\hbar\mathbf{k}$, where $\mu=m_1m_2/(m_1+m_2)$ is the reduced mass of the pair. The plane wave in turn is expanded in a standard sum over spherical harmonic functions $Y_{\ell m_\ell}(\hat{\mathbf{R}})$, where $\ell$ is the relative angular momentum, $m_\ell$ is its projection along a space fixed $z$ axis, and $\hat{\mathbf{R}}=\mathbf{R}/R$ is the direction vector on the unit sphere (Messiah, 1966). This expansion is called the partial wave expansion, and the various partial waves $\ell=0,1,2,\ldots$ are designated $s,p,d,\ldots$ waves.

If the potential $V(\mathbf{R})$ is isotropic, depending only on the magnitude of $\mathbf{R}$, there is no coupling among partial waves, each of which is described by the solution $\psi_\ell(R)=\phi_\ell(R)/R$ to the Schrödinger equation

$$-\frac{\hbar^2}{2\mu}\frac{d^2\phi_\ell(R)}{dR^2}+V_\ell(R)\phi_\ell(R)=E\phi_\ell(R), \tag{3}$$

where $V_\ell(R)=V(R)+\hbar^2\ell(\ell+1)/(2\mu R^2)$ includes the centrifugal potential, which is repulsive for $\ell>0$ and vanishes for the $s$ wave. We assume $V(R)\to 0$ as $R\to\infty$, so that $E$ represents the energy of the separated particles. This equation has a spectrum of $N_\ell$ bound state solutions at discrete energies $E_{n\ell}$ for $E<0$ and a continuous spectrum of scattering states with $E>0$. While bound states are normally labeled by vibrational quantum number $v=0,\ldots,N_\ell-1$ counting up from the bottom of the potential, we prefer to label threshold bound states by quantum number $n=-1,-2,\ldots$ counting down from the top of the potential for the last, next to last, etc. bound states. The bound state solutions $|n\ell\rangle$ are normalized to unity, $|\langle n\ell|n\ell\rangle|^2=1$, and $\phi_{n\ell}(R)=\langle R|n\ell\rangle\to 0$ as $R\to\infty$. The scattering solutions, representing the incident plane wave plus a scattered wave, approach

$$\phi_\ell(R,E) \to c\frac{\sin[kR - \pi\ell/2 + \eta_\ell(E)]}{\sqrt{k}} e^{i\eta_\ell(E)} \quad (4)$$

as $R\to\infty$, where $\eta_\ell(E)$ is the scattering phase shift and $c=\sqrt{2\mu/\pi\hbar^2}$ is a constant that ensures the wave function $|E\ell\rangle$ is normalized per unit energy, $\langle E\ell|E'\ell\rangle = \int_0^\infty \phi_\ell^*(R,E)\phi_\ell(R,E')dR = \delta(E-E')$. The scattering phase shift is the key parameter that incorporates the effect of the whole potential on the collision event.

Sadeghpour *et al.* (2000) reviewed the special properties of scattering phase shift near a collision threshold when $k\to 0$. If $V(R)$ varies as $1/R^s$ at large $R$, then $\tan\eta_\ell \propto k^{2\ell+1}$ if $2\ell+1 \leqslant s-2$ and $\tan\eta_\ell \propto k^{s-2}$ if $2\ell+1 \geqslant s-2$. While Levinson's theorem shows that $\eta_\ell \to N_\ell \pi$ as $k\to 0$, we need not consider the $N_\ell\pi$ part of the phase shift in this review. For van der Waals potentials with $s=6$, the threshold $\tan\eta_\ell$ varies as $k$ and $k^3$ for $s$ and $p$ waves and as $k^4$ for all other partial waves. The properties of $s$-wave collisions are of primary interest for cold neutral atom collisions, where near threshold, a more precise statement of the variation of $\tan\eta_0$ with $k$ is given by the effective range expansion,

$$k\cot\eta_0(E) = -1/a + \tfrac{1}{2}r_0k^2, \quad (5)$$

where $a$ is called the $s$-wave scattering length and $r_0$ is the effective range. For practical purposes, it often suffices to retain only the scattering length term and use $\tan\eta_0(E)=-ka$. Depending on the potential, the scattering length can have any value, $-\infty < a < +\infty$.

When the scattering length is positive and sufficiently large, that is, large compared to the characteristic length scale of the molecular potential (see Sec. II.B.1), the last $s$-wave bound state of the potential, labeled by index $n=-1$ and $\ell=0$, is just below threshold with a binding energy $E_b=-E_{-1,0}$ given by Eq. (2) in the Introduction. The domain of universality, where scattering and bound state properties are solely characterized by the scattering length and mass, is discussed in recent reviews (Braaten and Hammer, 2006; Köhler *et al.*, 2006). The universal bound state wave function takes on the form $\phi_{-1,0}(R)=\sqrt{2/a}\exp(-R/a)$ at large $R$. Such a state exists almost entirely at long range beyond the outer classical turning point of the potential. Such a bound state is known as a "halo state," also studied in nuclear physics (Riisager, 1994) and discussed in Sec. V.B.2.

### 1. Collision channels

The atoms used in cold collision experiments generally have spin structure. For each atom $i=1$ or 2 in a collision the electronic orbital angular momentum $\mathbf{L}_i$ is coupled to the total electronic spin angular momentum $\mathbf{S}_i$ to give a resultant $\mathbf{j}_i$, which in turn is coupled to the nuclear spin $\mathbf{I}_i$ to give the total angular momentum $\mathbf{f}_i$. The eigenstates of each atom are designated by the composite labels $q_i$. At zero magnetic field these labels are $f_im_i$, where $m_i$ is the projection of $\mathbf{f}_i$. For example, alkali-metal atoms that are commonly used in Feshbach resonance experiments have $^2S_{1/2}$ electronic ground states

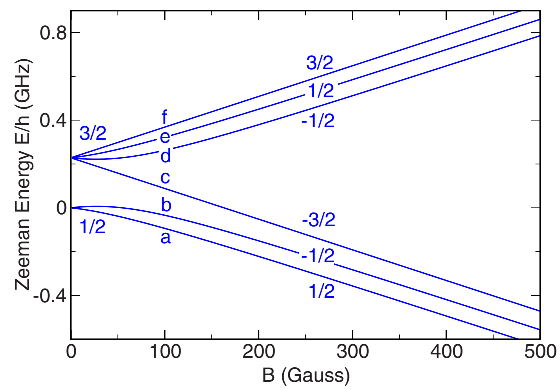


FIG. 5. (Color online) Atomic energy levels of the $^6$Li atom, which has $S=1/2$, $I=1$, and $f=1/2$ and 3/2. The figure shows both the projection $m$ of $f$ and the alphabetical shorthand notation $q_i$=a, b, c, d, e, and f used to label the levels in order of increasing energy.

with quantum numbers $L_i=0$ and $S_i=1/2$, for which there are only two values of $f_i=I_i-1/2$ and $I_i+1/2$ when $I_i\neq 0$. Whether $f_i$ is an integer or half an odd integer determines whether the atom is a composite boson or fermion.

A magnetic field $\mathbf{B}$ splits these levels into a manifold of Zeeman sublevels. Only the projection $m_i$ along the field remains a good quantum number, and $B=0$ levels with the same $m_i$ but different $f_i$ can be mixed by the field. Even at high field, where the individual $f_i$ values no longer represent good quantum numbers, the $f_i$ value still can be retained as a label, indicating the value at $B=0$ with which the level adiabatically correlates.

Figure 5 shows the Zeeman energy levels versus $B$ for the $^6$Li atom, a fermion, according to the classic Breit-Rabi formula (Breit and Rabi, 1931). The two $f_i$ levels are split at $B=0$ by the hyperfine energy, $E_{\rm hf}/h=228$ MHz. At large fields the lower group of three levels is associated with the quantum number $m_S=-1/2$, while the upper group has $m_S=+1/2$. The figure also shows our standard notation for atomic Zeeman levels for any species and any field strength. We label states by lower case Roman letters a, b, c,… in order of increasing energy. Some prefer to label the levels in order numerically as 1, 2, 3… . The notation $q_i$ can symbolically refer to the $f_im_i$, alphabetical, or numerical choice of labeling

The collision event between two atoms is defined by preparing the atoms in states $q_1$ and $q_2$ while they are separated by a large distance $R$, then allowing them to come together, interact, and afterward separate to two atoms in states $q_1'$ and $q_2'$. If the two final states are the same as the initial ones, $q_1,q_2=q_1',q_2'$, the collision is said to be elastic, and the atoms have the same relative kinetic energy $E$ before and after the collision. If one of the final states is different from an initial state, the collision is said to be inelastic. This often results in an energy release that causes a loss of cold atoms when the energetic atoms escape from the shallow trapping potential. We concentrate primarily on collisions where the two-body inelastic collision rate is zero or else very small in comparison to the elastic rate since this corresponds in practice to most cases of practical experimental interest. This condition is necessary for efficient evaporative cooling or to prevent rapid decay of the cold gas. Section III.A.2 discusses how atom loss due to three-body collisions can be used to detect the presence of two-body resonances.

In setting up the theory for the collision of two atoms, the scattering channels are defined by the internal states of the two atoms 1 and 2 and the partial wave, $|\alpha\rangle = |q_1 q_2\rangle |\ell m_\ell\rangle$, where $\langle \hat{R} | \ell m_\ell \rangle = Y_{\ell m_\ell}(\hat{\mathbf{R}})$. Since for collisions in a magnetic field the quantum number $M = m_1 + m_2 + m_\ell$ is strictly conserved, a scattering channel can be conveniently labeled by specifying the set of quantum numbers $\{q_1 q_2 \ell M\}$. For $s$ waves, where $\ell = m_\ell = 0$ and $M = m_1 + m_2$, it is only necessary to specify the quantum numbers $\{q_1 q_2\}$ to label a channel.

When the two atoms are of the same isotopic species, the wave function must be symmetric (antisymmetric) with respect to exchange of identical bosons (fermions). We assume such symmetrized and normalized functions as described by Stoof *et al.* (1988). Exchange symmetry ensures that identical atoms in identical spin states can only collide in $s, d, \ldots$ waves for the case of bosons and in $p, f, \ldots$ waves in the case of fermions; in all other cases, collisions in all partial waves are allowed.

The channel energy $E_\alpha = E(q_1) + E(q_2)$ is the internal energy of the separated atoms. Assume that the atoms are prepared in channel $\alpha$ with relative kinetic energy $E$ so that the total energy is $E_{\text{tot}} = E_\alpha + E$. Any channel $\beta$ with $E_\beta \leqslant E_{\text{tot}}$ is called an open channel and any channel with $E_\beta > E_{\text{tot}}$ is called a closed channel. A collision can produce atoms in an open channel after the collision, but not in a closed channel, since the atoms do not have enough energy to separate to the product atoms.

#### 2. Collision rates

The partial collision cross section for starting in open channel $\alpha$ with relative kinetic energy $E$ and ending in open channel $\beta$ can be expressed in terms of the $S_{\alpha,\beta}(E)$ element of the multichannel unitary scattering matrix $\mathbf{S}$. The cross section for elastic scattering at energy $E$ in channel $\alpha$ is

$$\sigma_{\text{el},\alpha}(E) = g_\alpha (\pi/k^2) |1 - S_{\alpha,\alpha}(E)|^2, \tag{6}$$

whereas the unitarity property of $\mathbf{S}$ allows us to express the cross section for loss of atoms from channel $\alpha$ as

$$\sigma_{\text{loss},\alpha}(E) = g_\alpha (\pi/k^2) [1 - |S_{\alpha,\alpha}(E)|^2]. \tag{7}$$

The corresponding partial elastic and inelastic rate coefficients $K_{\text{el},\alpha}(E)$ and $K_{\text{loss},\alpha}(E)$ are found by multiplying these partial cross sections by the relative collision velocity $v = \hbar k / \mu$. The factor $g_\alpha = 1$ except for certain special cases involving identical particles. The factor $g_\alpha = 2$ for describing thermalization or inelastic collisions in a normal Maxwellian gas of two atoms of the same species in identical spin states. Inelastic decay of a pure Bose-Einstein condensate has $g_\alpha = 1$ (Kagan *et al.*, 1985; Stoof *et al.*, 1989).

If only one open channel $\alpha$ is present, collisions are purely elastic and $S_{\alpha,\alpha}(E) = \exp[2i\eta_\alpha(E)]$. For $s$ waves the real-valued tan $\eta_\alpha(E) \to -ka_\alpha$ as $k \to 0$ and $a_\alpha$ is the scattering length for channel $\alpha$. When other open channels are present, the amplitude $|S_{\alpha,\alpha}(E)|$ is no longer unity, and for $s$ wave we can represent the complex phase $\eta_\alpha(E) \to -k\tilde{a}_\alpha$ for $k \to 0$ in terms of a complex scattering length (Bohn and Julienne, 1996; Balakrishnan *et al.*, 1997)

$$\tilde{a}_\alpha = a_\alpha - ib_\alpha, \tag{8}$$

where $a$ and $b$ are real, and $1 - |S_{\alpha,\alpha}(E)|^2 \to 4kb_\alpha \geqslant 0$ as $k \to 0$. The threshold behavior is

$$\sigma_{\text{el},\alpha}(E) = 4\pi g_\alpha (a_\alpha^2 + b_\alpha^2) \tag{9}$$

for the $s$-wave elastic collision cross section and

$$K_{\text{loss},\alpha}(E) = (2h/\mu) g_\alpha b_\alpha \tag{10}$$

for inelastic collisions that remove atoms from channel $\alpha$. Both $\sigma_{\text{el},\alpha}$ and $K_{\text{loss},\alpha}$ approach constant values when $E$ is sufficiently small.

The unitarity property of the $S$ matrix also sets an upper bound on the cross sections. Since there is a rigorous upper bound of $|S_{\alpha,\alpha}(E)| \leqslant 1$, we find that the elastic scattering cross section is maximum,

$$\sigma_{\text{el},\alpha}(E) = (4\pi/k^2) g_\alpha, \tag{11}$$

for any channel $\alpha$ (and thus any partial wave $\ell$) when $S_{\alpha,\alpha}(E) = -1$. Furthermore, $\sigma_{\text{loss},\alpha}(E)$, if nonvanishing, has a maximum value of $\sigma_{\text{loss},\alpha}(E) = g_\alpha \pi / k^2$ when $S_{\alpha,\alpha}(E) = 0$. These limits are called the unitarity limits of the cross sections. For $s$-wave collisions this limit is approached at quite low energy given by $E \approx \hbar^2 / (2\mu a_\alpha^2)$, where $ka_\alpha \approx 1$.

In order to compare with experimental data the partial rate coefficients must be summed over partial waves and thermally averaged over the distribution of relative collision velocities at temperature $T$. This defines the total rate coefficients $K_{\text{el},q_1 q_2}(T)$ and $K_{\text{loss},q_1 q_2}(T)$ when the atoms are prepared in states $q_1$ and $q_2$, respectively. Often the temperatures are sufficiently small that only the $s$-wave entrance channel contributes.

#### 3. Resonance scattering

The idea of resonance scattering in atomic and molecular systems has been around since the earliest days of quantum physics, as described in the Introduction. A conventional "resonance" occurs when the phase shift changes rapidly by $\approx \pi$ over a relatively narrow range of energy due to the presence of a quasibound level of the system that is coupled to the scattering state of the colliding atoms. Such a resonance may be due to a quasibound level trapped behind a repulsive barrier of a single potential or may be due to some approximate bound state which has a different symmetry and potential from that of the colliding atoms. The former is commonly known as a shape resonance, whereas the latter is often called a Feshbach resonance, in honor of Herman Feshbach, who developed a theory and a classification scheme for resonance scattering phenomena in the context of nuclear physics (Feshbach, 1958, 1962). We will follow here Fano's configuration interaction treatment of resonant scattering (Fano, 1961), which is common in atomic physics. A variety of treatments of the two-body physics of resonances in the context of ultracold Bose gases has been given by Timmermans *et al.* (1999), Duine and Stoof (2004), Góral *et al.* (2004), Marcelis *et al.* (2004), and Raoult and Mies (2004).

We first consider the standard scattering picture away from any collision threshold defined by a two-channel Hamiltonian $H$. Assume that we can describe our system to a good approximation by two uncoupled "bare" channels, as schematically shown in Fig. 1. One is the open background scattering channel $|\mathrm{bg}\rangle$ with scattering states $|E\rangle=\phi_{\mathrm{bg}}(R,E)|\mathrm{bg}\rangle$ labeled by their collision energy $E$. The other is the closed channel $|c\rangle$ supporting a bound state $|C\rangle=\phi_c(R)|c\rangle$ with eigenenergy $E_c$. The functions $\phi_c(R)$ and $\phi_{\mathrm{bg}}(R,E)$ are the solutions to Eq. (3) for the background potential $V_{\mathrm{bg}}(R)$ and the closed channel potential $V_c(R)$, respectively. Here $\phi_c(R)$ is normalized to unity. The scattering in the open channel is characterized by a background phase shift $\eta_{\mathrm{bg}}(E)$. When the Hamiltonian coupling $W(R)$ between the two channels is taken into account, then the two states become mixed or dressed by the interaction, and the scattering phase picks up a resonant part due to the bound state embedded in the scattering continuum,

$$\eta(E) = \eta_{\mathrm{bg}}(E) + \eta_{\mathrm{res}}(E), \tag{12}$$

where $\eta_{\mathrm{res}}(E)$ takes on the standard Breit-Wigner form (Mott and Massey, 1965; Taylor, 1972),

$$\eta_{\mathrm{res}}(E) = -\tan^{-1}\left(\frac{\frac{1}{2}\Gamma(E_c)}{E-E_c-\delta E(E_c)}\right). \tag{13}$$

The interaction $W(R)$, which vanishes at large $R$, determines two key features of the resonance, namely, its width,

$$\Gamma(E) = 2\pi|\langle C|W(R)|E\rangle|^2, \tag{14}$$

and its shift $\delta E$ to a new position at $E_c+\delta E(E)$,

$$\delta E(E) = \mathcal{P}\int_{-\infty}^{\infty}\frac{|\langle C|W(R)|E'\rangle|^2}{E-E'}dE', \tag{15}$$

where $\mathcal{P}$ implies a principal part integral, which includes a sum over the contribution from any discrete bound states in the spectrum of the background channel. When the resonance energy is not near the channel threshold, it is normally an excellent approximation to take the width and shift as energy-independent constants, $\Gamma(E_c)$ and $\delta E(E_c)$, evaluated at the resonance energy $E_c$, as in Eq. (13). The resonance phase changes by $\approx\pi$ when $E$ varies over a range on the order of $\Gamma$ from below to above resonance.

The essential difference between conventional and threshold resonance scattering is that if $E_c$ is close to the open channel threshold at $E=0$, the explicit energy dependence of the width and shift become crucial (Bohn and Julienne, 1999; Marcelis *et al.*, 2004; Julienne and Gao, 2006),

$$\eta_{\mathrm{res}}(E) = -\tan^{-1}\left(\frac{\frac{1}{2}\Gamma(E)}{E-E_c-\delta E(E)}\right). \tag{16}$$

The threshold laws for the $s$-wave width and shift as $k\to 0$ are

$$\tfrac{1}{2}\Gamma(E) \to (ka_{\mathrm{bg}})\Gamma_0, \tag{17}$$

$$E_c + \delta E(E) \to E_0, \tag{18}$$

where $\Gamma_0$ and $E_0$ are $E$-independent constants. Since $\Gamma(E)$ is positive definite, $\Gamma_0$ has the same sign as $a_{\mathrm{bg}}$. Combining these limits with the background phase property, $\eta_{\mathrm{bg}}(E)\to -ka_{\mathrm{bg}}$, and, for the sake of generality, adding a decay rate $\gamma/\hbar$ for the decay of the bound state into all available loss channels give in the limit of $k\to 0$

$$\tilde{a} = a - ib = a_{\mathrm{bg}} + \frac{a_{\mathrm{bg}}\Gamma_0}{-E_0 + i(\gamma/2)}. \tag{19}$$

The unique role of scattering resonances in the ultracold domain comes from the ability to tune the threshold resonance position $E_0$ through zero by varying either an external magnetic field with strength $B$ or optical field with frequency $\nu$.

Both magnetically and optically tunable resonances are treated by the same theoretical formalism given above, although the physical mechanisms determining the coupling and tuning are quite different. In the case of a magnetically tunable resonance, the channel can often be chosen so that $\gamma$ is zero or small enough to be ignored, whereas optical resonances are always accompanied by decay processes $\gamma$ due to decay of the excited state. The resonance strength $\Gamma_0$ is fixed for magnetic resonances, but $\Gamma_0(I)$ for optical resonances can be turned off and on by varying the laser intensity $I$. It may also be possible to gain some control over $\Gamma_0$ using a combination of electric and magnetic fields (Marcelis *et al.*, 2008).

In the case of a magnetically tunable resonance, there is a difference $\delta\mu=\mu_{\mathrm{atoms}}-\mu_c$ between the magnetic moment $\mu_{\mathrm{atoms}}$ of the separated atoms and the magnetic moment $\mu_c$ of the bare bound state $|C\rangle$. Thus, the energy $E_c$ of the state $|C\rangle$ relative to the channel energy of the separated atoms,

$$E_c = \delta\mu(B - B_c), \tag{20}$$

can be tuned by varying the magnetic field, and $E_c$ is zero at a magnetic field equal to $B_c$. Then, given that $\gamma=0$, the scattering length takes on the simple form given in Eq. (1),

$$a(B) = a_{bg} - a_{bg}\Delta/(B - B_0), \tag{21}$$

where

$$\Delta = \Gamma_0/\delta\mu \quad \text{and} \quad B_0 = B_c + \delta B \tag{22}$$

are the width and the position of the singularity in the scattering length, shifted due to the interaction between the closed and open channels by an amount $\delta B = -\delta E/\delta\mu$. Note that $\Delta$ has the same sign as $\delta\mu/a_{bg}$. Figure 2 schematically shows the scattering length near the point of resonance $B_0$.

The complex scattering length of an optically tunable resonance at laser frequency $\nu$ includes the collisional loss due to excited state decay (Fedichev, Kagan, *et al.*, 1996; Bohn and Julienne, 1999),

$$\tilde{a}(\nu,I) = a_{bg} + \frac{a_{bg}\Gamma_0(I)}{h[\nu - \nu_c - \delta\nu(I)] + i(\gamma/2)}, \tag{23}$$

where the optically induced width $\Gamma_0(I)$ and shift $\delta\nu(I)$ are linear in $I$, and $\nu_c$ represents the frequency of the unshifted optical transition between the excited bound state and the collisional state of the two atoms at $E=0$.

Whenever bound state decay is present, whether for magnetically or optically tunable resonances, Eq. (19) shows that resonant control of the scattering length,

$$a = a_{bg} - a_{res}\frac{\gamma E_0}{E_0^2 + (\gamma/2)^2}, \tag{24}$$

is accompanied by collisional loss given by

$$b = \frac{1}{2}a_{res}\frac{\gamma^2}{E_0^2 + (\gamma/2)^2}. \tag{25}$$

The resonant length parameter

$$a_{res} = a_{bg}\Gamma_0/\gamma \tag{26}$$

is useful for defining the strength of an optical resonance (Bohn and Julienne, 1997; Ciuryło *et al.*, 2005) or any other resonance with strong decay (Hutson, 2007). Figure 6 gives an example of such a resonance. The scattering length has its maximum variation of $a_{bg} \pm a_{res}$ at $E_0 = \pm\gamma/2$, where $b = a_{res}$. Resonances with $a_{res} \leq |a_{bg}|$ only allow relatively small changes in scattering length, yet $b$ remains large enough that they are typically accompanied by large inelastic rate coefficients. On the other hand, if $a_{res} \gg |a_{bg}|$, losses can be overcome by using large detuning since the change in scattering length is $a - a_{bg} = -a_{res}(\gamma/E_0)$ when $|E_0| \gg \gamma$, whereas $b/|a - a_{bg}| = \frac{1}{2}|\gamma/E_0| \ll 1$.

The resonance length formalism is quite powerful. By introducing the idea of an energy-dependent scattering length (Blume and Greene, 2002; Bolda *et al.*, 2002) it can be extended to Feshbach resonances in reduced dimensional systems such as pancake or cigar-shaped optical lattice cells (Naidon and Julienne, 2006).

While this discussion has concentrated on resonant scattering properties for $E>0$, the near-threshold resonant properties of bound Feshbach molecules for energy $E<0$ are important aspects of Feshbach physics [see Fig. 2 and Köhler *et al.* (2006)]. In particular, as the bound

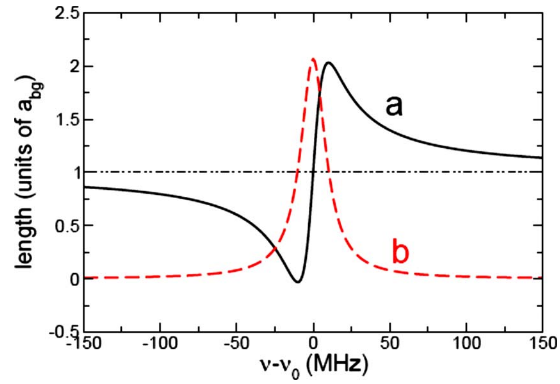


FIG. 6. (Color online) Scattering length for an optically tunable Feshbach resonance as a function of laser tuning $\nu - \nu_0$. The lengths $a$ and $b$ are defined in Eqs. (24) and (25). Here $a_{bg} = 5.29$ nm, $\Gamma_0/h = 21$ MHz at $I = 500$ W/cm$^2$, $a_{res} = 5.47$ nm, and $\gamma/h = 20$ MHz. Numerical values for the strength and spontaneous linewidth of the resonance are typical for $^{87}$Rb and are taken from Fig. 1 of Theis *et al.*, 2004.

state becomes more deeply bound, the closed channel character of the bound state increases and the binding energy $E_b$ is no longer described by the universal expression in Eq. (2). The dressed or true molecular bound state of the system with energy $-E_b$ is a mixture of closed and background channel components,

$$|\psi_b(R)\rangle = \sqrt{Z}\phi_c(R)|c\rangle + \chi_{bg}(R)|bg\rangle, \tag{27}$$

where $0 \leq Z \leq 1$ represents the fraction of the eigenstate $|\psi_b(R)\rangle$ in the closed channel component (Duine and Stoof, 2003). Unit normalization of $|\psi_b(R)\rangle$ ensures that $\int|\chi_{bg}(R)|^2 dR = 1 - Z$. Since the variation of the energy $-E_b$ with a parameter $x$ of the Hamiltonian satisfies the Hellman-Feynmann theorem $\partial(-E_b)/\partial x = \langle\psi_b|\partial H/\partial x|\psi_b\rangle$, it follows from Eq. (27) that

$$Z = \partial(-E_b)/\partial E_c = \delta\mu_b/\delta\mu. \tag{28}$$

Here $\delta\mu_b = \partial E_b/\partial B = \mu_{atoms} - \mu_b$ is the difference between the magnetic moment of the separated atoms and the magnetic moment $\mu_b$ of the dressed molecular eigenstate. Since $\delta\mu_b$ vanishes in the limit $B \to B_0$, where $E_b \to 0$ according to the universality condition in Eq. (2), then $Z$ vanishes in this limit also. Section II.C.5 develops more specific properties and conditions for $E_b$ and $Z$ in this limit.

### B. Basic molecular physics

Most atoms that can be trapped at ultracold temperatures have ground $S$ states with zero electronic orbital angular momentum ($L=0$) as for alkali-metal or alkaline-earth-metal atoms. The collision between two atoms is controlled by the electronic Born-Oppenheimer interaction potential(s) between them. All potentials are isotropic for the interaction of two $S$-state atoms. We restrict our discussion of molecular physics to such cases. Figure 7 shows as an example the $^1\Sigma_g^+$ and $^3\Sigma_u^+$ potentials for two ground state $^2S$ Li atoms, which are analogous to

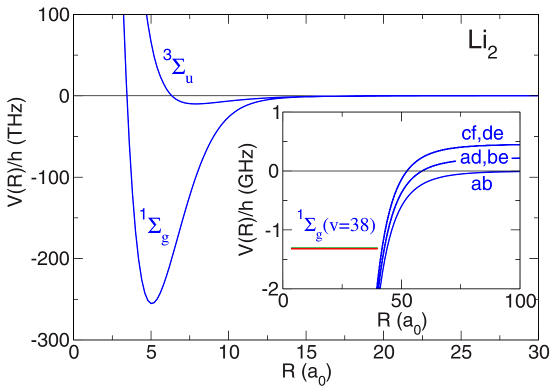


FIG. 7. (Color online) Molecular potentials $V(R)/h$ vs $R$ of the two electronic states of $Li_2$ that correlate with two separated $^2S$ atoms. The inset shows an expanded view of the long-range $s$-wave potentials of $^6$Li at $B=0$, indicating the five hyperfine states of the separated atoms (see Fig. 5) for which the total angular momentum has projection $M=0$. The inset also shows the last two nearly degenerate bound states (unresolved on the figure) of the $^6Li_2$ molecule from a coupled-channel calculation. It is a good approximation to label these nearly degenerate levels as the $I=0$ and 2 components of the total nuclear spin $\mathbf{I}=\mathbf{I}_1+\mathbf{I}_2$ of the last $v=38$ vibrational level of the $^1\Sigma_g^+$ potential.

the similar potentials for the $H_2$ molecule or other alkali-metal atoms. The superscripts 1 and 3 refer to singlet and triplet couplings of the spins of the unpaired electrons from each atom, i.e., the total electron spin $\mathbf{S}=\mathbf{S}_1+\mathbf{S}_2$ has quantum numbers $S=0$ and 1. The $\Sigma$ refers to zero projection of electronic angular momentum on the interatomic axis for the $S$-state atoms, and $g$ ($u$) refers to *gerade* (*ungerade*) electronic inversion symmetry with respect to the center of mass of the molecule. The $g$ ($u$) symmetry is absent when the two atoms are not of the same species.

The Born-Oppenheimer potentials are often available from *ab initio* or semiempirical sources. When $R$ is sufficiently small, typically less than $R_{ex}\approx 1$ nm for alkali-metal atoms, electron exchange and chemical bonding effects determine the shape of the potentials. For $R \gg R_{ex}$, the potentials are determined by the long-range dispersion interaction represented by a sum of second-order multipolar interaction terms.

### 1. van der Waals bound states and scattering

Many aspects of ultracold neutral atom interactions and of Feshbach resonances, in particular, can be understood qualitatively and even quantitatively from the scattering and bound state properties of the long-range van der Waals potential. The properties of this potential relevant for ultracold photoassociation spectroscopy have been reviewed by Jones *et al.* (2006). Its analytic properties are discussed by Mott and Massey (1965), Gribakin and Flambaum (1993), and Gao (1998b, 2000).

In the case of $S$-state atoms, the leading term in the long-range part of all Born-Oppenheimer potentials for a given atom pair has the same van der Waals potential characterized by a single $C_6$ coefficient for the pair. Consequently, all $q_1q_2$ spin combinations have the long-range potential

$$V_\ell(R) = -\frac{C_6}{R^6} + \frac{\hbar^2}{2\mu}\frac{\ell(\ell+1)}{R^2}. \tag{29}$$

A straightforward consideration of the units in Eq. (29) suggests that it is useful to define length and energy scales,

$$R_{\mathrm{vdW}} = \frac{1}{2}\left(\frac{2\mu C_6}{\hbar^2}\right)^{1/4} \quad \text{and} \quad E_{\mathrm{vdW}} = \frac{\hbar^2}{2\mu}\frac{1}{R_{\mathrm{vdW}}^2}. \tag{30}$$

Gribakin and Flambaum (1993) defined an alternative van der Waals length scale which they called the mean scattering length,

$$\bar{a} = [4\pi/\Gamma(1/4)^2]R_{\mathrm{vdW}} = 0.955\,978\ldots R_{\mathrm{vdW}}, \tag{31}$$

where $\Gamma(x)$ is the gamma function. A corresponding energy scale is $\bar{E}=\hbar^2/(2\mu\bar{a}^2)=1.09\,422\ldots E_{\mathrm{vdW}}$. The parameter $\bar{a}$ occurs frequently in formulas based on the van der Waals potential. Table I gives the values of $R_{\mathrm{vdW}}$ and $E_{\mathrm{vdW}}$ for several cases. Values of $C_6$ for other systems are tabulated by Tang *et al.* (1976), Derevianko *et al.* (1999), and Porsev and Derevianko (2006).

The van der Waals energy and length scales permit a simple physical interpretation (Julienne and Mies, 1989). A key property for ultracold collisions is that $C_6/R^6$ becomes large compared to the collision energy $E$ when $R<R_{\mathrm{vdW}}$. Thus, the wave function for any partial wave oscillates rapidly with $R$ when $R<R_{\mathrm{vdW}}$ since the local momentum $\hbar k(R)=\sqrt{2\mu[E-V(R)]}$ becomes large compared to the asymptotic $\hbar k$. On the other hand, when $R>R_{\mathrm{vdW}}$, the wave function approaches its asymptotic form with oscillations on the scale determined by the long de Broglie wavelength of the ultracold collision. The energy scale $E_{\mathrm{vdW}}$ determines the nature of the connection between the long- and short-range forms of the wave function. The de Broglie wavelength $\lambda=2\pi(R_{\mathrm{vdW}})$ for $E=E_{\mathrm{vdW}}$. When $E\ll E_{\mathrm{vdW}}$ so that $\lambda \gg R_{\mathrm{vdW}}$, a WKB connection cannot be made near $R_{\mathrm{vdW}}$ between the asymptotic $s$ wave and the short-range wave function [see Fig. 15 of Jones *et al.* (2006)]. Consequently, the quantum properties of the collision are manifest for $E<E_{\mathrm{vdW}}$.

The van der Waals length also characterizes the extent of vibrational motion for near-threshold bound state. The outer turning point for classical motion for all low $\ell$ bound states is on the order of $R_{\mathrm{vdW}}$. The wave function for $\ell=0$ oscillates rapidly for $R<R_{\mathrm{vdW}}$ and decays exponentially as $e^{-k_bR}$ for $R\gg R_{\mathrm{vdW}}$, where $\hbar^2k_b^2/(2\mu)$ is the binding energy. The only case where the wave function extends far beyond $R_{\mathrm{vdW}}$ is that of the last $s$-wave bound state for the case of the universal halo molecule, where $a\gg R_{\mathrm{vdW}}$ (see Secs. II.A and V.B.2).

The van der Waals potential determines the interaction over a wide zone between $R_{\mathrm{vdW}}$ and the much smaller $R_{ex}$ where chemical forces become important. Thus, near-threshold bound and scattering state proper-

TABLE I. Characteristic van der Waals scales $R_{\mathrm{vdW}}$ and $E_{\mathrm{vdW}}$ for several atomic species (1 amu $=1/12$ mass of a $^{12}$C atom, 1 a.u.$=1E_h a_0^6$ where $E_h$ is a hartree and 1 $a_0=0.052\,917\,7\ldots$ nm).

| Species | Mass (amu) | $C_6$ (a.u.) | $R_{\mathrm{vdW}}$ ($a_0$) | $E_{\mathrm{vdW}}/k_B$ (mK) | $E_{\mathrm{vdW}}/h$ (MHz) |
|---|---|---|---|---|---|
| $^6$Li | 6.0151223 | 1393.39[a] | 31.26 | 29.47 | 614.1 |
| $^{23}$Na | 22.9897680 | 1556[b] | 44.93 | 3.732 | 77.77 |
| $^{40}$K | 39.9639987 | 3897[b] | 64.90 | 1.029 | 21.44 |
| $^{40}$Ca | 39.962591 | 2221[c] | 56.39 | 1.363 | 28.40 |
| $^{87}$Rb | 86.909187 | 4698[d] | 82.58 | 0.2922 | 6.089 |
| $^{88}$Sr | 87.905616 | 3170[c] | 75.06 | 0.3497 | 7.287 |
| $^{133}$Cs | 132.905429 | 6860[e] | 101.0 | 0.1279 | 2.666 |

[a]Yan *et al.*, 1996.
[b]Derevianko *et al.*, 1999.
[c]Porsev and Derevianko, 2002.
[d]van Kempen *et al.*, 2002.
[e]Chin, Vuletić *et al.*, 2004.

ties are determined to a large extent by the long-range van der Waals potential. The effect of short range is then contained within the *phase* of the wave function or, equivalently, the logarithmic derivative (Moerdijk and Verhaar, 1994; Vogels *et al.*, 2000). More precisely, for any $R_z$ satisfying $R_{\mathrm{ex}} < R_z \ll R_{\mathrm{vdW}}$ so that $k(R_z) \gg k$, the wave function phase is nearly independent of $E$ and almost the same for all near-threshold bound or scattering states. In fact, the phase is nearly independent of partial wave $\ell$ as well since the centrifugal potential is typically small compared to the van der Waals potential for such an $R_z$. Using this phase as a boundary condition for propagating the wave function to large $R$ in the asymptotic domain determines the energy-dependent scattering phase $\eta_\ell(E)$ and bound state energies. In fact the phase of the wave function in the zone $R_{\mathrm{ex}} < R_z \ll R_{\mathrm{vdW}}$ is uniquely related to the $s$-wave scattering length (Gao, 1998a). Consequently, to a good approximation the near-threshold bound states and scattering properties for all low partial waves are determined by the $s$-wave scattering length, the $C_6$ constant, and the reduced mass (Gao, 2001).

Gao (2000) worked out the energies $E_{n,\ell}$ of the bound states of all partial waves for a van der Waals potential as a function of the $s$-wave scattering length, where $n=-1,-2,\ldots$ is the vibrational quantum number and $\ell$ is the rotational quantum number of the bound state. He showed that the energies of weakly bound states have a $\Delta\ell=4$ periodicity. Figure 8 shows bound state energies as a function of $\ell$ for two values of $a$. In the left panel $a=\pm\infty$ so there is a $s$-wave bound state with $E=0$. The figure shows that for $\ell=4$ there is also bound state with $E/E_{\mathrm{vdW}}=0$. In fact Gao (2000) showed for $\ell=8,12,\ldots$ that there will be a bound state at zero energy as well. The right panel of Fig. 8 shows that when $a=\bar{a}$ there is a bound state at zero energy for $\ell=2$. There will also be a bound state at zero energy for $\ell=6,10,\ldots$.

Figure 8 can also be used to define the concept of "energy bins" in which, regardless of the value of $a$, there must be a bound state. Bins are most easily defined by starting from a case with a bound state at zero binding energy. By changing the short-range logarithmic derivative its binding energy can be increased or its energy lowered and at some point the binding energy is so large that a new bound state appears at zero binding energy. This is exactly the situation shown in Fig. 8(a) for $s$ and $g$ waves. In other words, for $s$ waves there must be a $n=-1$ bound state between $-39.5E_{\mathrm{vdW}}$ and $0E_{\mathrm{vdW}}$, while for $g$ waves there must be a $n=-1$ bound state between $-191E_{\mathrm{vdW}}$ and $0E_{\mathrm{vdW}}$. The $n=-2$ $s$-wave bound

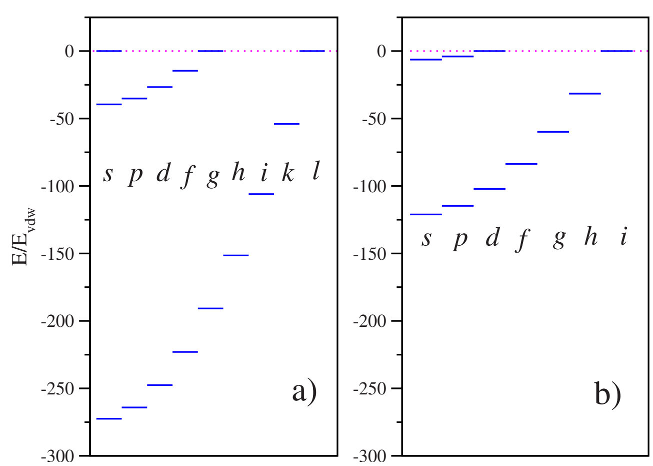


FIG. 8. (Color online) Bound state energies of the last vibrational levels of two atoms interacting via a van der Waals potential as a function of partial wave $\ell$. The zero of energy is at two free atoms with zero collision energy ("at threshold"). The lowest partial waves are shown. (a) Shows the bound state structure up to $\ell=8$ when the scattering length of the colliding atoms is infinite or equivalently there is an $s$-wave bound state with zero binding energy. (b) The bound state structure up to $\ell=6$ when the scattering length is $a=0.956\ldots R_{\mathrm{vdW}}=\bar{a}$ or equivalently there is a $d$-wave bound state with zero binding energy. The length $R_{\mathrm{vdW}}$ and energy $E_{\mathrm{vdW}}$ are defined in the text. Adapted from Gao, 2000.

state appears between $-272E_{\mathrm{vdW}}$ and $-39.5E_{\mathrm{vdW}}$. Figure 8(b) can similarly be used to define the bins for other waves.

When the scattering length is large compared to $\bar{a}$ and positive, a simple expression for the van der Waals correction to the binding energy of the last $s$-wave bound state can be worked out (Gribakin and Flambaum, 1993),

$$E_{-1,0}=-\hbar^2/[2\mu(a-\bar{a})^2]. \tag{32}$$

The universal formula in Eq. (2) only applies in the limit that $a\gg\bar{a}$ and $|E_{-1,0}|\ll E_{\mathrm{vdW}}$. Gao (2004) worked out higher order corrections to the binding energy due to the van der Waals potential, which can be recast as

$$E_{-1,0}=-\frac{\hbar^2}{2\mu(a-\bar{a})^2}\left[1+\frac{g_1\bar{a}}{a-\bar{a}}+\frac{g_2\bar{a}^2}{(a-\bar{a})^2}+\cdots\right]. \tag{33}$$

Here $g_1=\Gamma(1/4)^4/6\pi^2-2=0.9179\ldots$ and $g_2=(5/4)g_1^2-2=-0.9468\ldots$ are constants.

Similarly, the effective range of the potential in Eq. (5) is also determined from the van der Waals potential, given the $s$-wave scattering length (Gao, 1998a; Flambaum et al., 1999),

$$r_0=\frac{\Gamma(1/4)^4}{6\pi^2}\bar{a}\left[1-2\frac{\bar{a}}{a}+2\left(\frac{\bar{a}}{a}\right)^2\right], \tag{34}$$

where $\Gamma(1/4)^4/(6\pi^2)\approx 2.9179$. When $a\gg\bar{a}$, this simplifies to $r_0=2.9179\bar{a}$. Note that $r_0$ diverges as $a\to 0$.

The energy levels of the van der Waals potential are not exact due to the slight influence from the actual short-range potential and extremely long-range retardation corrections. They are, nevertheless, relatively accurate guides to the expected energy spectrum for real molecules. For example, when the scattering length is slightly larger than $\bar{a}$, which corresponds to Fig. 8(b) with all bound states shifted to slightly more positive energies, the $d$-wave bound state becomes a shape resonance, that is, a decaying quasibound state with $E>0$ trapped behind the $d$-wave centrifugal barrier. For $^{23}$Na and $^{87}$Rb the experimentally observed scattering length is 10–20 % larger than $\bar{a}$ and, indeed, in both cases a $d$-wave shape resonance has been observed under various circumstances (Boesten et al., 1997; Samuelis et al., 2000; Buggle et al., 2004; Thomas et al., 2004). Similarly, a $p$-wave shape-resonance occurs when $a$ is slightly larger than $2\bar{a}$ as for $^{40}$K (DeMarco et al., 1999) and $^{171}$Yb (Kitagawa et al., 2008). In addition Kitagawa et al. (2008) showed how the scattering length and binding energies of the last few bound states for the single potential of the Yb+Yb interaction are related as the reduced mass is changed using different isotopic combinations of Yb atoms. The scattering length and binding energies can be "tuned" over a wide range by choosing different pairs of atoms among the seven stable isotopes of Yb.

The $\delta\ell=4$ characteristic of van der Waals potentials also has practical consequences for ultracold scattering. For $^{85}$Rb the scattering length has been found to be large compared to $R_{\mathrm{vdW}}$ and a $g$-wave shape resonance has been observed (Boesten, Tsai, et al., 1996). For $^{133}$Cs the scattering length is large compared to $R_{\mathrm{vdW}}$, and numerous $g$-wave bound states with binding energies much smaller than $E_{\mathrm{vdW}}$ were observed by Chin, Vuletić, et al. (2004) at low magnetic field. In fact, some of these bound states appear as magnetic Feshbach resonances in the collision of two Cs atoms. Recently, a weakly bound $l=8$ or $l$-wave state has been observed as well (Mark, Ferlaino, et al., 2007).

#### 2. Entrance- and closed channel dominated resonances: Resonance strength

The van der Waals theory is useful for characterizing and classifying the basic properties of the resonances discussed in Sec. II.A.3 by expressing lengths in units of $\bar{a}$ and energies in units of $\bar{E}$ [see Eq. (31)]. The numerator of the resonant term in Eq. (19) defines a resonance strength parameter to be $a_{\mathrm{bg}}\Gamma_0$, where $\Gamma_0=\delta\mu\Delta$ [see Eq. (22)]. It is helpful to define a dimensionless resonance strength parameter $s_{\mathrm{res}}$ to be

$$s_{\mathrm{res}}=r_{\mathrm{bg}}\frac{\Gamma_0}{\bar{E}}=\frac{a_{\mathrm{bg}}}{\bar{a}}\frac{\delta\mu\Delta}{\bar{E}}, \tag{35}$$

where $r_{\mathrm{bg}}=a_{\mathrm{bg}}/\bar{a}$ is the dimensionless background scattering length. The sign of $s_{\mathrm{res}}$ is always positive. The resonance phase in Eq. (16) is determined by the tunable resonance position and the resonance width and shift. In the limit $E\to 0$, both the width

$$\tfrac{1}{2}\Gamma(E)=(k\bar{a})(\bar{E}s_{\mathrm{res}}) \tag{36}$$

and the shift (Góral et al., 2004; Julienne and Gao, 2006)

$$\delta E=\frac{1-r_{\mathrm{bg}}}{1+(1-r_{\mathrm{bg}})^2}(\bar{E}s_{\mathrm{res}}) \tag{37}$$

are proportional to $\bar{E}s_{\mathrm{res}}$. Section II.B.5 describes widths and shifts for some typical resonances. Sections II.C.3–II.C.5 give additional analytic properties of threshold scattering and bound states associated with Feshbach resonances and show how Eq. (37) can be derived.

The strength parameter $s_{\mathrm{res}}$ allows us to classify Feshbach resonances into two limiting cases. Stoll and Köhler (2005) and Köhler et al. (2006) used $\eta=1/s_{\mathrm{res}}$ to do this. When $s_{\mathrm{res}}\gg 1$, the resonance is called an entrance channel dominated resonance. Here the near-threshold scattering and bound states have the spin character of the entrance channel for detuning $E_0$ over a large fraction of the width $\Gamma_0$ and thus for $B-B_0$ over a large fraction of the resonance width $\Delta$. In this regime, the resonance can be well modeled by the $B$-dependent scattering length of Eq. (1). The bound state is universal with $Z\ll 1$ [see Eq. (27)] over this large detuning range and with a binding energy well approximated by Eq. (2).

Resonances of this type have the largest resonance width $\Delta$ and are conventionally called "broad resonances."

Resonances with $s_{\text{res}} \ll 1$ are called closed channel dominated resonances. Here the near-threshold scattering and bound states have the spin character of the entrance channel only over a small fraction of the width $\Gamma_0$ near $E_0=0$ and thus over a small fraction of the resonance width $\Delta$ near $B=B_0$. A universal bound state only exists over this small detuning range. Thus, the closed channel fraction $Z$ is only small near $B=B_0$ and is near unity over a wide detuning range away from $B=B_0$. Such resonances need to be modeled by a coupled-channel description. Resonances of this type often have a small width $\Delta$ and are conventionally called "narrow resonances."

It should be emphasized that the conventional use of "broad" or "narrow" resonances referring to those that can or cannot be modeled by single channel model is not rigorously defined. Exceptions exist where resonances with apparently broad widths are actually closed channel dominated. The terms introduced here, entrance and closed channel dominances, better reflect the nature of the near-threshold states over a detuning range on the order of the width $\Delta$ and can be unambiguously assigned to a resonance by evaluating $s_{\text{res}}$.

Section II.B.5 illustrates the differences between entrance and closed channel dominated resonances by giving specific examples of such resonances. Section II.C.5 develops a simple model for the bound states for any type of resonance and shows that the norm $Z$ of the closed channel part vanishes in the limit that $E_0 \to 0$ near the point of resonance $B_0$ even for closed channel dominated resonances. Szymanska *et al.* (2005) discussed in detail the implication of the distinction between open and closed channel dominances for the modeling of many-body systems, a topic that is beyond the scope of this review.

The Appendix shows the wide range of resonance strengths $s_{\text{res}}$ and widths $\Delta$ observed for various alkali atom resonances. Broad resonances with $\Delta$ larger than ~1 G tend to have $s_{\text{res}}>1$ and thus be entrance channel dominated ones. Narrow resonances with $\Delta$ smaller than ~1 G tend to have $s_{\text{res}}<1$ and thus be closed channel dominated ones. A notable exceptions is the $^7$Li 737 G resonance with $s_{\text{res}}<1$ that is very broad yet tends toward being closed channel dominated (see Sec. II.B.5).

Equation (36) allows us to address the question whether a sharp resonance feature appears at small but finite collision energy above threshold. A condition for having a sharp resonance is that the width $\frac{1}{2}\Gamma(E)$ should be smaller than the collision energy $E$. It is convenient to rewrite Eq. (36) as $\frac{1}{2}\Gamma(E)=(s_{\text{res}}/k\bar{a})E$. For an entrance channel dominated resonance with $s_{\text{res}} \gg 1$ and $k\bar{a}<1$ or $E<\bar{E}$, it follows that $\frac{1}{2}\Gamma(E)>E$. Thus, there can be no sharp resonance features evident in the above-threshold phase $\eta(E,B)$ of an entrance channel dominated resonance when $E<\bar{E}$. A sharp resonance feature can only appear when $E \gg \bar{E}$. Nygaard *et al.* (2006) illustrated this case for a resonance involving $^{40}$K atoms. On the other hand, for a closed channel dominated resonance with $s_{\text{res}} \ll 1$ a sharp resonance feature in $\eta(E,B)$ with $\frac{1}{2}\Gamma(E) \ll E$ can appear immediately above threshold.

### 3. Coupled-channel picture of molecular interactions

While many insights can be gained from the properties of the long-range van der Waals potential, actual calculations require taking into account the full molecular Hamiltonian, including not only the full range of the Born-Oppenheimer potentials but also the various spin-dependent couplings among them. In general, the potential should be viewed as a spin-dependent potential matrix, the elements of which account for the interaction among the various spin states of the atoms. The wave function for atoms prepared in channel $\alpha$ can be written as a coupled-channel expansion in the separated atom spin basis described in Sec. II.A.1 (Mott and Massey, 1965; Stoof *et al.*, 1988; Gao, 1996; Mies *et al.*, 2000; Hutson *et al.*, 2008),

$$|\psi_\alpha(R,E)\rangle = \sum_\beta |\beta\rangle \phi_{\beta\alpha}(R,E)/R. \tag{38}$$

The allowed states $|\beta\rangle$ in this expansion are those that have the same projection quantum number $M=m_1+m_2+m_\ell$ (see Sec. II.A.1). In addition parity conservation implies that all partial waves $\ell_\beta$ in the expansion are even if $\ell_\alpha$ is even and odd if $\ell_\alpha$ is odd.

Substituting Eq. (38) in the Schrödinger equation gives the coupled-channel equations for the vector $\boldsymbol{\phi}(R,E)$,

$$-\frac{\hbar^2}{2\mu}\frac{d^2\boldsymbol{\phi}(R,E)}{dR^2} + \mathbf{V}(R)\boldsymbol{\phi}(E,R) = E\boldsymbol{\phi}(E,R). \tag{39}$$

The solutions to these coupled equations give the bound and scattering states of the interacting atoms. The potential matrix $\mathbf{V}(R)$ gives the matrix elements of the Hamiltonian between the channel basis sets. It takes on the following form in the asymptotic spin basis:

$$V_{\alpha\beta} = [E_\alpha + \hbar^2\ell_\alpha(\ell_\alpha+1)/(2\mu r^2)]\delta_{\alpha\beta} + V_{\text{int},\alpha\beta}(R). \tag{40}$$

The interaction matrix $V_{\text{int}}(R)$ contains the electronic Born-Oppenheimer potentials discussed in Sec. II.B and the relativistic electron spin-dependent interactions,

$$\mathbf{V}_{\text{int}}(R) = \mathbf{V}_{\text{el}}(R) + \mathbf{V}_{\text{ss}}(R). \tag{41}$$

For collisions of $S$ state atoms the term $\mathbf{V}_{\text{el}}(R)$ represents the strong isotropic electronic interaction that is diagonal in $\ell$ and $m_\ell$ but off diagonal in the atomic channel quantum numbers $q_1q_2$. The diagonal elements $V_{\text{el},\alpha\alpha}$ vary at long range as the van der Waals potential (see Fig. 7). It has normally been unnecessary to include small retardation or nonadiabatic corrections to long-range molecular potentials in order to fit experimental data on ground state collisions within their experimental error [see, e.g., Kitagawa *et al.* (2008)]. The off-diagonal elements $V_{\text{el},\alpha\beta}$, where $\beta \neq \alpha$, decrease exponentially at large $R$ as the exchange potential becomes small compared to the atomic hyperfine splitting for $R>R_{\rm ex}$. The $\mathbf{V}_{\rm el}$ coupling is responsible for elastic scattering and inelastic spin-exchange collisions and gives rise to the largest resonance strengths.

The term $\mathbf{V}_{\rm ss}(r)$ in Eq. (41) represents weak relativistic spin-dependent interactions. These include the spin-spin dipole interaction (Stoof *et al.*, 1988; Moerdijk *et al.*, 1995) and the second-order spin-orbit interaction (Kotochigova *et al.*, 2000), important for heavy atoms (Leo *et al.*, 2000). The two contributions are both anisotropic and are off diagonal in both $q_1q_2$ and $\ell$. Thus, $\mathbf{V}_{\rm ss}(r)$ couples different partial waves. At long range $\mathbf{V}_{\rm ss}(r)$ is proportional to $\alpha^2/R^3$, where $\alpha=1/137.0426$ is the fine structure constant. This anisotropic potential only contributes diagonal terms for partial waves $\ell \geqslant 1$ and does not contribute to the potential $V_{{\rm int},\alpha\alpha}(R)$ when $\alpha$ represents an $s$-wave channel. The $\mathbf{V}_{\rm ss}(r)$ coupling is responsible for weak inelastic relaxation and normally gives rise to small resonance strengths.

The Born-Oppenheimer potentials are normally never known with sufficient accuracy to permit accurate calculations of threshold scattering properties. Consequently, it is usually necessary to vary the short-range potentials over some range of $R<R_{\rm ex}$ to calibrate theoretical models so that they reproduce measured threshold bound state or scattering data. In some cases the van der Waals coefficients are accurately known, whereas in other cases they need to be varied to fit the data as well. Once this is done, coupled-channel theoretical models typically are robust and predictive of near-threshold collision and bound state properties. Some examples of high quality theoretical models based on fitting Feshbach resonance data are given by van Abeelen and Verhaar (1999a) for $^{23}$Na, Chin *et al.* (2000) and Leo *et al.* (2000) for $^{133}$Cs, Marte *et al.* (2002) for $^{87}$Rb, Bartenstein *et al.* (2005) for $^{6}$Li, Werner *et al.* (2005) for $^{52}$Cr, and Ferlaino *et al.* (2006) and Pashov *et al.* (2007) for $^{40}$K $^{87}$Rb. Information on other models can be found in the references listed in Secs. III.B and III.C.

#### 4. Classification and molecular physics of Feshbach resonances

The previous sections have laid the groundwork for classifying and understanding the properties of Feshbach resonance states in ultracold collisions of ground $S$-state atoms. This classification can be made according to the quantum numbers $\{q_1q_2\ell M|q_c\ell_c\}$, where $\{q_1q_2\ell M\}$ characterize the entrance channel (see Sec. II.A.1) and $\{q_c\ell_c\}$ characterize the "bare" closed channel bound state that gives rise to the resonance. Such a bound state has the same $M$ as the entrance channel. Some possible choices for quantum numbers comprising the composite $q_c$ are given below.

It is important to note that $\ell_c$ need not be the same as the entrance channel partial wave $\ell$. Parity conservation ensures that $|\ell-\ell_c|$ is even. In the case of two $\mathbf{L}=0$ atoms the $\mathbf{V}_{\rm el}$ term is isotropic and only gives rise to nonzero matrix elements when $\ell_c=\ell$. On the other hand, $\ell_c$ can be different from $\ell$ for the anisotropic $\mathbf{V}_{\rm ss}$ term. We are primarily concerned with entrance channel $s$ waves, although some resonances with $p$-wave (e.g., $^{6}$Li, $^{40}$K, and $^{133}$Cs) or $d$-wave ($^{52}$Cr) entrance channels are known in the $\mu$K domain.

TABLE II. Classification of magnetic Feshbach resonances in collisions of ultracold atoms. The type of the resonance is labeled by the partial wave $\ell_c$ of the closed channel bound state rather than the entrance channel partial wave $\ell$. Almost all cases known experimentally have $\ell=0$ or 1. Note that identical bosons (fermions) in identical spin states can only interact with even (odd) partial waves. All other cases permit both even and odd partial waves.

| Type | $\ell$ | $\ell_c$ |
|---|---|---|
| $s$-wave resonance | 0, 2,… | 0 |
| $p$-wave resonance | 1, 3,… | 1 |
| $d$-wave resonance | 0, 2,… | 2 |
| $f$-wave resonance | 1, 3,… | 3 |
| $g$-wave resonance | 0, 2,… | 4 |

We find that it is convenient to designate resonances according to the value of the closed channel bound state quantum number $\ell_c$, as shown in Table II. If $\ell_c$ is even (odd), we assume an $s$- ($p$-) wave entrance channel unless otherwise stated. The strongest resonances with the largest widths $\Delta$ are $s$-wave resonances with $\ell=\ell_c=0$ and are due to the $\mathbf{V}_{\rm el}$ term in the Hamiltonian. A number of weak resonances with small $\Delta$ are known where the $s$-wave entrance channel is coupled through the $\mathbf{V}_{\rm ss}$ term to bound states with even $\ell_c$ such as 2 or 4. Following Table II the latter are designated as $d$- or $g$-wave resonances, respectively. For example, $d$-wave resonances are known for $^{87}$Rb (Marte *et al.*, 2002) and $g$-wave resonances for Cs (Chin, Vuletić, *et al.*, 2004). For $s$-wave entrance channels the $g$-wave resonances are only possible due to second-order coupling in $\mathbf{V}_{\rm ss}$. Entrance channel $p$ waves can be coupled to resonant bound states of odd $\ell_c=1$ or 3, although the latter would tend to be quite weak and rarely observed.

The long-range potential $V_{{\rm el},\alpha\beta}(R)$ is diagonal for the interaction of two ground state alkali-metal atoms for all combinations $q_1q_2$ of Zeeman sublevels, and all channels have the same van der Waals coefficient $C_6$. Consequently each channel will have a spectrum of vibrational and rotational levels for a van der Waals potential as shown in Fig. 8. The $n=-1,-2,\ldots$ levels associated with closed spin channels $\alpha'$ can become scattering resonances for entrance channel $\alpha$ if they exist near energy $E_\alpha$. The value of $n$ can be one of the values comprising the set of approximate quantum numbers $q_c$. Some examples of the use of $n$ in resonance classification are given by Marte *et al.* (2002) for $^{87}$Rb (see Fig. 14) or Köhler *et al.* (2006) for $^{85}$Rb. The vibrational quantum number can be either $n$, counting down from the top, or $v$, counting up from the bottom of the well.

The approximate spin quantum numbers in $q_c$ are determined by whatever set of quantum numbers that blocks the Hamiltonian matrix into nearly diagonal parts. This will depend on the nature of the coupling among the various angular momenta of the problem so that no unique general scheme can be given. For alkali-metal dimers the spacing between vibrational levels, which is on the order of tens of $E_{\mathrm{vdW}}$ as seen from Fig. 8, must be compared to the spacing between the channel energies $E_\alpha$. For example, in a light molecule such as $^6Li_2$ or $^{23}Na_2$ they are large compared to the atomic hyperfine splitting $E_{\mathrm{hf}}=|E_{I+1/2}-E_{I-1/2}|$ and Zeeman interactions. In this case, the vibrational levels are to a good approximation classified according to the electronic spin coupling, $S=0$ or 1, of the respective $^1\Sigma_g^+$ and $^3\Sigma_u^+$ Born-Oppenheimer potentials, with additional classification according to their nuclear spin substructure. van Abeelen and Verhaar (1999a) and Laue *et al.* (2002) gave an example of such a classification for $^{23}Na_2$ and Simonucci *et al.* (2005) gave an example for $^6Li_2$.

In contrast to light species, heavy species such as $Rb_2$ or $Cs_2$ have vibrational spacings that are smaller than $E_{\mathrm{hf}}$, so that near-threshold bound states of the $^1\Sigma_g^+$ and $^3\Sigma_u^1$ potentials are strongly mixed by the hyperfine interaction. The near-threshold molecular states do not correspond to either $S=0$ or 1 but often can be characterized by the approximate quantum number $f_c$, where $\mathbf{f}=\mathbf{f}_1+\mathbf{f}_2$. As with the $f_1$ or $f_2$ atomic quantum numbers, $f_c$ is not a good quantum number at large $B$ but can be used as a label according to the low field state with which it adiabatically correlates. Marte *et al.* (2002) gave examples of such resonance classification for $^{87}Rb$ and Chin, Vuletić, *et al.* (2004) and Köhler *et al.* (2006) do so for $^{133}Cs$ and $^{85}Rb$, respectively. Hutson *et al.* (2008) described improved computational methods for calculating the coupling between bound state levels and characterized a number of experimentally observed avoided crossings (Mark, Ferlaino, *et al.*, 2007) between $Cs_2$ levels having different approximate quantum numbers.

### 5. Some examples of resonance properties

We use the fermionic species $^6Li$ to illustrate some basic features of Feshbach resonances. Figure 5 shows the atomic Zeeman levels. The inset of Fig. 7 shows the five channels and the potentials $V_{\alpha\alpha}(R)$ at long range needed to describe the $s$-wave collision of an $q_1=a$ atom with a $q_2=b$ atom. These five channels summarized in Table III have the same van der Waals $C_6$ coefficient and the same projection $M=0$. Due to the light mass, the last bound state of the van der Waals potential must lie in a "bin," that is, $39.5E_{\mathrm{vdW}}/h=24.3$ GHz deep.

Figure 7 shows that the last two $M=0$ coupled-channel $s$-wave bound states for $B=0$ have the character of the $n=-1$ or $v=38$ level of the $^1\Sigma_g^+$ potential. They have a binding energy of $\approx 1.38$ GHz relative to the separated atom energy $E_{ab}$, associated with the positive scattering length of $a=45.17a_0$ of the $S=0$ singlet potential (Bartenstein *et al.*, 2005). The two levels have total nuclear spin $I=0$ or 2 and projection $m_I=0$, where $\mathbf{I}=\mathbf{I}_1+\mathbf{I}_2$. The next bound states below threshold are three $M=0$ spin components of the $v=9$ level of the $^3\Sigma_u^+$ potential, far below threshold with binding energies $\approx 24$ GHz near the bottom of the $n=-1$ bin. These deeply bound levels are associated with the large negative scattering length of $-2140a_0$ for the $S=1$ potential (Abraham *et al.*, 1997; Bartenstein *et al.*, 2005).

TABLE III. Separated atom channel labels for the five $s$-wave $M=0$ channels of $^6Li$. The $(f_1f_2)$ quantum numbers are only exact at $B=0$.

| $\alpha$ | $(f_1f_2)$ | $m_{f_1},m_{f_2}$ |
|---|---|---|
| $ab$ | $(\frac{1}{2}\frac{1}{2})$ | $+\frac{1}{2},-\frac{1}{2}$ |
| $ad$ | $(\frac{1}{2}\frac{3}{2})$ | $+\frac{1}{2},-\frac{1}{2}$ |
| $be$ | $(\frac{1}{2}\frac{3}{2})$ | $-\frac{1}{2},+\frac{1}{2}$ |
| $cf$ | $(\frac{3}{2}\frac{3}{2})$ | $-\frac{3}{2},+\frac{3}{2}$ |
| $de$ | $(\frac{3}{2}\frac{3}{2})$ | $+\frac{1}{2},-\frac{1}{2}$ |

Figure 9 shows how the channel energies and the energies of the last two $M=0$ $s$-wave bound states of the $^6Li_2$ molecule vary with magnetic field. Simonucci *et al.* (2005) gave a detailed description of the molecular physics of these multichannel bound states. At high $B$ field, $E_{ab}$ varies linearly with $B$ with a slope of nearly $dE_{ab}/dB=-2\mu_B$, where $\mu_B$ is the Bohr magneton. Since both bound states have $S=0$ character near $B=0$, their magnetic moment vanishes, i.e., $dE_c/dB=0$ near $B=0$. The $I=2$ state crosses $E_{ab}$ near $B=543$ G, where it interacts weakly with the $ab$ entrance channel and makes a very narrow Feshbach resonance, as shown in Fig. 11. On the other hand, the energy of the strongly interacting $I=0$ bound state changes dramatically above about 540 G and becomes nearly parallel to the energy of the

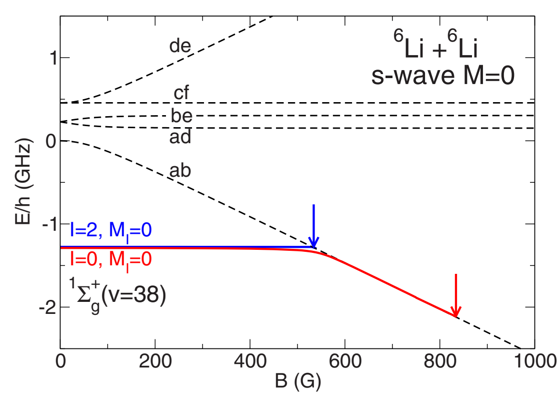


FIG. 9. (Color online) Last coupled-channel bound states of the $^6Li_2$ dimer with $M=0$. The arrows indicate the locations of the 543 and 834 G Feshbach resonances, where the binding energy of a threshold bound state equals 0. While the low $B$ field $I=2$ $^1\Sigma_g^+(v=38)$ level retains its spin character as it crosses threshold near 543 G, the $I=0$ level mixes with the entrance channel and switches near $\approx 550$ G to a bound level with $ab$ spin character, eventually disappearing as a bound state when it crosses threshold at 834 G.

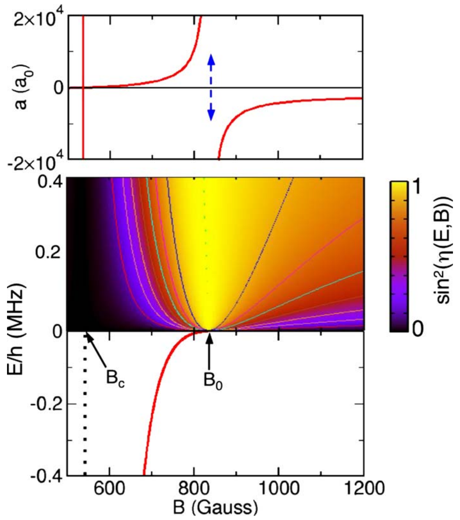


FIG. 10. (Color online) Near-threshold bound and scattering state properties of the $^6$Li *ab* channel. The upper panel shows the coupled-channel scattering length vs magnetic field $B$ using the model of Bartenstein *et al.* (2005). The double-headed arrow indicates the point of singularity $B_0$ for the broad resonance near 834 G, which is an entrance channel dominated resonance with width $\Delta = 300$ G and $s_{\text{res}} = 59$ (see Secs. II.A.3 and II.B.2). There also is a narrow resonance with a singularity near 543 G. The lower panel shows for $E < 0$ the energy of the bound state (solid line) that merges with the continuum at $B_0$. The zero of energy at each $B$ is the *ab* channel energy $E_{ab}(B)$. An energy of $E/h = 0.4$ MHz is equivalent to $E/k_B = 19$ $\mu$K. The universal bound state energy from Eq. (2) is indistinguishable on the scale of this graph from the coupled-channel bound state energy. The nearly vertical dotted line shows the energy of the bare bound state $E_c(B)$ of $^1\Sigma_g^+(v=38, I=0)$ character that crosses threshold at $B_c$ near 540 G. The shaded contour plot for $E > 0$ shows $\sin^2 \eta(E,B)$. The broad light-colored region near the point of resonance indicates the region where $\sin^2 \eta \approx 1$ and the cross section is near its maximum value limited by the unitarity property of the $S$ matrix. Since $s_{\text{res}} \gg 1$ the width $\Gamma(E)$ in Eq. (36) is larger than $E$ in the near-threshold region so that there is no above-threshold resonance feature in the collision cross section vs $E$.

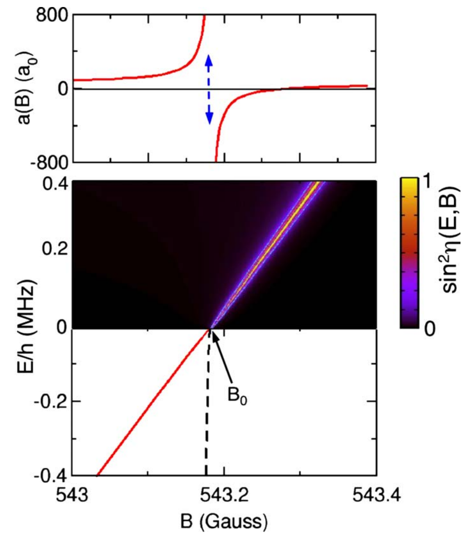


FIG. 11. (Color online) Expanded view near 543 G of Fig. 10. The upper panel shows the coupled-channel scattering length vs magnetic field strength $B$, where the double-headed arrow indicates the calculated point of singularity $B_0$ for the narrow resonance at 543.18 G with a width of $\Delta = 0.10$ G in excellent agreement with the measured resonance at 543.26(10) G (Strecker *et al.*, 2003). This is a closed channel dominated resonance with $s_{\text{res}} = 0.001$. The lower panel shows for $E < 0$ the energy of the coupled-channel bound state that merges with the continuum at $B_0$. The dashed line shows the universal bound state energy from Eq. (2). Universality does not apply for detunings over most of the width of the resonance but is only applicable in an extremely narrow range very close to $B_0$. The shaded contour plot of $\sin^2 \eta(E,B)$ for $E > 0$ shows a very narrow and sharp resonance emerging above threshold with a width $\Gamma(E) \ll E$, with a linear variation of position with $B$ and with a very small domain of unitarity of the $S$ matrix.

*ab* entrance channel. This state switches to $S=1$ character near the 540 G crossing region and transforms into the $v=10$ level of the $^3\Sigma_u^+$ potential at higher $B$. This level becomes a very weakly bound "universal" halo state of dominantly entrance channel character above around 650 G and does not disappear until it reaches the $E_{ab}$ threshold near 834 G (Bartenstein *et al.*, 2005), where it makes a very broad Feshbach resonance, shown in Fig. 10.

Figure 10 shows the near-threshold bound and scattering state properties of the $^6$Li *ab* channel between 500 and 1200 G, while Fig. 11 shows an expanded view of the narrow resonance near 543 G. The energy range is typical of the ultracold domain. The two figures illustrate two extremes of resonance behavior. The 834 G resonance is strongly open channel dominated with $s_{\text{res}} = 59$ [see Eq. (35)] and is well represented by a universal halo bound state of entrance channel character over a large fraction of its width $\Delta$. The 543.2 G resonance is strongly closed channel dominated with $s_{\text{res}} = 0.001$. It exhibits open channel character and universal behavior only over a negligible detuning range spanning at most a few $\mu$G when $B$ is tuned near $B_0$.

It is instructive to examine the wave functions for the coupled-channel bound states with the same binding energy near each resonance. For example, the binding energies in Figs. 10 and 11 are $\approx 200$ kHz near 700 and 543.1 G, respectively. We calculate that the projection $Z$ on the closed channel components, $Z = 1 - n_\alpha$, are 0.002 and 0.98 for these respective cases, where $n_\alpha = \int_0^\infty |\phi_{ab,ab}(R)|^2 dR$ is the norm of the entrance channel component $\phi_{ab,ab}(R)$ of the bound state from the coupled-channel expansion in Eq. (38). The small projection $Z$ at 700 G is in good agreement with the value measured by Partridge *et al.* (2005) (see Fig. 30). These projections for levels with the same near-threshold binding energy illustrate the very different character of entrance and closed channel dominated resonances.

The width $\Delta$ itself does not determine whether a resonance is entrance or closed channel dominated. Rather, it is necessary to apply the criterion in Eq. (35). A good example of this is provided by the bosonic $^7$Li system,

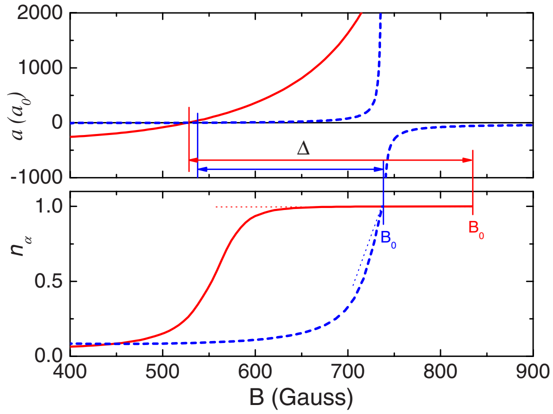


FIG. 12. (Color online) Scattering length and entrance channel fraction for the $^6$Li 834 G open channel dominated resonance (solid lines) and the $^7$Li 737 G resonance (dashed lines), which is tending toward closed channel dominance. The narrow $^6$Li resonance is not shown. The upper panel shows the scattering length $a(B)$ vs magnetic field strength $B$, whereas the lower panel shows the norm $n_\alpha(B)$ of the entrance channel spin component of the coupled-channel wave function. The vertical lines indicate the location $B_0$ of each resonance, and the horizontal double arrows indicate the width $\Delta$ of each. The dotted lines on the lower panel indicates the slope of $n_\alpha(B)=1-Z(B)$ predicted near the resonance position $B_0$ by Eq. (51) of Sec. II.C.5. While both resonances have quite large $\Delta$, the $^6$Li 834 G one is clearly "open channel dominated" with $1-Z(B)$ remaining near unity when $|B-B_0|$ ranges over half of its width. On the other hand, the 737 G $^7$Li resonance has $s_{\rm res}=0.80$ and is tending toward being "closed channel dominated" since $1-Z(B)$ drops off rapidly from unity as $|B-B_0|$ increases from resonance, with $n_\alpha(B)>0.5$ only for $|(B-B_0)/\Delta|<0.11$. Furthermore, this resonance has a universal bound state (not shown) only over a relatively small fraction of its width, with the calculated binding energy departing from Eq. (2) by 10% when $|(B-B_0)/\Delta|=0.06$.

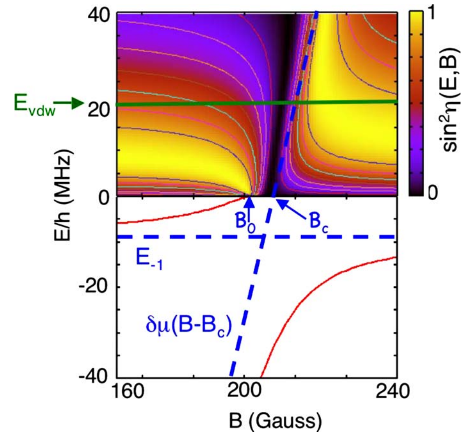


FIG. 13. (Color online) Bound states and scattering phase near the $^{40}$K *ab* 202 G resonance. The energy is between $E/h=\pm 40$ MHz ($E/k_B=\pm 1.9$ mK) where the zero of energy is taken to be the separated atom energy of an *a* and a *b* atom. The horizontal solid line shows $E_{\rm vdW}/h=21$ MHz. The horizontal dashed line shows the last bare bound state energy $E_{-1}$ of the background potential and the sloping dashed line shows the bare resonance level with energy $\delta\mu(B-B_c)$, where $\delta\mu/h=2.35$ MHz/G. The resonance width $\Delta=7.8$ G (Greiner *et al.*, 2003). The solid lines for $E<0$ indicate the coupled-channel dressed energies of the $^{10}K_2$ molecule. Away from resonance these approach the bare energies. The strong avoided crossing between the two bare states leads to the shift in the point of singularity $B_0$ from the bare crossing at $B_c$. For positive energies the interference between the background and resonant phases is evident. Since this is an open channel dominated resonance with $s_{\rm res}=2$, no sharp resonant feature appears in $\sin^2\eta(E,B)$ vs $E$ for $0<E<E_{\rm vdW}$. A sharp resonance feature only emerges when $E\gg E_{\rm vdW}$.

which has a very broad resonance in the *aa* channel near 737 G with a width of 192 G (Khaykovich *et al.*, 2002; Strecker *et al.*, 2002; Junker *et al.*, 2008; Pollack *et al.*, 2009), where *a* represents the state which correlates with the $|f=1,\ m=1\rangle$ state at $B=0$. Because the background scattering length is nearly two orders of magnitude smaller for this $^7$Li case than for the 843 G $^6$Li resonance, the $s_{\rm res}$ parameter for the $^7$Li *aa* resonance is only 0.80 instead of 59. Consequently, this broad $^7$Li resonance is tending toward closed channel dominance according to our classification scheme and only has a small region of universality spanning a few G when $B$ is tuned near $B_0$. Figure 12 shows the pronounced differences between the $^6$Li *ab* and $^7$Li *aa* resonances in spite of the similar magnitudes of their widths (see also Sec. II.C.5).

In order to illustrate the difference between the bare and dressed resonance states introduced in Sec. II.A.3. Figure 13 shows the coupled-channel bound state energies and scattering phases in the near-threshold region for the $^{40}$K *ab* channel. The *a* and *b* states correlate at $B=0$ with the $|f=\frac{9}{2},m=-\frac{9}{2}\rangle$ and $|f=\frac{9}{2},m=-\frac{7}{2}\rangle$ atomic states of fermionic $^{40}$K. This resonance was observed by Loftus *et al.* (2002) and Regal *et al.* (2003a) and has additionally been characterized by Szymanska *et al.* (2005) and Nygaard *et al.* (2006). The actual eigenstates of the dressed system (solid lines) result from the avoided crossing of the ramping closed channel bare state energy $E_c=\delta\mu(B-B_c)$ and the last bare bound state at $E_{-1}$ of the background potential (dashed lines). The shift in the location of the singularity in $a(B)$ at $B_0$ from the threshold crossing of the bare state at $B_c$ is given from Eq. (37),

$$B_0-B_c=\Delta r_{\rm bg}(1-r_{\rm bg})/[1+(1-r_{\rm bg})^2]. \qquad (42)$$

This same formula predicts the large difference between $B_0$ and $B_c$ evident in Fig. 10 for the broad $^6$Li *ab* resonance.

Finally, we give an example of resonances for a heavy species $^{87}$Rb where classification of near-threshold bound states using the electronic spin $S=0$ and 1 quantum numbers is not possible. The bin size $\approx 0.240$ GHz for the last bound state is much less than the $^{87}$Rb ground state hyperfine splitting $E_{\rm hf}/h=6.835$ GHz so that the last few bound states of the $^{87}Rb_2$ molecule are mixed by the hyperfine interaction. Figure 14 shows the coupled-channel *s*-wave bound states calculated by Marte *et al.* (2002) for channels with $M=m_1+m_2=2$, 1,

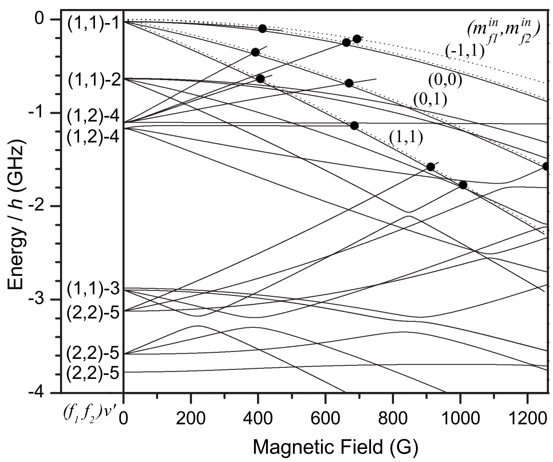


FIG. 14. Coupled-channel $^{87}$Rb $s$-wave bound states. The dotted lines show the channel energies for four different entrance channels with $f_1 = f_2 = 1$, labeled by the projection quantum numbers $(m_1, m_2)$. The bound state energies (solid lines) for these channels are shown as a function of magnetic field $B$ with quantum numbers $(f_1 f_2)n$ assigned at $B=0$, where $n$ is the vibrational quantum number in the $f_1 f_2$ channel counting down from the separated atom limit in that channel. A Feshbach resonance occurs when a bound state with quantum number $M = m_1 + m_2$ crosses a dissociation threshold having the same $M$ (solid dots). From Marte et al., 2002.

and 0. Unlike the $^6$Li case in Fig. 9, there are a number of bound states within a few GHz of threshold. The levels are labeled at $B=0$ by the spin quantum numbers $(f_1 f_2)$ of the separated atoms and the vibrational quantum number $n$ counting down from the separated atom dissociation limit. The figure shows the last three vibrational levels of the lowest $(f_1 f_2) = (11)$ separated atom limit. The $B=0$ energy of the (12) separated atom limit is $E_{\mathrm{hf}} = 6.835$ GHz and only the $n=-4$ vibrational level appears in this range. Similarly only the $n=-5$ level appears for the (22) separated atom limit. The closed channel dominated resonance ($s_{\mathrm{res}} = 0.17$) near 1007 G in the (11)$M=2$ channel has been used to make molecules in atomic gases (Dürr, Volz, Marte, and Rempe, 2004) and lattices (Thalhammer et al., 2006).

### C. Simplified models of resonance scattering

While coupled-channel models are valuable for understanding the near threshold molecular physics of scattering resonances and for highly quantitative predictive calculations for a range of $B$ field and multiple spin channels, they can be quite complicated to set up and use. Consequently, it is highly desirable to have simplified models that are accessible to experimental and theoretical researchers. Fortunately, a variety of high quality models is available, each valid over a limited domain of energy.

The key to practical approximations for the near threshold bound and scattering states for ultracold neutral atom interactions is the separation of the length and energy scales associated with the separated atoms, on the one hand, and the molecular interactions, on the other hand. The molecular interactions are characterized by various energy scales associated with the van der Waals potential, the potential at $R_{\mathrm{ex}}$, or the minimum of the potential. This scale should be compared with the hyperfine, Zeeman, and kinetic energies of the ultracold atoms. For ranges of internuclear separation $R$ where the molecular energy scale is much larger than the atomic one, the phases and amplitudes of the coupled-channel wave function components $\phi_{\alpha\beta}$ are nearly independent of energy and partial wave over an energy range on the order of the atomic scale. In effect, the short-range wave function provides an energy-independent boundary condition for connecting to the near-threshold asymptotic bound or scattering states, which are strongly energy dependent. While this separation of scales can be made explicit in methods based on long-range coupled-channel calculations (Tsai et al., 1997; van Abeelen and Verhaar, 1999a) or multichannel quantum defect methods (Julienne and Mies, 1989; Burke et al., 1998; Vogels et al., 1998; Raoult and Mies, 2004; Julienne and Gao, 2006), it remains implicit as the basis for many other approximation schemes.

A variety of simplified treatments shows that it is sufficient to use the basic framework in Sec. II.A.3 to parametrize threshold resonances in ultracold atoms. Thus, resonances are characterized by a reduced mass $\mu$, a background scattering length $a_{\mathrm{bg}}$, a tunable position $E_0$ selected by an external field, and an energy- and tuning-insensitive width $\Gamma_0$. Resonances that decay, whether by emission of light or by relaxation to lower energy open channels, can readily be treated by introducing the decay width $\gamma$ (Fedichev, Reynolds, et al., 1996; Bohn and Julienne, 1999; Köhler et al., 2005; Hutson, 2007). The review of Köhler et al. (2006) described how two-channel models can be especially effective when the resonance parameters are already known.

#### 1. Contact potential model

The simplest approximation for resonance scattering is to use the Fermi pseudopotential (Huang and Lee, 1957)

$$V(\mathbf{R}) = \frac{2\pi\hbar^2}{\mu} a(B) \delta(\mathbf{R}) \frac{\partial}{\partial R} R, \tag{43}$$

with a strength proportional to the scattering length $a(B)$. This zero-range delta-function pseudopotential is an excellent approximation for the full molecular interaction when $k|a(B)| \ll 1$ and $k\bar{a} \ll 1$ and becomes exact in the limit $E \to 0$. It can be used for positive or negative $a$, and its phase shift is $\tan \eta(E,B) = -ka(B)$. For $a>0$ it has a bound state given by the universal energy of Eq. (2).

If the resonance parameters $a_{\mathrm{bg}}$, $\Delta$, and $B_0$ are known, the effect of tuning near a resonance can then be fully incorporated using $a(B)$ from Eq. (1). For an entrance channel dominated resonance with $s_{\mathrm{res}} \gg 1$, so that the universal binding energy in Eq. (2) applies [see Eq. (32)], the scattering length is the only parameter needed to treat near-threshold bound states and scattering (Köhler *et al.*, 2006). However, more robust approximations are needed since universality will only apply for detunings that at most span a range on the order of the width $\Delta$ and can be much less, depending on $s_{\mathrm{res}}$.

### 2. Other approximations

Although the underlying molecular physics often involves a number of coupled channels, many resonances are isolated in energy and magnetic field. Then the properties of the bare resonance level are determined by energy scales large compared to the small kinetic energies of the ultracold domain and the level can be accurately approximated as coming from a single bound state channel, as in the Fano treatment summarized in Sec. II.A.3. A number of groups have developed a variety of simplified methods for characterizing the properties of ultracold scattering resonances, but we cannot review this work exhaustively or in detail. For example, Moerdijk *et al.* (1995), Timmermans *et al.* (1999), and Kokkelmans *et al.* (2002) introduced the standard Feshbach formalism of separating the system into bound and scattering subspaces, $Q$ and $P$, to characterize magnetically tunable resonances for ground state alkali-metal atoms. Góral *et al.* (2004) used a Green's function formalism and introduced a separable potential that is chosen to accurately represent the two-body scattering and bound states of the background channel. Marcelis *et al.* (2004) were especially interested in representing the case of a large negative $a_{\mathrm{bg}}$, which is relevant to the $^{85}$Rb system. Mies *et al.* (2000) used the resonances of two $^{23}$Na atoms to show how to reduce a coupled five-channel problem to an effective two-channel problem using a Lennard-Jones pseudopotential with the correct van der Waals coefficient. Nygaard *et al.* (2006) illustrated this method for the $^{40}$K system.

One model that shows great promise for practical and accurate fitting of resonance data is the asymptotic bound state model based on the work of Moerdijk *et al.* (1995). Rather than solving for the bound states of a set of coupled equations in order to locate resonance positions, it uses an expansion in the last bound states of the Born-Oppenheimer potentials. The model is far less computationally demanding than full coupled-channel calculations. Stan *et al.* (2004) used a simplified version of this model to characterize measured resonances due to the triplet molecular state in the $^6$Li+$^{23}$Na system. Recently, Wille *et al.* (2008) used this model to quantitatively characterize a number of resonances of $^6$Li+$^{40}$K that involved strong mixing of the singlet and triplet molecular states.

### 3. van der Waals resonance model

By introducing the van der Waals $C_6$ coefficient as an additional model parameter, the properties of bound and scattering states can be extended away from their very near-threshold domain into the domain where $k\bar{a} \gg 1$ and the binding energy is much larger than $E_{\mathrm{vdW}}$ or $\bar{E}$. The reason is that there is a large range of $R$, namely, $R_{\mathrm{ex}} < R < R_{\mathrm{vdW}}$, where the potential is accurately represented as $-C_6/R^6$ and is much larger in magnitude than $E_{\mathrm{vdW}}$. The properties of the van der Waals potential have been discussed in Sec. II.B.1.

Feshbach resonances are characterized by a width $\Gamma(E)$ and shift $\delta E(E)$. These are given in the $E \to 0$ limit by Eqs. (36) and (37), which depend on the dimensionless resonance strength $s_{\mathrm{res}}$ and $r_{\mathrm{bg}}$. The $E\to 0$ result can be generalized to finite energy by introducing two standard functions $C_{\mathrm{bg}}(E)^{-2}$ and $\tan\lambda_{\mathrm{bg}}(E)$ of multichannel quantum defect theory (MQDT) (Julienne and Mies, 1989; Mies and Raoult, 2000; Raoult and Mies, 2004),

$$\tfrac{1}{2}\Gamma(E) = \tfrac{1}{2}\bar{\Gamma} C_{\mathrm{bg}}(E)^{-2}, \tag{44}$$

$$\delta E(E) = \tfrac{1}{2}\bar{\Gamma} \tan \lambda_{\mathrm{bg}}(E), \tag{45}$$

where for the van der Waals background potential (Julienne and Gao, 2006)

$$\frac{\bar{\Gamma}}{2} = (\bar{E} s_{\mathrm{res}}) \frac{1}{1+(1-r_{\mathrm{bg}})^2} = \Gamma_0 \frac{r_{\mathrm{bg}}}{1+(1-r_{\mathrm{bg}})^2} \tag{46}$$

is proportional to $s_{\mathrm{res}}$ and is independent of energy. The MQDT functions have the following limiting form as $E\to 0$: $C_{\mathrm{bg}}(E)^{-2} = k\bar{a}[1+(1-r_{\mathrm{bg}})^2]$ and $\tan\lambda_{\mathrm{bg}}(E) = 1-r_{\mathrm{bg}}$. When $E \gg \bar{E}$, $C_{\mathrm{bg}}(E)^{-2} \to 1$ and $\tan\lambda_{\mathrm{bg}}(E) \to 0$. Consequently, $\Gamma(E)=\bar{\Gamma}$ and $\delta E(E)$ vanishes when $E$ becomes large compared to $\bar{E}$. If $|r_{\mathrm{bg}}| \gg 1$, the $C_{\mathrm{bg}}(E)^{-2}$ function has a maximum as a function of $E$ and $|\tan\lambda_{\mathrm{bg}}(E)|$ has decreased to half its $E=0$ value at $E \approx \hbar^2/[2\mu(a_{\mathrm{bg}}-\bar{a})^2]$.

The functions $C_{\mathrm{bg}}(E)$ and $\tan\lambda_{\mathrm{bg}}(E)$, as well as $\eta_{\mathrm{bg}}(E)$, depend on only three parameters, $C_6$, $\mu$, and $a_{\mathrm{bg}}$ (Julienne and Gao, 2006). The near-threshold phase $\eta(E)$ in Eq. (16) can be evaluated over a wide range of energy on the order of $\bar{E}$ and larger from a knowledge of these three parameters plus $s_{\mathrm{res}}$, the magnetic moment difference $\delta\mu$, and the resonant position $B_0$. The $\sin^2\eta(E,B)$ function evaluated using Eqs. (44) and (45) is virtually indistinguishable from the coupled-channel results shown in Figs. 10–13.

### 4. Analytic two-channel square well model

A very simple square well model, because it is analytically solvable, can capture much of the physics of near-threshold bound and scattering states. Bethe (1935) used such a model to successfully explain the threshold scattering of cold neutrons from atomic nuclei, where the neutron de Broglie wavelength was very large compared to the size of the nucleus. Kokkelmans *et al.* (2002) and Duine and Stoof (2004) introduced two-channel square well models to represent Feshbach resonances in ultracold atom scattering.

Figure 15 shows the bare background and closed channel potentials for a square well model where for convenience of analysis we take the width of the wells to be the van der Waals length $\bar{a}$. The background entrance

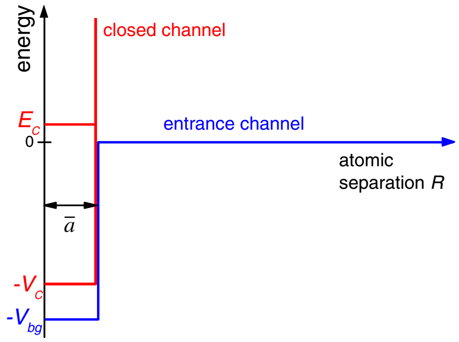


FIG. 15. (Color online) Two-channel square well model of a magnetic Feshbach resonance. The potential for the bare entrance background channel has a well depth $-V_{\mathrm{bg}}$. The spatial width is chosen to be $\bar{a}$ so as to simulate the length scale of a van der Waals potential. The potential for the bare closed channel has a well depth $-V_c$ relative to the separated atoms and is infinite for $R>\bar{a}$. The value of $V_{\mathrm{bg}}$ is chosen so that the background scattering length is $a_{\mathrm{bg}}$. The value of $V_c$ is chosen so that there is a bound state with energy $E_c$ near $E=0$. We assume that this energy varies with magnetic field as $E_c=\delta\mu(B-B_c)$, where $\delta\mu$ is a relative magnetic moment and $E_c=0$ at $B=B_c$.

channel and the closed channel are designated by $|\mathrm{bg}\rangle$ and $|c\rangle$, respectively. Using a two-state coupled-channel expansion as in Eq. (38), $|\psi(R,E)\rangle=|c\rangle\phi_c(R,E)/R+|\mathrm{bg}\rangle\phi_{\mathrm{bg}}(R,E)/R$, the potential matrix in Eq. (40) is

$$\mathbf{V}=\begin{cases}\begin{pmatrix}-V_c & W\\ W & -V_{\mathrm{bg}}\end{pmatrix} & \text{for } R<\bar{a}\\ \begin{pmatrix}\infty & 0\\ 0 & 0\end{pmatrix} & \text{for } R>\bar{a}.\end{cases} \tag{47}$$

The off-diagonal matrix element $W$ describes the weak coupling between the two channels.

In order to simulate a magnetically tuned Feshbach resonance, the model parameters need to be chosen so as to give the correct parameters for that resonance. The well depth $V_{\mathrm{bg}}$ is chosen so that the background channel scattering length is $a_{\mathrm{bg}}$. The well depth $V_c$ is chosen so that the well has a bare bound state at $E_c$. The tuning of the bound state as $E_c=\delta\mu(B-B_c)$ can be simulated by varying $V_c$ linearly with the external magnetic field $B$. Finally, weak coupling requires $|W|\ll|V_{\mathrm{bg}}-V_c|$. The coupling parameter $W$ can then be chosen to give the right resonance width $\Gamma(E)=2ka_{\mathrm{bg}}\delta\mu\Delta$ at low energies [see Eq. (17)] using the known resonance width $\Delta$. Analytically calculating the matrix element defining $\Gamma(E)$ in Eq. (14) relates $W$ to $\Delta$ as follows:

$$2V_cW^2/(V_{\mathrm{bg}}-V_c)^2=[r_{\mathrm{bg}}/(1-r_{\mathrm{bg}})^2]\delta\mu\Delta. \tag{48}$$

With the chosen parameters, the square well model yields analytic forms for the scattering phase shift as in Eq. (16) and the scattering length as in Eq. (1).

The square well model also permits an analytic evaluation of the weakly bound state below the continuum. Assuming an eigenstate $|\psi_b\rangle$ exists at energy $-E_b=-\hbar^2k_b^2/(2\mu)<0$ and $|a_{\mathrm{bg}}|\gg\bar{a}$, we get

$$k_b=\frac{1}{a_{\mathrm{bg}}-\bar{a}}+\frac{\Gamma_{\mathrm{sq}}/2}{\bar{a}(E_b+E_c)}, \tag{49}$$

where $\Gamma_{\mathrm{sq}}/2=\delta\mu\Delta r_{\mathrm{bg}}(1-r_{\mathrm{bg}})^{-2}$. Marcelis *et al.* (2004) derived a similar result for a contact potential. Note that when the coupling term $W\to 0$ so that $\Gamma_{\mathrm{sq}}\to 0$, the solutions $E_b=-E_c$ and $E_b=\hbar^2/[2\mu(a_{\mathrm{bg}}-\bar{a})^2]$ correspond to the bare states of the square well in the closed and open channel (for $a_{\mathrm{bg}}>\bar{a}$) as expected. Since the resonant singularity in the scattering length occurs when $E_b\to 0$, taking this limit of Eq. (49) allows us to calculate the resonance energy shift $\delta E=\delta\mu(B_0-B_c)$ as

$$\delta E=\Gamma_{\mathrm{sq}}(1-r_{\mathrm{bg}})/2. \tag{50}$$

Both Eqs. (50) and (49) can also be derived from the van der Waals model with $\Gamma_{\mathrm{sq}}$ replaced by $\bar{\Gamma}=\Gamma_{\mathrm{sq}}[1+(r_{\mathrm{bg}}-1)^{-2}]$. Note that $\Gamma_{\mathrm{sq}}$ and $\bar{\Gamma}$ are nearly the same for $|r_{\mathrm{bg}}|\gg 1$. The modified version of Eq. (50) is equivalent to Eqs. (37) and (42), derived from the van der Waals model.

Lange *et al.* (2009) extended the above model to precisely determine the scattering length and the resonance parameters in the magnetic field regime where multiple Feshbach resonances overlap.

### 5. Properties of Feshbach molecules

A variety of properties of Feshbach molecules can be calculated by solving Eq. (49) for the binding energy $E_b$. For example, the closed channel fraction $Z$ of the eigenstate can be found by differentiating $E_b$ with respect to $E_c$ [see Eq. (28)]. In the limit $B\to B_0$ where $E_b$ vanishes and $a\to+\infty$, we have

$$Z=\frac{1}{\zeta}\left|\frac{B-B_0}{\Delta}\right|, \tag{51}$$

where the dimensionless proportionality constant

$$\zeta=\frac{1}{2}s_{\mathrm{res}}|r_{\mathrm{bg}}|=\frac{r_{\mathrm{bg}}^2}{2}\frac{|\delta\mu\Delta|}{\bar{E}} \tag{52}$$

determines the rate at which the Feshbach molecular state deviates from the entrance channel dominated regime or, equivalently, the halo molecule regime, when $B$ is tuned away from $B_0$. Equation (51) shows that having a small closed channel fraction $Z\ll 1$ requires the magnetic field to be close to resonance, $|B-B_0|\ll\zeta|\Delta|$. Figure 12 of Sec. II.B.5 compares $1-Z$ from Eq. (51) for the respective open and closed channel dominated $^6$Li 834 G and $^7$Li 737 G resonances.

For open channel dominated resonances, where $s_{\mathrm{res}}\gg 1$, it is usually true that $|r_{\mathrm{bg}}|\geqslant 1$ and $\zeta\gg 1$, and $Z$ remains small over a large fraction of the resonance width $\Delta$. The bound state wave function takes on primarily entrance channel character over this range (see the examples of the $^6$Li 834 G or $^{40}$K 202 G resonances in Fig. 16). Closed channel dominated resonances have $s_{\mathrm{res}}\ll 1$ and small $\zeta\ll 1$. Consequently, $Z$ remains small only over a small range of the resonance (see the example of

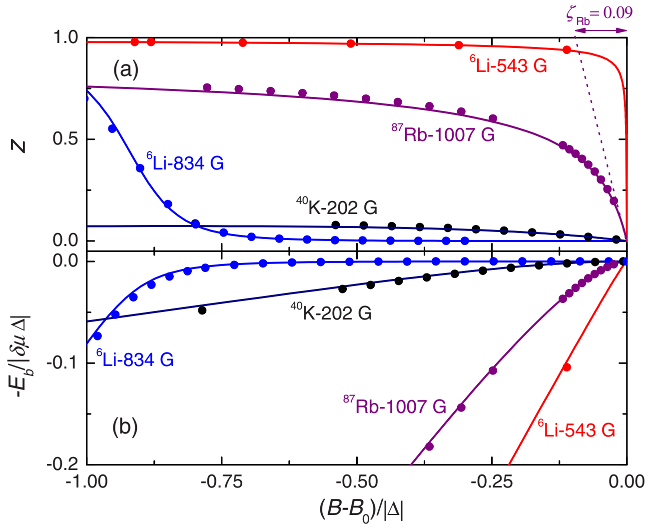


FIG. 16. (Color online) Closed channel fraction (a) and energy (b) of weakly bound molecular states as a function of magnetic field for selected Feshbach resonances. The dots are from coupled-channel calculations as described in Sec. II.B.3. The solid curves are calculated based on Eq. (49), Eq. (28), and the parameters given in the Appendix. The slope of $Z$ at $B=B_0$ defines the $\zeta$ parameter; an example for the $^{87}$Rb 1007 G resonance is shown as the dashed line with $\zeta_{\mathrm{Rb}}=0.09$. This $^{87}$Rb resonance and the $^6$Li 543 G one are closed channel dominated and have $s_{\mathrm{res}},\zeta<1$. The $^6$Li 834 G and the $^{40}$K 202 G resonances are open channel dominated resonances with $s_{\mathrm{res}},\zeta>1$.

the $^{87}$Rb 1007 G or $^6$Li 543 G resonances in Fig. 16). A small $\zeta_{\mathrm{Rb}}=0.09$ for the Rb 1007 G resonance implies that the molecular state is entrance channel dominated only within ~9% of the resonance width. In the Appendix $\zeta$ is listed for several other resonances.

Expanding Eq. (49) at small binding energies, the molecular binding energy has the following form in the threshold limit:

$$E_b=\hbar^2/[2\mu(a-\bar{a}+R^*)^2], \tag{53}$$

where $R^*=\bar{a}/s_{\mathrm{res}}$. This expression applies in the limit that $a\gg\bar{a}$ and $a\gg 4R^*$. The binding energy $E_b$ shows two corrections to the universal $1/a^2$ threshold law in Eq. (2). One is the finite range correction $\bar{a}$ shown in Eq. (32); the other one, $R^*$, introduced by Petrov (2004), is unique to Feshbach resonances. The correction $R^*$ is negligibly small for open channel dominated resonances with $s_{\mathrm{res}}\gg 1$. Closed channel dominated resonances can have large $R^*\gg\bar{a}$. Such resonances only have a regime with a bound state of predominant entrance channel character near $B_0$ where $a\gg 4R^*$. This condition is consistent with the one given previously, namely, $|B-B_0|\ll\zeta|\Delta|$.

## III. FINDING AND CHARACTERIZING FESHBACH RESONANCES

Magnetically tunable Feshbach resonances have been experimentally observed in essentially all alkali-metal species, in some mixtures of different alkali-metal atoms, as well as for Cr atoms. Experimental data on the resonance positions have in many cases enabled the construction of accurate models to describe the near-threshold behavior, including scattering properties and molecular states. We first review the various experimental approaches to identify and characterize Feshbach resonances in Sec. III.A and then discuss observations of Feshbach resonances for alkali-metal atoms in Sec. III.B and various other systems in Sec. III.C.

### A. Experimental methods

Experimental approaches to detect magnetic Feshbach resonances can be classified into several types. After some general considerations in Sec. III.A.1, we will discuss detection by inelastic collisional trap loss in Sec. III.A.2, by elastic collision properties in Sec. III.A.3, and by loss in the presence of optical radiation in Sec. III.A.4. Finally, Sec. III.A.5 discusses precision radiofrequency spectroscopy of Feshbach molecules.

#### 1. General considerations

*a. What is the magnetic field range to be explored?*

The typical spacing between two Feshbach resonances can be estimated from the ratio of the energy splitting between closed channel molecular levels and the relative magnetic moment $\delta\mu$ between the entrance channel and the closed channel. The vibrational energy splitting between near-threshold bound states is determined by the long-range van der Waals potential to be on the order of $100E_{\mathrm{vdW}}$ (see Sec. II.B.1). For alkali-metal atoms $\delta\mu$ is on the order of two Bohr magneton $2\mu_B=2.8$ MHz/G and six times larger for $^{52}$Cr. For atoms with a small hyperfine splitting compared to $100E_{\mathrm{vdW}}$, Feshbach resonances are induced by the last bound states. This leads to a typical $s$-wave Feshbach resonance separation of ~10 000 G for $^6$Li and ~100 G for $^{52}$Cr. For atoms with hyperfine splittings much larger than $100E_{\mathrm{vdW}}$, resonances can be induced by much deeper bound states in the closed channel (see Fig. 14 for $^{87}$Rb), and the expected spacings can be estimated accordingly.

The density of Feshbach resonances increases when higher partial wave scattering and multiple closed hyperfine channels, defined in Sec. II.B.3, are included. The relevant number of channels is determined by the angular momentum dependence of the molecular potentials and identical particle statistics. For alkali-metal atoms there are on the order of ten closed channels for the lowest partial wave $\ell=0$. The number of channels increases rapidly for higher partial waves. The ultralow temperature usually limits scattering to $s$- and sometimes $p$-wave entrance channels, but coupling to molecular states with up to $\ell_c=4$ has been observed (see Tables II and IV).

For species without unpaired electrons, e.g., Sr and Yb, one expects no or limited magnetic tunability because there is no electron contribution to the magnetic moment and the nuclear contribution is very small. In these systems, Feshbach resonances can possibly be optically induced (see Sec. VI.A).

*b. What is the required magnetic field resolution?*

The width of the resonance generally determines the magnetic field resolution required for detection. Many $s$-wave Feshbach resonances have widths larger than 1 G (see the Appendix). High partial wave Feshbach resonances are typically much narrower because of the weaker Feshbach coupling strength. Usually, a resolution in the milligauss range is required to detect $d$- or $g$-wave Feshbach resonances.

*c. How to trap atoms for collision studies?*

Optical dipole traps, reviewed by Grimm *et al.* (2000), are the main tool to confine cold atoms for collision studies related to Feshbach resonances. Optical potentials trap atoms in any sublevel of the electronic ground state and permit investigation of collisions in any corresponding spin channel. For many experimental applications, the lowest atomic state is of particular interest, which is a high-field seeking state and can therefore not be trapped magnetically. Optical dipole traps allow for the application of arbitrary homogenous magnetic fields without affecting the trapping potential. In contrast, magnetic traps can only confine atoms in low-field seeking states, and the application of a magnetic bias field for Feshbach tuning can strongly influence the trap parameters. This limits the application of Feshbach tuning in magnetic traps to very few situations.

*d. How low a temperature is needed to observe the resonances?*

In most experiments, a temperature of a few $\mu$K is sufficiently low to observe a clear resonant structure in inelastic collisional loss. Collision studies can be performed with thermal samples, BECs, or degenerate Fermi gases. Elastic collision measurements are more complex. Enhancement of elastic collision rates near Feshbach resonances is more prominent at lower temperatures $<1$ $\mu$K. On the other hand, suppression of elastic collision rates due to a zero crossing of the scattering length can be easily seen well above 1 $\mu$K (see Sec. III.A.3).

**2. Inelastic loss spectroscopy**

Resonant losses are the most frequently observed signatures of Feshbach resonances in cold atom experiments. These losses can be induced by two- or three-body processes. Loss occurs because of the release of internal energy into the motion when colliding atoms end up in a lower internal state or when a molecule is formed. The gain in kinetic energy is on the order of the Zeeman energy, the hyperfine energy, or the molecular vibrational energy, depending on the inelastic channel, and is generally so large that all atoms involved in the collisions are lost. Near a Feshbach resonance, inelastic loss is strongly enhanced because the Feshbach bound states have strong couplings to inelastic outgoing channels.

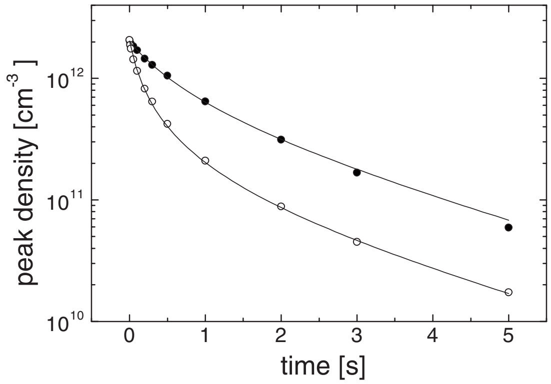


FIG. 17. Time evolution of the peak atomic density in a cloud of $^{133}$Cs atoms in the $|f=4,m=-4\rangle$ state at $T=5.3$ $\mu$K. The solid circles show the off-resonant evolution at $B=140$ G, whereas the open circles show the on-resonant evolution at $B=205$ G (open circles), where a Feshbach resonance is located. The fit is based on Eq. (55) with $L_3=0$ and the peak density corresponds to $2\sqrt{2}\bar{n}$. From Chin, Vuletić, *et al.*, 2004.

Two- and three-body collision losses can be quantified based on the evolution of the atom number $N(t)$, which for a single species satisfies

$$\dot{N}(t) = -\frac{N(t)}{\tau} - \int [L_2 n^2(\mathbf{r},t) + L_3 n^3(\mathbf{r},t)] d^3r, \tag{54}$$

where $\tau$ is the one-body lifetime, typically determined by background gas collisions, $n(\mathbf{r},t)$ is the position- and time-dependent atomic density distribution, and $L_2$ ($L_3$) is the thermally averaged two-body (three-body) loss coefficient.

The loss equation can be further simplified under the assumption that thermalization is much faster than inelastic loss. For example, for a thermal cloud with temperature $T$ in a three-dimensional (3D) harmonic trap, one finds

$$\dot{\bar{n}}(t) = -\frac{\bar{n}(t)}{\tau} - L_2 \bar{n}(t)^2 - (4/3)^{3/2} L_3 \bar{n}(t)^3, \tag{55}$$

where $\bar{n} = N\bar{\omega}^3(4\pi k_B T/m)^{-3/2}$ is the mean density; $m$ is the atomic mass and $\bar{\omega}$ is the geometric mean of the three trap vibrational frequencies. Examples of density-dependent loss curves are shown in Fig. 17.

The trap loss coefficient $L_2$ is related to the inelastic loss coefficient in Sec. II.A.2 by $L_2 = K_{\text{loss}}(T)$, where we have assumed that both atoms are lost in one collision event. Near a Feshbach resonance, $L_2$ is enhanced and has a Lorentzian profile at low temperatures (see Sec. II.A.3 for more details on inelastic scattering resonances). Two-body collision loss has been observed in many cold atom system (see Fig. 18 for an example).

Three-body loss, as described by the loss coefficient $L_3$ in Eq. (54), is also strongly enhanced near Feshbach resonances. In many experiments cold atoms are polarized in the lowest ground state and two-body inelastic

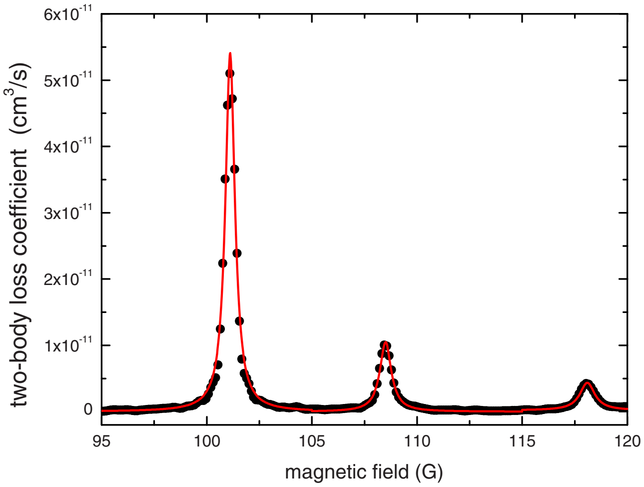


FIG. 18. (Color online) Two-body inelastic loss coefficient of cesium atoms in the $|f=3,m=-3\rangle$ state as a function of magnetic field. The loss coefficient is extracted from the atomic density evolution, as shown in Fig 17. Three resonances are identified here. The solid line is a Lorentzian fit. From Chin, Vuletić, *et al.*, 2004.

collisions (in the *aa* channel) do not occur so that three-body recombination loss is the dominant trap loss process. Three-body recombination occurs when three atoms interact and form a diatomic molecule and a free atom. In this process, the molecular binding energy is released into the kinetic energies of the outgoing molecule and the third atom, which except for very small molecular binding energies leads to immediate trap loss.

In the first experimental report on atomic Feshbach resonances, Inouye *et al.* (1998) observed very fast trap loss of a sodium BEC near a Feshbach resonance. In this experiment, three-body recombination is the leading trap loss process. Recombination losses induced by Feshbach resonances have been observed and studied in numerous later experiments, for example, by Roberts *et al.* (2000) on $^{85}$Rb, by Marte *et al.* (2002) and Smirne *et al.* (2007) on $^{87}$Rb, and by Weber *et al.* (2003a) on $^{133}$Cs.

For bosonic atoms with large scattering length $a \gg \bar{a}$ and low temperatures, $L_3$ scales generally as $a^4$ (Fedichev, Reynolds, *et al.*, 1996; Esry *et al.*, 1999; Nielsen and Macek, 1999; Braaten and Hammer, 2006) but with additional quantum features (resonance and interference effects) as discussed in Sec. VI.C on Efimov physics. For fermionic atoms the situation is more complicated because of Pauli suppression effects (see Sec. IV.B), but generally a loss feature accompanies a Feshbach resonance.

#### 3. Elastic collisions

Elastic collisions refer to scattering processes in which the colliding atoms only change their motional state but not the internal state. The cross section $\sigma_{\mathrm{el}}$ for elastic *s*-wave collisions follows from Eq. (6). Neglecting the effective range correction [$r_0=0$ in Eq. (5)], one obtains the simple expression

$$\sigma_{\mathrm{el}}(E) = g4\pi a^2/(1+k^2a^2), \tag{56}$$

where $a$ depends on magnetic field $B$ and $g$ is the symmetry factor introduced in Sec. II.A.2. Near a Feshbach resonance, the scattering length becomes very large. The elastic *s*-wave cross section is $g4\pi a^2$ at very low energy as $k\to 0$ and approaches its upper bound $g4\pi/k^2$ in the unitarity limit at finite $k$ where $ka \gtrsim 1$. The latter can be reached in the $\mu$K regime if $a$ becomes very large.

A strong enhancement of the thermally averaged elastic collision rate $n\langle\sigma_{\mathrm{el}}v\rangle$ can indicate the occurrence of a Feshbach resonance. One experimental approach is to measure the thermalization rate, which is proportional to the elastic collision rate as $\kappa n\langle\sigma_{\mathrm{el}}v\rangle$. Here $\kappa$ are numerically calculated as 2.7 in the low temperature $k\to 0$ limit (Monroe *et al.*, 1993) and 10.5 in the unitarity limit (Arndt *et al.*, 1997). Similarly, DeMarco *et al.* (1999) found $\kappa=4.1$ for *p*-wave collisions in Fermi gases. Finding Feshbach resonances based on analyzing thermalization rates was reported by Vuletić *et al.* (1999) on $^{133}$Cs atoms and by Loftus *et al.* (2002) on $^{40}$K.

Near a resonance the thermalization rate can be limited under hydrodynamic conditions, which are reached when the cross section is so large that the collision rate in the trap exceeds the trap frequency (Vuletić *et al.*, 1999). The maximum collision rate is also bounded by the unitarity limit when $a$ is large. In both cases resonance structure that is due to elastic scattering can become less evident near $B_0$.

Another efficient method to identify Feshbach resonances based on elastic collisions is to locate the zero crossing of the scattering length, that is, the magnetic field for which the scattering length vanishes near resonance where $B=B_0+\Delta$ [see Eq. (1)]. This can be monitored by measuring atom loss resulting from elastic collisions during the process of evaporation. Thermalization and evaporation loss are suppressed at the zero crossing. Schemes to locate the zero crossing have been applied to $^{85}$Rb by Roberts *et al.* (1998), $^{133}$Cs by Chin *et al.* (2000), $^{40}$K by Loftus *et al.* (2002), $^{6}$Li by Jochim *et al.* (2002) and O'Hara, Hemmer, *et al.* (2002), and $^{40}$K-$^{87}$Rb mixture by Zaccanti *et al.* (2006). An example is shown in Fig. 19. While the zero crossing is evident, no resonance feature is seen near $B_0=834$ G.

Finally, resonant changes of elastic scattering can also be revealed through the detection of collision shifts in atomic clock experiments (Marion *et al.*, 2004) and by measurements of the mean-field interaction in Bose-Einstein condensates (Inouye *et al.*, 1998; Cornish *et al.*, 2000; Regal *et al.*, 2003b) (see discussion in Sec. IV.A.2).

#### 4. Radiative Feshbach spectroscopy

Radiative Feshbach spectroscopy makes use of red- or blue-detuned light to detect the variation of the collisional wave function near a Feshbach resonance. The amplitudes of both the open and closed channel compo-

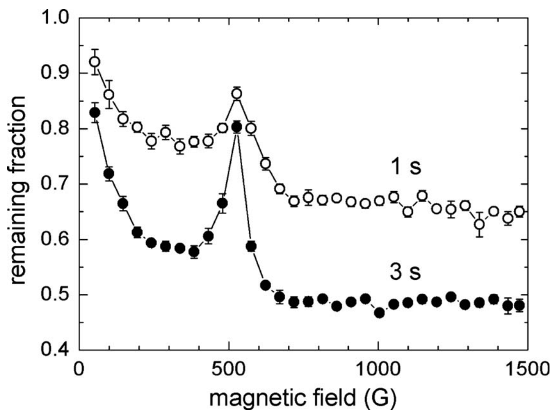


FIG. 19. Fraction of trapped atoms remaining after evaporation of $^6$Li atoms in an optical dipole trap after 1 s (open circles) and 3 s (closed circles) hold times. The peak near 530 G indicates a minimum of evaporative loss. This minimum results from the zero crossing of the scattering length induced by the broad 834 G Feshbach resonance. From Jochim *et al.*, 2002.

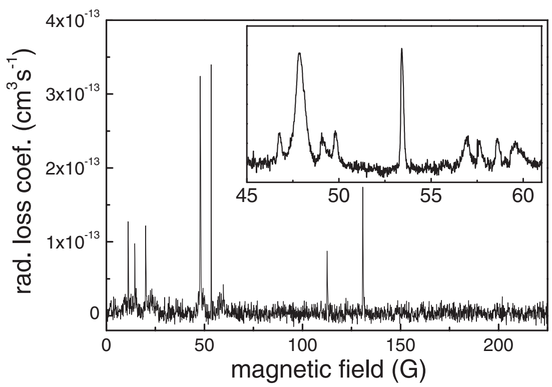


FIG. 20. Radiatively induced atom loss vs magnetic field due to a far blue-detuned laser beam applied to a sample of $^{133}$Cs atoms confined in an optical dipole trap at a temperature of 3 $\mu$K. The laser wavelength is tuned 5 nm above the free atomic transition to excite the colliding atoms to a repulsive molecular state. Once excited, the atoms quickly dissociate and are lost from the trap. Multiple narrow Feshbach resonances were observed. The inset shows an expanded view with more resonances resolved. From Chin *et al.*, 2003.

nents of the wave function are strongly modified for distances on the order of or less than $\bar{a}$ when $B$ is tuned near resonance. This is evident for the closed channel component since the outer turning point will be on the order of $\bar{a}$ (see Sec. II.B.1). The optical transition induces loss of atoms by excitation of atom pairs at such separations.

Courteille *et al.* (1998) adopted the idea of radiative spectroscopy to identify a Feshbach resonance in $^{85}$Rb. In this experiment, a photoassociation laser beam (Jones *et al.*, 2006) is held at a fixed frequency to the red of the strong $S \rightarrow P$ atomic transition and serves as a sensitive probe to measure the resonance position $B_0$. The light excites the colliding pair of atoms to an excited molecular level in a state with an attractive potential. The excited level decays by spontaneous emission, giving rise to atom loss. The experiment monitors the atom loss as $B$ is varied near $B_0$, thus locating the resonance.

In contrast, Chin *et al.* (2003) applied a laser with far blue detuning to detect Feshbach resonances in cesium samples. The blue-detuned light excites a molecular state with a repulsive potential so that the atoms are repelled, accelerated from one another, and lost from the trap. This method requires less detailed knowledge of molecular structure than the previous method. In this experiment, multiple narrow $p$-, $d$-, $f$-, and $g$-wave resonances were identified in two different collision channels of cesium atoms (see Fig. 20).

#### 5. Binding energy measurements

The detection methods discussed previously provide good ways to determine the existence of resonances and their positions. Measurements of the magnetic-field-dependent binding energies of near-threshold Feshbach molecules can yield information to precisely determine the scattering properties near a specific resonance (see Fig. 2 and Sec. II.C.5).

Regal *et al.* (2003a) and Bartenstein *et al.* (2005) employed rf spectroscopy on Feshbach molecules to measure very small molecular binding energies. An example of the rf spectroscopy is shown in Fig. 21. In this experiment, weakly bound molecules are first prepared near the Feshbach resonance (see Sec. V.A). An rf field is then applied to drive either a "bound-free" transition, which dissociates the molecules, or a "bound-bound" transition, which converts them into a different molecular state. Based on the line-shape functions calculated by Chin and Julienne (2005), binding energy of Feshbach molecules can be measured to 1 kHz. These kind of precise data can be combined with theoretical modeling to determine the position and the width of the resonance.

Other efforts to spectroscopically probe weakly bound states include oscillating magnetic field spectroscopy employed by Thompson *et al.* (2005a) and Papp and Wieman (2006) and rf and microwave techniques by Mark, Ferlaino, *et al.* (2007) and Zirbel, Ni, Ospelkaus, Nicholson, *et al.* (2008). Using the theoretical models described in Sec. II.C.4 Lange *et al.* (2009) showed how Feshbach resonance parameters can be extracted from molecular binding energy measurements.

### B. Homonuclear alkali-metal systems

Feshbach resonances have been found and characterized in essentially all single-species alkali-metal systems. The scattering properties show vast differences between the various species and also between different isotopes of the same species. Each system is unique and has particular properties. Here we give a brief account for each species or isotope, ranging from first observations to the best current knowledge, and we discuss the characteristic properties. A table of important resonances can be found in the Appendix.

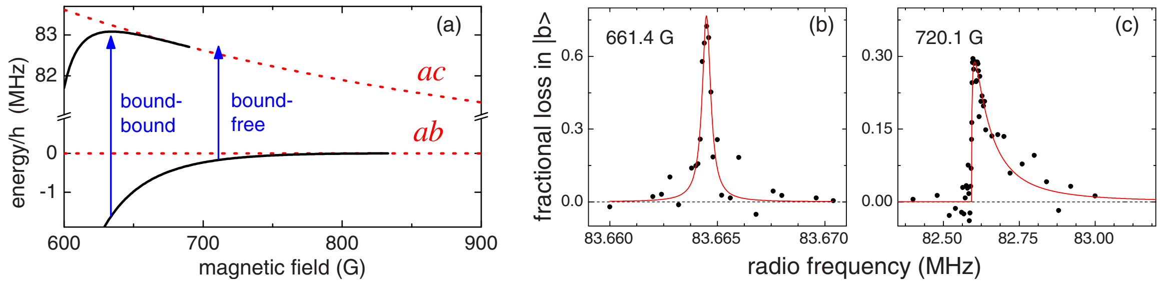


FIG. 21. (Color online) Investigation of Feshbach resonances in the lowest two scattering channels in $^6$Li with radio-frequency (rf) spectroscopy on ultracold molecules. In this experiment, $10^5$ molecules, initially prepared in the *ab* channel and confined in a dipole trap, are radiatively excited to the *ac* channel. The rf excitation line shape shows a markedly different behavior below and above 690 G. (a) The molecular bound state (solid) and channel energies (dotted) for the two channels. Below 690 G, a weakly bound state exists in the *ac* channel, and a bound-bound transition is possible (arrow). Above 690 G, no weakly bound state exists in the *ac* channel, and only a bound-free transition that dissociates the molecules is possible (blue arrow). (b) The observed narrow and symmetric bound-bound excitation line shape at 661.4 G. (c) The observed broad and asymmetric bound-free line shape at 720.1 G. The disappearance of a bound state in *ac* indicates that a Feshbach resonance occurs in this channel. Adapted from Bartenstein *et al.*, 2005.

**1. Lithium**

Lithium has two stable isotopes, one fermionic ($^6$Li) and one bosonic ($^7$Li).

$^6$Li—In 1998 Houbiers *et al.* (1998) predicted Feshbach resonances in cold collisions of fermionic $^6$Li. Experimental evidence for a prominent resonance was established by monitoring inelastic decay (Dieckmann *et al.*, 2002) and elastic collision properties (Jochim *et al.*, 2002; O'Hara, Hemmer, *et al.*, 2002). These experiments showed large variations in loss and thermalization rates as a function of the magnetic field strength for equal mixtures of the lowest two hyperfine ground states *a* and *b* prepared in an optical dipole trap. Because of the fermionic nature of $^6$Li even partial-wave scattering and, in particular, *s*-wave scattering only occur between atoms in unlike hyperfine states. Consequently, if the gas is sufficiently cold such that the $\ell > 0$ centrifugal barriers are higher than the temperature of the gas, *s*-wave collisions in the *ab* channel represent the essential thermalization mechanism. Jochim *et al.* (2002) and O'Hara, Hemmer, *et al.* (2002) reported a strongly suppressed thermalization rate near 530 G, indicating the zero crossing of the scattering length in the *ab* channel. Most recently, Du *et al.* (2008) located the zero crossing to $527.5 \pm 0.2$ G. Dieckmann *et al.* (2002) observed enhanced inelastic loss near 680 G, about 150 G below the actual resonance location ($B_0 = 834$ G). Note that this particular resonance is extraordinarily broad ($\Delta \approx -300$ G). Further experiments by Bourdel *et al.* (2003) and Gupta *et al.* (2003) provided confirmation of this Feshbach resonance.

In order to further pinpoint the resonance position, Bartenstein *et al.* (2005) conducted radio-frequency spectroscopy on Feshbach molecules in the *ab* channel as described in Sec. III.A.4. The resonance could be located with an uncertainty of 1.5 G, more than two orders of magnitude smaller than its width. Broad resonances in two other entrance channels (*ac* and *bc*) were reported as well.

Strecker *et al.* (2003) identified a narrow *s*-wave resonance at 543.25 G in the *ab* channel and Zhang *et al.* (2004) and Schunck *et al.* (2005) observed three *p*-wave resonances near 200 G, one in each of the channels *aa*, *ab*, and *bb*. All of these observed resonances are induced by *s*- and *p*-wave rotational levels of the $v = 38$ bound state of the singlet $X\,^1\Sigma_g^+$ potential, as shown in Fig. 9 for *s*-wave resonances.

The two *s*-wave resonances in the *ab* channel illustrate the concept of resonance strength, as described in Sec. II.B.2. The broad resonance at 834 G is strongly entrance channel dominated, while the narrow resonance at 543 G is an extreme case of a closed channel dominated resonance. The former has an extraordinarily large magnetic field range of universal behavior, while that for the latter is vanishingly small (detunings of a few $\mu$G or less); see Sec. II.C.5 and Fig. 16. This has important consequences for molecules formed near these resonances.

The broad resonance at 834 G in the *ab* channel is used to create molecular Bose-Einstein condensates and fermionic superfluids. This will be discussed in Sec. IV.B.

$^7$Li—Moerdijk and Verhaar (1994) predicted Feshbach resonances in collisions of bosonic $^7$Li atoms in $|f=1, m=1\rangle$ (*aa* channel). Strecker *et al.* (2002) identified a zero crossing of the scattering length induced by a broad Feshbach resonance. This resonance was used to study the formation of bright solitons by Khaykovich *et al.* (2002) and Strecker *et al.* (2002) at small and negative scattering lengths near the zero crossing (see also Sec. IV.A.3). In these early experiments, the resonance position was estimated to 720 G. Later measurements by Junker *et al.* (2008) and Pollack *et al.* (2009) accurately pinpointed the resonance position and the zero crossing to 736.8(2) and 543.6(1) G, respectively.

Gross and Khaykovich (2008) observed two resonances in the state $|f=1, m=0\rangle$ (*bb* channel). A narrower one was found at 831(4) G with a width of 7 G, while a broader one (width of 34 G) was located at ~884 G. In between these two resonances, a zero crossing was found at 836(4) G.

**2. Sodium**

Inouye *et al.* (1998) pioneered experimental research in locating Feshbach resonances. In an optically trapped BEC of $^{23}$Na (the only stable isotope) with all atoms in the lowest hyperfine state $|f=1,m=1\rangle$, they identified resonances at 853 and 907 G. A third resonance in a different channel at 1195 G was later reported by Stenger *et al.* (1999). All three resonances are narrow and *s* wave in nature. The 1998 experiment showed both strongly enhanced trap loss and the dispersive tuning of the scattering length near the 907 G resonance (see Fig. 3).

The experimental determination of the resonances has enabled detailed models of the interaction potentials between ultracold Na atom (van Abeelen and Verhaar, 1999a). These models were further refined by Samuelis *et al.* (2000) based on conventional molecular spectroscopy in combination with photoassociation data.

The Feshbach resonance at 907 G was used to create ultracold $Na_2$ molecules (Xu *et al.*, 2003) and to demonstrate coherent molecule optics (Abo-Shaeer *et al.*, 2005); see also Sec. V.A.1.

**3. Potassium**

Potassium has three stable isotopes, two of them are bosonic ($^{39}$K and $^{41}$K) and one is fermionic ($^{40}$K).

$^{39}$K—In 1996 Boesten, Vogels, *et al.* (1996) predicted Feshbach resonance locations in collisions between $^{39}$K atoms. Their results were based on spectroscopic data of binding energies of rovibrational states of the $X\,^1\Sigma_g^+$ and $^3\Sigma_u^+$ potentials. The data, however, were not sufficiently complete to give quantitative resonance locations, but they did show that the likelihood of resonances was large. Another early prediction of resonance locations was made by Bohn *et al.* (1999).

Feshbach resonances in $^{39}$K were observed at 402 G, analyzed by D'Errico *et al.* (2007), and applied to create a tunable BEC of this species (Roati *et al.*, 2007). The zero crossing of the scattering length near the broad 402 G resonance has found intriguing applications for atom interferometry with noninteracting condensates (Fattori, D'Errico, *et al.*, 2008); see also Sec. IV.A.4. This resonance has an intermediate character between that of an entrance channel and a closed channel dominated resonance.

$^{40}$K—Early predictions on Feshbach resonances in $^{40}$K were made by Bohn *et al.* (1999). The first experimental observation was reported by Loftus *et al.* (2002), who demonstrated resonant control of elastic collisions via the 202 G resonance in a mixture of the lowest two spin states (*ab* channel). One year later, the same group reported on a *p*-wave resonance at 199 G (Regal *et al.*, 2003b); they measured the resonantly enhanced elastic collision rate of atoms in the second-lowest hyperfine state (*bb* channel) at a temperature of 3 $\mu$K. At an even lower temperature and by monitoring the collision-induced heating rate, Ticknor *et al.* (2004) found that this resonance is actually a doublet. This doublet structure in the *p*-wave resonance is due to a small energy splitting between the $|\ell=1,m_\ell=0\rangle$ and $|\ell=1,m_\ell=\pm1\rangle$ molecular states. The anisotropic nature of the *p*-wave resonances has found interesting applications in low-dimensional traps (Günter *et al.*, 2005).

In spin mixtures with *s*-wave interactions, Regal and Jin (2003) and Regal *et al.* (2003b) identified 10-G-wide *s*-wave Feshbach resonances in the *ab* and *ac* channels at 201.6(6) and 224.21(5) G, respectively, by monitoring the thermalization rate and mean-field shifts. These resonances provide a convenient tool to study strongly interacting Fermi gases and fermionic condensates (see Secs. IV.B).

$^{41}$K—A Feshbach resonance was recently observed by Kishimoto *et al.* (2009) at 51.4 G in the *cc* channel. The observation confirmed a theoretical prediction by D'Errico *et al.* (2007), which was based on experimental data available for the other potassium isotopes.

**4. Rubidium**

$^{85}$Rb—Courteille *et al.* (1998) reported a Feshbach resonance in a magnetically trapped thermal sample by observing enhanced photoassociative loss (see Sec. III.A.4). This result confirmed the prediction by Vogels *et al.* (1997). van Abeelen *et al.* (1998) suggested using photoassociation as a probe to identify Feshbach resonances. By monitoring inelastic loss, Roberts *et al.* (1998) determined the position of this 10-G-wide resonance to be at 155 G. Claussen *et al.* (2003) then used a BEC to perform a high-precision spectroscopic measurement of the molecular binding energy and determined the resonance parameters $B_0$ and $\Delta$ within 20 mG.

Attainment of BEC in $^{85}$Rb crucially depended on the existence of the 155 G resonance (see Sec. IV.A.1). Only in a 10 G window near the resonance the scattering length is positive and Cornish *et al.* (2000) were able to Bose condense $^{85}$Rb. As the first available BEC with widely tunable interactions the system has received considerable attention (see Sec. IV.A.3). Coherent atom-molecule coupling (Donley *et al.*, 2002) and the formation of ultracold $^{85}Rb_2$ molecules (Thompson *et al.*, 2005a) were reported based on this Feshbach resonance.

$^{87}$Rb—Marte *et al.* (2002) conducted a systematic search for Feshbach resonances in bosonic $^{87}$Rb. For atoms polarized in various combinations of magnetic sublevels in the $f=1$ hyperfine manifold, more than 40 resonances were observed between 300 and 1200 G by monitoring atom loss in an optical dipole trap. These resonances are induced by *s*- and *d*-wave bound states and are all very narrow. For the *s*-wave states, the underlying molecular structure is shown in Fig. 14. The widest and most often used resonance is located at 1007 G and has a width of 0.2 G. In different experiments, Erhard *et al.* (2004) and Widera *et al.* (2004) observed a low-field resonance near 9 G in the *ae* channel.

Several resonances in $^{87}$Rb have been used to form ultracold Feshbach molecules. They are formed by ramping the magnetic field through the resonance (Dürr, Volz, Marte, and Rempe, 2004); see Sec. V.A.1. The potential of combining Feshbach resonances with optical lattices has been demonstrated in a series of experiments with $^{87}$Rb (Thalhammer *et al.*, 2006; Volz *et al.*, 2006; Winkler *et al.*, 2006; Syassen *et al.*, 2007) (see Sec. VI.B).

#### 5. Cesium

Cesium, for which the isotope $^{133}$Cs is the only stable one, was proposed as the first alkali-metal species in which Feshbach resonances could be observed (Tiesinga *et al.*, 1993). With the limited state of knowledge of the interaction potentials no quantitative predictions could be made. The first observation of Feshbach resonances in cesium collisions was published seven years later (Vuletić *et al.*, 1999).

Vuletić *et al.* (1999), Chin *et al.* (2000), and Chin, Vuletić, *et al.* (2004) reported on more than 60 Feshbach resonances of various types using several detection schemes. These include *s*-, *p*-, *d*-, *f*-, and *g*-wave resonances in ten different scattering channels. Vuletić *et al.* (1999) used cross-axis thermalization rates to identify resonances in the lowest *aa* channel and used trap loss measurements in the *gg* channel. Chin *et al.* (2000) reported many more resonances by preparing the atoms in other internal states and by monitoring the evaporation rates to more efficiently measure the elastic cross section. The resonances provided Leo *et al.* (2000) with the essential information to precisely determine the interaction potentials of ultracold cesium.

Narrow resonances were observed by Chin *et al.* (2003) and Chin, Vuletić, *et al.* (2004) using radiative Feshbach spectroscopy (see Sec. III.A.4). In these experiments $^{133}$Cs atoms were illuminated by a far blue-detuned laser beam, whose wavelength was optimized to only remove atoms near a resonance. These resonances are induced by *g*-wave bound states and are only strong enough to be observed due to the large second-order spin-orbit coupling of cesium atoms. The observed resonances are at low magnetic fields, which can be understood as a consequence of the large background scattering length in the *aa* collision channel (see Sec. II.B.1). In addition, *l*-wave Feshbach molecules have been produced by Mark, Ferlaino, *et al.* (2007) and Knoop *et al.* (2008); their coupling to the *s*-wave continuum is too weak to lead to observable resonances in collision experiments. Finally, Lee *et al.* (2007) predicted a broad *s*-wave resonance at ~800 G in the *aa* channel. This is a magnetic field regime that has not been experimentally explored yet.

Figure 22 shows the scattering length in the *aa* channel. It has a zero crossing at 17.1 G (Chin, Vuletić, *et al.*, 2004; Gustavsson *et al.*, 2008) and multiple narrow resonances below 50 G. The gradual change in *a* from $-2500a_0$ to $500a_0$ across 30 G in the figure is actually the tail of a broad resonance with $B_0=-12$ G (see the Appendix). The negative $B_0$ follows from fitting to Eq. (1). Both the narrow and broad resonances have provided favorable conditions for many exciting experiments. This included the attainment of BEC with Cs atoms, a Bose condensate (Weber *et al.*, 2003a), the formation of $Cs_2$ (Chin *et al.*, 2003; Herbig *et al.*, 2003), the observation of resonances between ultracold molecules (Chin *et al.*, 2005), and studies on Efimov physics (see Sec. VI.C).

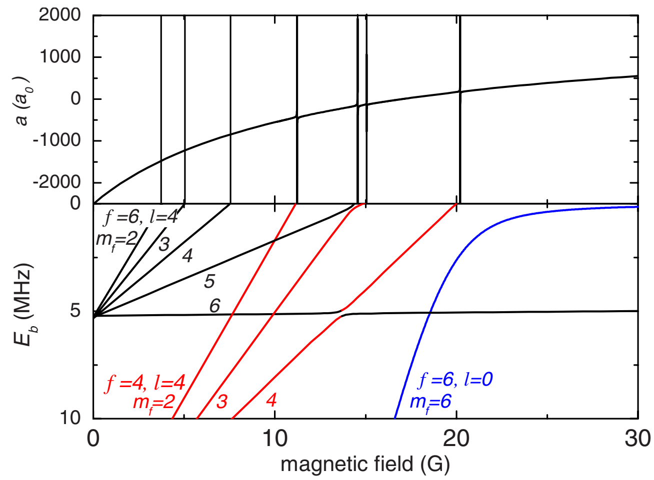


FIG. 22. (Color online) Scattering length and bound state energies for cesium atoms in the lowest internal state as a function of magnetic field. From Chin, Vuletić, *et al.*, 2004.

### C. Heteronuclear and other systems

Most of the experimental and theoretical attention so far has been focused on locating and using magnetic Feshbach resonances in single-species alkali-metal atom gases. Over the last five years, however, considerable progress has also been made in locating Feshbach resonance in other atomic species and in mixtures of alkali-metal atoms. These systems are investigated for various reasons. Of particular interest is the promise of more exotic quantum many-body behavior (Micheli *et al.*, 2006; Bloch *et al.*, 2008; Menotti *et al.*, 2008).

Heteronuclear systems provide the path to prepare mixtures of bosonic and fermionic quantum degenerate gases. Intriguing applications include the creation of fermionic molecules in an atomic Bose-Fermi mixture (Ospelkaus, Ospelkaus, Humbert, Ernst, *et al.*, 2006; Zirbel, Ni, Ospelkaus, D'Incao, *et al.*, 2008) and novel quantum phases of fermions with unequal masses (Petrov *et al.*, 2007). Feshbach resonances provide means to tune the interactions between different species in order to explore quantum phases in various regimes.

Atoms with magnetic moments interact via the long-range magnetic dipole-dipole interaction $V_{ss}$ in addition to the van der Waals and more short-range interactions. For alkali-metal atoms the effect of this dipole-dipole interaction on collective behavior is small. In atomic species with much larger magnetic moments, however, the dipole-dipole interaction can have a significant impact on the many-body behavior of the gas (Goral *et al.*,

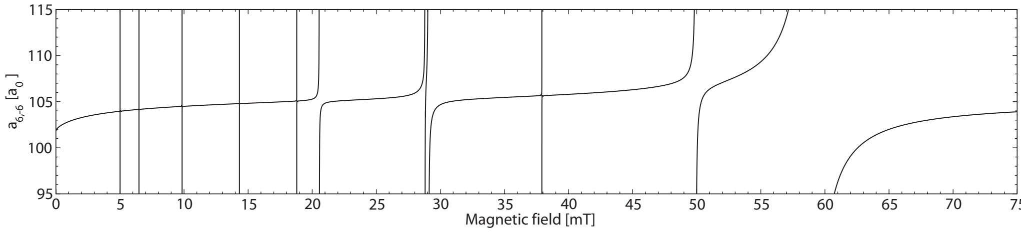


FIG. 23. Scattering length of $^{52}$Cr atoms vs magnetic field. The feature near 29 mT is a pair of nearly degenerate Feshbach resonances. From Werner *et al.*, 2005.

2000; Santos *et al.*, 2003; Santos and Pfau, 2006). In an atomic species such as chromium (Sec. III.C.1), magnetic Feshbach resonances can be used to tune the relative strength of the short-range interactions and the long-range dipole-dipole interaction (Yi and You, 2002; Lahaye *et al.*, 2007).

Another way to create exotic many-body systems is by pairing different atomic species into Feshbach molecules, which can then be converted into deeply bound molecules with a large electric dipole moment. Such a moment gives rise to large dipolar interactions, orders of magnitude larger than possible with magnetic dipole moments. These molecules, which are either bosonic or fermionic, have many applications in dipolar molecular quantum gases (Micheli *et al.*, 2006; Büchler *et al.*, 2007) and quantum computation (DeMille, 2002).

#### 1. Chromium

In 2005 Griesmaier *et al.* (2005) announced BEC of $^{52}$Cr atoms. This species has a magnetic moment that is six times larger than that for alkali-metal atoms. Subsequently, Stuhler *et al.* (2005) showed that the expansion of a cigar-shaped chromium condensate depended on the relative orientation of the magnetic moment and the elongated condensate, which for the first time showed the effects of the dipole-dipole interaction in a quantum-degenerate gas.

Werner *et al.* (2005) measured 14 magnetic Feshbach resonances in $^{52}$Cr in the energetically lowest magnetic sublevel. Feshbach resonances were detected by measuring, after a fixed hold time, the number of remaining atoms as a function of magnetic field. Atom loss could only have occurred by enhanced three-body recombination near the resonance. Figure 23 shows the $s$-wave scattering length as a function of magnetic field derived from the observed locations of the Feshbach resonances and a multichannel scattering model of the collision. Most of the resonances are $g$-wave resonances with the exception of one of the two nearly degenerate resonances at 29 mT and those at 50 and 59 mT. These three resonances have $d$-wave character. Moreover, Werner *et al.* (2005) also assigned two resonances as originating from $d$-wave collisions and coupling to an $s$-wave closed channel, i.e., $\ell=2$ and $\ell_c=0$ according to the notation discussed in Sec. II.B.4. Note that these resonances do not show up in the $s$-wave scattering length as shown in Fig. 23. One of these unusual resonances was investigated by Beaufils *et al.* (2009).

#### 2. Mixed species

K+Rb—The first mixed system to receive a detailed effort to locate Feshbach resonances was a mixture fermionic $^{40}$K and bosonic $^{87}$Rb atoms (Simoni *et al.*, 2003). Based on experimentally determined inelastic and elastic rate coefficients at zero magnetic field they predicted the location of 15 Feshbach resonances with an uncertainty ranging from 10 to 100 G.

Inouye *et al.* (2004) presented the first direct determination of the magnetic field location of three Feshbach resonances. The two atomic species, each in their energetically lowest hyperfine state, were optically trapped. As shown in Fig. 24 the Feshbach resonances were detected by measuring, after a fixed hold time, the number of remaining atoms as a function of magnetic field. The atom loss is due to three-body recombination.

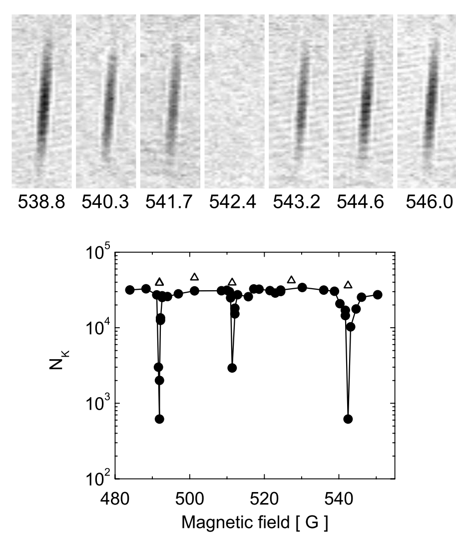


FIG. 24. Observation of Feshbach resonances in $^{40}$K+$^{87}$Rb. The top panel shows in-trap absorption images of $^{40}$K atoms after a fixed hold time of ≈1 s at various magnetic fields. The label on each image gives the magnetic field in Gauss. No $^{40}$K atoms could be seen at 542.2 G. The bottom panel shows the number of remaining $^{40}$K atoms after the fixed hold time as a function of magnetic field. Narrow features are observed at 492, 512, and 543 G. Adapted from Inouye *et al.*, 2004.

Ferlaino et al. (2006) confirmed the positions of these three resonances and found nine additional resonances. Theoretical modeling uniquely assigned each resonance and determined the scattering lengths of the $X\,^1\Sigma^+$ and $a\,^3\Sigma^+$ Born-Oppenheimer potentials to about 2%. The difference between the experimental Feshbach locations and those of the best-fit theory was less than 1 G for all resonances. The experimental uncertainty in the resonance locations was 0.2 G.

Ferlaino et al. (2006) also predicted the location of resonances of several isotopic combinations. For the bosonic $^{39}$K and $^{87}$Rb collision with both atoms in their lowest hyperfine state Roati et al. (2007) confirmed the location of one such resonance. It was found at 317.9 G well within the uncertainties quoted by Ferlaino et al. (2006). Klempt et al. (2007) observed a number of new Feshbach resonances, constructed an accurate potential model, and predicted resonances in other isotopic KRb combinations. Simoni et al. (2008) presented a refined near-threshold model for scattering and bound-state calculations for all isotopic combinations of K and Rb.

Feshbach resonances in mixtures of $^{40}$K and $^{87}$Rb have been applied to the creation of Feshbach molecules in optical traps (Zirbel, Ni, Ospelkaus, D'Incao, et al., 2008; Zirbel, Ni, Ospelkaus, Nicholson, et al., 2008) and in single sites of an optical lattice (Ospelkaus, Ospelkaus, Humbert, Ernst, et al., 2006); see Sec. VI.B.1. Recently these fermionic molecules have been transferred to more deeply bound levels (Ospelkaus et al., 2008); see Sec. V.B. Furthermore, interspecies interaction tuning has been exploited to study the collective behavior of a $^{40}$K+$^{87}$Rb Bose-Fermi mixture (Ospelkaus, Ospelkaus, Humbert, Sengstock, and Bongs, 2006) and to realize a tunable double species BEC in a $^{41}$K+$^{87}$Rb Bose-Bose mixture (Thalhammer et al., 2008).

Li+Na—Stan et al. (2004) observed three magnetic Feshbach resonances in the interaction between a degenerate fermionic $^6$Li gas and a Bose-Einstein condensate of Na. The resonances were observed by detecting atom loss when sweeping the magnetic field at constant rate through the resonances. Atom loss could only have occurred from three-body recombination or from molecule formation during the sweep. The observed resonances at 746.0, 759.6, and 795.6 G are $s$-wave resonances. In a recent theoretical study based on this experimental input data, Gacesa et al. (2008) derived precise values of the triplet and singlet scattering lengths for the $^6$Li-Na and the $^7$Li-Na combination. Moreover they predict a variety of additional Feshbach resonances within an experimentally attainable field range.

$^6$Li+$^{40}$K—Wille et al. (2008) described the observation of 13 Feshbach resonances in fermionic $^6$Li and $^{40}$K in various hyperfine states. Their theoretical analysis, which relies on the model developed by Stan et al. (2004) and discussed in Sec. II.C.2, indicated that the resonances were either $s$- or $p$-wave resonances. This isotopic combination is a prime candidate for the study of strongly interacting Fermi-Fermi mixtures.

Na+Rb—Predictions of Feshbach resonance locations based on analysis of high-resolution Fourier spectroscopy of the molecular $X\,^1\Sigma_g^+$ and $a\,^3\Sigma_u^+$ states in a 600 K beam of NaRb molecules are described by Bhattacharya et al. (2004) and Pashov et al. (2005). For example, Pashov et al. (2005) predicted for the ultracold collision between $^{23}$Na and $^{85}$Rb, both in the energetically lowest hyperfine state, $s$-wave Feshbach resonances at 170 and 430 G with an uncertainty of about 50 G. This uncertainty is sufficiently small that the predictions will be helpful for planning experiments which can accurately locate the resonances.

Initial experiments on other combinations of mixed atomic species have been performed. Feshbach resonances have been reported in the $^6$Li+$^{87}$Rb system by Deh et al. (2008), in the $^7$Li+$^{87}$Rb system by Marzok et al. (2009), and in the $^{87}$Rb+$^{133}$Cs system by Pilch et al. (2009).

### 3. Isotopic mixtures

A special case of a mixed system is that where different isotopes of the same element are combined. In particular, isotopic mixtures of Rb, K, and Li have been studied. Isotopic mixtures of K or Li are of particular interest as both fermionic and bosonic isotopes exist.

Feshbach resonances in isotopic mixtures of rubidium have recently been observed. Papp and Wieman (2006) found two $s$-wave Feshbach resonances in the collision of $^{85}$Rb and $^{87}$Rb when both isotopes are in their lowest hyperfine state. Their magnetic field locations of 265.44(0.15) and 372.4(1.3) G are consistent with the predictions of Burke et al. (1998).

van Kempen et al. (2004) predicted the location of $^6$Li+$^7$Li Feshbach resonances. When both isotopes are in the lowest hyperfine state resonances occur between 200 and 250 G as well as between 550 and 560 G. Four of these resonances have been observed by Zhang et al. (2005).

In predictions for isotopic mixtures "mass scaling" is often used. As the interatomic potentials are to good approximation independent of the isotopic composition of the dimer, the only thing that changes is the (reduced) mass of the dimer. Corrections are due to the breakdown of the Born-Oppenheimer approximation. Seto et al. (2000) and van Kempen et al. (2002) showed that for Rb the experimental data on $^{85}$Rb $^{85}$Rb, $^{85}$Rb $^{87}$Rb, and $^{87}$Rb $^{87}$Rb are consistent with mass scaling. A new analysis that includes the 2006 observations of Papp and Wieman (2006) is needed.

For the lithium system van Kempen et al. (2004) showed that mass scaling is insufficient to explain the observed data for the homonuclear $^6$Li+$^6$Li and $^7$Li+$^7$Li systems. Consequently, van Kempen et al. (2004) quoted a few Gauss uncertainty for the location of $^6$Li+$^7$Li Feshbach resonances from the breakdown of mass scaling.

## IV. CONTROL OF ATOMIC QUANTUM GASES

Tuning two-body interactions via Feshbach resonances is the experimental key to control collective phenomena in degenerate quantum gases. This has found numerous applications, both with atomic Bose-Einstein condensates (Cornell and Wieman, 2002; Ketterle, 2002) and with degenerate Fermi gases (Inguscio *et al.*, 2008).

The different decay properties of Bose and Fermi gases near Feshbach resonances play a crucial role for the experiments. For Bose gases, resonant two-body scattering in general leads to rapid decay via three-body collisions, as have discussed in context with loss spectroscopy on Feshbach resonances in Sec. III.A.2. Three-body decay limits the practical applicability of Feshbach tuning to Bose gases, restricting the experiments to the dilute gas regime where the scattering length is small compared to typical interparticle separations. In contrast, Fermi gases can be remarkably stable near $s$-wave Feshbach resonances (Petrov *et al.*, 2004).

For atomic Bose-Einstein condensates in the dilute gas regime (Sec. IV.A), the collective behavior can be described in a mean-field approach. In strongly interacting Fermi gases (Sec. IV.B), the role of the scattering length is much more complex. Here Feshbach tuning can be used to control the nature of fermionic pairing in different superfluid regimes.

### A. Bose-Einstein condensates

In experiments on atomic BEC, the role of Feshbach tuning can be divided into two parts. First, the control of collision properties can be essential for the attainment of BEC. Second, the possibility to control the mean-field interaction opens up a variety of interesting applications.

#### 1. Attainment of BEC

Some atomic species offer favorable collision properties for the attainment of BEC without any necessity of interaction tuning; $^{87}$Rb and $^{23}$Na are the most prominent examples (Cornell and Wieman, 2002; Ketterle, 2002). In other cases, however, Feshbach tuning is essential either to produce large condensates ($^{7}$Li) or to achieve BEC at all ($^{85}$Rb, $^{133}$Cs, and $^{39}$K).

First consider the general question what is a "good" scattering length $a$ for making a BEC. To begin, $a$ should be positive because condensates undergo collapse at negative scattering length when the number of condensed atoms exceeds a relatively small critical value (Bradley *et al.*, 1997). Moreover, $a$ should not be too small because a sufficiently large elastic collision rate is required for evaporative cooling toward BEC; the cross section for elastic collisions between identical bosons is $8\pi a^2$. Finally, the scattering length should not be too large to avoid rapid decay by three-body collisions (Roberts *et al.*, 2000; Weber *et al.*, 2003b) as three-body decay scales as $a^4$ (Fedichev, Reynolds, *et al.*, 1996; Braaten and Hammer, 2006). In practice these conditions result in typical values for a good value of $a$ between a few ten and a few hundred times the Bohr radius $a_0$. In detail, the optimum value for $a$ depends on the confinement properties of the trap and behavior of inelastic decay.

For $^{7}$Li, early magnetic trapping experiments showed BEC in the internal state $f=2$, $m=2$, where the scattering length $a=-27a_0$ is small and negative (Bradley *et al.*, 1995, 1997); here the number of condensate atoms was limited through collapse to only a few hundred. Later experiments (Khaykovich *et al.*, 2002; Strecker *et al.*, 2002) on optically trapped $^{7}$Li in the internal state $f=1$, $m=1$ exploited the 737 G Feshbach resonance to tune the scattering length from its very small background value ($a_{\mathrm{bg}}\approx+5a_0$) to sufficiently large positive values, typically in a range between $+40a_0$ and $+200a_0$. Evaporative cooling then resulted in condensates with up to $3\times10^5$ atoms. More recently, Gross and Khaykovich (2008) exploited Feshbach tuning in the state $f=1$, $m=0$ for the all-optical production of a BEC. They obtained favorable conditions for efficient evaporative cooling at 866 G, where the scattering length is about $+300a_0$.

Bose-Einstein condensation of $^{85}$Rb was achieved by evaporative cooling in a magnetic trap (Cornish *et al.*, 2000) exploiting the broad resonance at 155 G (Sec. III.B.4) in the state $f=2$, $m=-2$ to tune the scattering length to positive values. The large negative background scattering length $a_{\mathrm{bg}}=-443a_0$ would limit the number of condensate atoms to less than 100. Two stages of cooling were performed. The first stage used a magnetic field of 250 G, where the scattering length $a$ is close to its background value; the second was close to the resonance at 162.3 G, where $a=+170a_0$. This procedure optimized the ratio of elastic to inelastic collision rates (Roberts *et al.*, 2000) for the temperatures occurring during these stages.

Feshbach tuning played a crucial role for the attainment of BEC in $^{133}$Cs (Weber *et al.*, 2003a; Kraemer *et al.*, 2004). The condensate was produced in an optical trap in the state $f=3$, $m=3$. In this lowest internal state, two-body decay is energetically forbidden, and the scattering length $a(B)$ shows a large variation at low magnetic fields (Fig. 22), which is due to a broad Feshbach resonance at $-12$ G. In a first evaporative cooling stage a shallow large-volume optical trap was employed, and a large scattering length of $a=+1200a_0$ at $B=73$ G provided a sufficiently large elastic collisions rate at rather low atomic densities. The second cooling stage employed a much tighter trap. Here, at much higher densities, an optimum magnetic field of 21 G was found, where $a=+210a_0$. Highly efficient evaporation led to the attainment of BEC. Later experiments revealed a minimum of three-body decay in this magnetic field region (Kraemer *et al.*, 2006); see also Sec. VI.C.2.

For the attainment of BEC in $^{39}$K, Roati *et al.* (2007) employed a mixture with $^{87}$Rb atoms with both species being in their internal ground states. First, an interspecies Feshbach resonance near 318 G was used to optimize sympathetic cooling; the interspecies scattering length was tuned to $+150a_0$ by choosing a magnetic field of 316 G. Then, after the removal of the Rb atoms, final evaporative cooling toward BEC was performed near the 402 G resonance of $^{39}$K (Sec. III.B.3) with the scattering length tuned to a positive value of $+180a_0$.

#### 2. Condensate mean field

Trapped atomic BECs in the dilute-gas regime are commonly described (Dalfovo *et al.*, 1999) by the Gross-Pitaevskii equation for the condensate wave function $\Phi$,

$$i\hbar\frac{\partial}{\partial t}\Phi = \left(-\frac{\hbar^2\nabla^2}{2m} + V_{\text{ext}} + V_{\text{mf}}\right)\Phi, \tag{57}$$

where $V_{\text{ext}}$ is the external trapping potential. Interactions are taken into account by the mean-field potential

$$V_{\text{mf}} = (4\pi\hbar^2 a/m)n, \tag{58}$$

where the atomic number density $n$ is related to $\Phi$ by $n=|\Phi|^2$. This mean field enters the Gross-Pitaevskii equation as a nonlinearity and leads to many interesting phenomena.

In the Thomas-Fermi regime of large condensates with $a>0$ one can neglect the kinetic energy term and obtain the equilibrium density distribution of a BEC,

$$n = \frac{m}{4\pi\hbar^2 a}(\mu - V_{\text{ext}}), \tag{59}$$

which applies for $\mu > V_{\text{ext}}$; otherwise $n=0$. For a given particle number $N$, the chemical potential $\mu$ follows from the normalization condition $N=\int nd^3r$.

In many cases of practical relevance, stable condensates with positive $a$ are confined in harmonic traps and are in the Thomas-Fermi regime. The condensate is then characterized by the Thomas-Fermi radius $r_{\text{TF}}$ given as the radius at which the external trapping potential equals the chemical potential and the peak number density $n_0$. These two quantities follow the scaling laws

$$r_{\text{TF}} \propto a^{1/5}, \quad n_0 \propto a^{-3/5}. \tag{60}$$

Figure 25 shows how the size of a trapped $^{85}$Rb condensate increases when the Feshbach resonance at 155 G is approached. The *in situ* measurements were used to experimentally determine $a(B)$ (Cornish *et al.*, 2000). The results are in good agreement with later measurements of the molecular binding energy, which allowed for a more precise determination of the scattering properties near the Feshbach resonance (Claussen *et al.*, 2003).

The mean-field approach is valid for scattering lengths which are small compared to the typical interparticle distance. The prospect to observe beyond-mean-field effects in BECs (Dalfovo *et al.*, 1999) has been an important motivation for experiments near Feshbach resonances at large $a$. In atomic Bose gases, however, the fast inelastic decay makes it very difficult to observe such phenomena. Papp *et al.* (2008) finally demonstrated beyond-mean-field behavior by Bragg spectroscopy on a $^{85}$Rb BEC. In molecular BECs created in atomic Fermi gases (Sec. IV.B.1), the collisional stability facilitates the observation of beyond-mean-field behavior by simpler means. For example, Altmeyer *et al.* (2007) observed beyond-mean-field behavior by studying collective oscillations of a $^6Li_2$ molecular BEC.

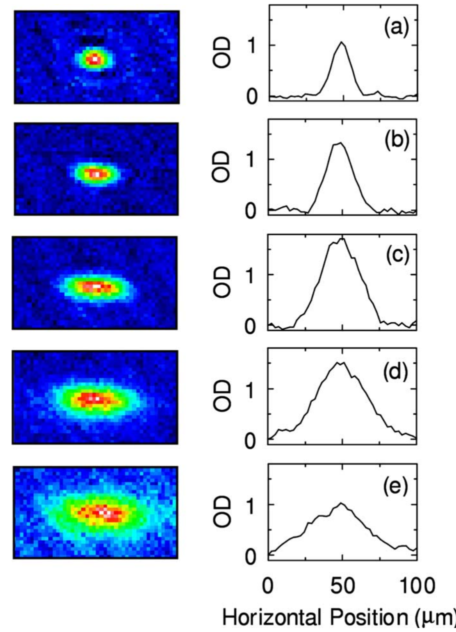


FIG. 25. (Color online) *In situ* images and density profiles showing the variation of the equilibrium size of a magnetically trapped $^{85}$Rb BEC close to a Feshbach resonance. With decreasing magnetic field (a)–(e), the scattering length increases from a very small positive value at 165.2 G (zero crossing at 165.8 G) to a very large value of $a \approx +6000a_0$ at 156.4 G (resonance position at 155.0 G). From Cornish *et al.*, 2000.

#### 3. Controlled collapse and bright solitons

For negative scattering lengths the condensate mean field is attractive. The resulting nonlinearity can then lead to a condensate collapse and to the formation of bright matter-wave solitons. To study phenomena of this kind by Feshbach tuning, the general experimental strategy is to first produce a stable BEC at positive $a$. Then, the attractive interaction is introduced by changing $a$ to negative values. Experiments of this class have been performed with $^{85}$Rb (Donley *et al.*, 2001; Roberts *et al.*, 2001; Cornish *et al.*, 2006), $^7$Li (Khaykovich *et al.*, 2002; Strecker *et al.*, 2002), and $^{133}$Cs (Weber *et al.*, 2003a; Rychtarik *et al.*, 2004).

Exploiting the 155 G Feshbach resonance in $^{85}$Rb, Roberts *et al.* (2001) investigated the stability of a BEC with attractive interactions. They first produced the condensate in a magnetic trap at a moderate positive scattering length. They then slowly changed the atom-atom interaction from repulsion to attraction by ramping the magnetic field into the region of negative scattering length. With increasing attractive interaction they observed an abrupt transition in which atoms were ejected from the condensate. These measurements of the onset

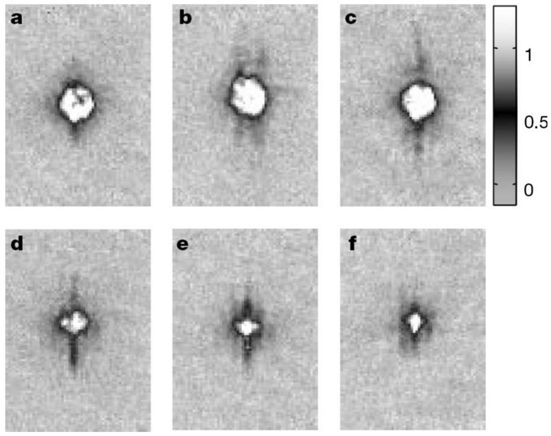


FIG. 26. Striking phenomena have been observed in the controlled collapse of a $^{85}$Rb BEC. The images show the formation of "jets," where streams of atoms with highly anisotropic velocities are ejected by the collapsing condensate. From Donley *et al.*, 2001.

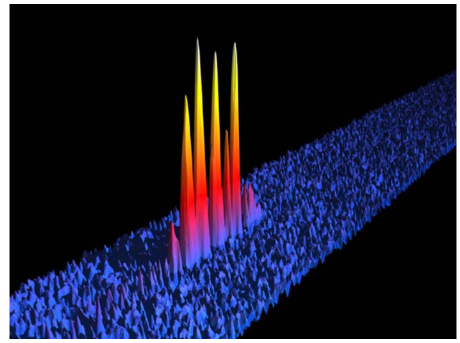

FIG. 27. (Color online) A train of matter-wave solitons created from an optically trapped BEC of $^{7}$Li atoms (Strecker *et al.*, 2002). The individual solitons contain up to about 5000 atoms. Courtesy of Randall Hulet.

of condensate collapse provided a quantitative test of the stability criterion for a BEC with attractive interactions.

The controlled collapse in $^{85}$Rb following a sudden change of $a$ led to the spectacular observation of a "Bosenova," a condensate implosion with fascinating and unexpected properties (Donley *et al.*, 2001). An anisotropic burst of atoms was observed that exploded from the condensate during the early stage of collapse (Fig. 26), leaving behind a highly excited long-lived remnant condensate. Strikingly, the number of atoms in the remnant BEC was significantly larger than the critical number for a collapse. The surprising fact that the remnant BEC did not undergo further collapse was later explained by its fragmentation into bright solitons (Cornish *et al.*, 2006).

Condensate collapse experiments were also used to detect the presence of a small BEC of Cs atoms in an optical surface trap (Rychtarik *et al.*, 2004). While a thermal gas did not show loss when the scattering length was suddenly switched to negative values, the condensate showed up in the sudden onset of collapse-induced loss.

Bright solitons were observed in experiments on $^{7}$Li atoms near the broad 737 G Feshbach resonance. Khaykovich *et al.* (2002) produced a BEC by evaporative cooling at $a \approx 40a_0$ in an optical trap. They then released the BEC into a one-dimensional optical waveguide and studied the propagation of the resulting matter-wave packet for an ideal gas ($a=0$) and a gas with a small attractive mean-field interaction ($a=-4a_0$). In the latter case, they observed the dispersion-free propagation that is characteristic for a soliton. In a similar experiment Strecker *et al.* (2002) created a train of solitons (see Fig. 27) from an optically trapped $^{7}$Li BEC by abruptly switching the scattering length from $200a_0$ to $-3a_0$. They also observed the propagation of the solitons in the trap and their mutual repulsion. These spectacular experiments on bright solitons highlight the analogy between bright matter-wave solitons and optical solitons in fibers and thus the intimate connection between atom optics with BECs and light optics.

#### 4. Noninteracting condensates

The zero crossing of the scattering length near a Feshbach resonance can be used to realize noninteracting ideal-gas condensates. BECs of $^{7}$Li, $^{39}$K, $^{85}$Rb, and $^{133}$Cs are good candidates to reduce $|a|$ to very small values on the order of $a_0$ or smaller.

To explore noninteracting condensates with $^{133}$Cs Weber *et al.* (2003a) and Kraemer *et al.* (2004) exploited the zero crossing near 17 G and studied expansion after release from the trap. The scattering length was abruptly changed to zero when the condensate was released from the trap. An extremely slow expansion was observed with a release energy as low as $k_B \times 50$ pK (see Fig. 28). The surprising observation that the release energy is a factor of 5 below the kinetic energy associated with the motional ground state of the trap is explained by the fact that the initial size of the expanding matter-wave packet is determined by the repulsive condensate self-interaction before release, which is larger than the bare ground state of the trap. The momentum spread is thus significantly smaller. In contrast, a slow change of $a$ to zero before release would have ideally resulted in a wave packet with position and momentum spread corresponding to the bare ground state.

Besides the small equilibrium size of the condensate, a vanishing scattering length has profound consequences for the collective behavior of a BEC. The sound velocity ($\propto na^{1/2}$) is vanishingly small so that all excitations will become particlelike and not phononlike. Moreover, the healing length ($\propto na^{-1/2}$) becomes very large, which may be applied in experiments on rotating condensates (Madison *et al.*, 2000) to increase the core size of vortices.

Noninteracting condensates are promising for the observation of phenomena that are masked by interacting effects, as, e.g., phenomena on a lower energy scale. In atom interferometry the mean-field interaction of a condensate is a substantial systematic error source, as

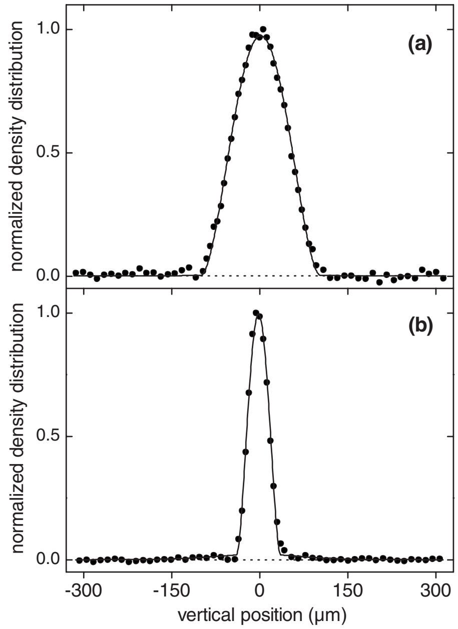


FIG. 28. Density profiles of a Cs BEC after 100 ms of expansion at (a) $a=210a_0$ and (b) $a=0$. The expansion energy of the noninteracting condensate is as low as $k_B\times 50$ pK. From Kraemer *et al.*, 2004.

Gupta *et al.* (2002) observed in the context of photon recoil measurements. Roati *et al.* (2004) studied Bloch oscillations in an optical lattice under the influence of gravity. They showed that, for interacting bosons, the oscillations lost contrast much faster than for identical fermions without $s$-wave interaction. A noninteracting BEC combines the advantages of an ultralow momentum spread with very long observation times. Two recent experiments have reported on long-lived Bloch oscillations with BECs of $^{133}$Cs (Gustavsson *et al.*, 2008) and $^{39}$K (Fattori, D'Errico, *et al.*, 2008), which is an important advance toward high-precision atom interferometry. This could, for example, open up new possibilities for precision measurements of gravitational effects (Carusotto *et al.*, 2005).

Another intriguing application of the zero crossing of a Feshbach resonance was demonstrated by Lahaye *et al.* (2007) with a BEC of $^{52}$Cr atoms. This species exhibits a very large magnetic dipole-dipole interaction because of its magnetic moment of $6\mu_B$. When the isotropic contact interaction is reduced by tuning the scattering length close to zero, the magnetic dipole interaction dominates. In $^{52}$Cr this was achieved near the 589 G Feshbach resonance (Fig. 23). The resulting dipolar quantum gas represents a model system for a "quantum ferrofluid," the anisotropic properties of which have been attracting considerable interest (Menotti *et al.*, 2008). In further work on $^{52}$Cr BEC near the zero of the scattering length, Lahaye *et al.* (2008) investigated the controlled collapse of the system and demonstrated its complex dynamics and Koch *et al.* (2008) studied the stability of the dipolar condensate depending on the trap geometry. The effect of the magnetic dipole interaction has also been observed in noninteracting condensates made of alkali atoms with magnetic moments of the order of $1\mu_B$ for $^{39}$K by Fattori, Roati, *et al.* (2008) and for $^{7}$Li by Pollack *et al.* (2009). The recent observation of Anderson localization of matter waves in a disordered optical potential by Roati *et al.* (2008) represents a further exiting application of a noninteracting condensate.

### B. Degenerate Fermi gases

In experiments on ultracold Fermi gases (Inguscio *et al.*, 2008), Feshbach resonances serve as a key to explore many-body physics in the strongly interacting regime (Bloch *et al.*, 2008). This regime is realized when the scattering length exceeds the interparticle spacing and connects the field of ultracold atoms to fundamental questions in various fields of physics, such as high $T_c$ superconductors, nuclear matter, neutron stars, and the quark-gluon plasma. The first Feshbach resonance in a Fermi gas was observed by Loftus *et al.* (2002). O'Hara, Hemmer, Gehm, *et al.* (2002) produced the first strongly interacting Fermi gas. Since then the research field has undergone rapid developments with many exciting achievements (Inguscio *et al.*, 2008).

The decay properties of ultracold Fermi gases are strongly influenced by Pauli's exclusion principle (Esry *et al.*, 2001; Petrov, 2003; Suno *et al.*, 2003; Petrov *et al.*, 2004). Three-body recombination processes in one- and two-component Fermi gases necessarily involve identical particles. This generally leads to a suppression of loss as compared to Bose gases or systems with three nonidentical particles. The majority of recent experiments on Fermi gases (Inguscio *et al.*, 2008) has focused on two-component spin mixtures of $^{6}$Li or $^{40}$K with resonant $s$-wave interactions, realized near broad entrance-channel dominated resonances. In such systems, it is possible to realize a resonant $s$-wave interaction ($a\to\pm\infty$) practically without any decay. Nevertheless, these resonances are accompanied by subtle loss features (Dieckmann *et al.*, 2002), which do not appear at the resonance center but at the side where the scattering length is positive. In contrast to the remarkable stability near this special $s$-wave scenario, three-body collisions near a $p$-wave Feshbach resonance usually lead to significant loss (Regal *et al.*, 2003b; Zhang *et al.*, 2004; Schunck *et al.*, 2005).

Here, as prominent examples for the application of Feshbach tuning, we review the attainment of BEC of molecules (Sec. IV.B.1) and studies of the BEC Bardeen-Cooper-Schrieffer (BCS) crossover and the observation of fermion superfluidity (Sec. IV.B.2).

#### 1. BEC of molecules

Bose-Einstein condensation of molecules was created in atomic Fermi gases of $^{6}$Li (Jochim *et al.*, 2003b; Zwierlein *et al.*, 2003; Bourdel *et al.*, 2004) and $^{40}$K (Greiner *et al.*, 2003). The molecules are weakly bound dimers at the side of an entrance channel dominated $s$-wave Feshbach resonance where the scattering length is positive and very large. These dimers are formed in a halo state (Sec. V.B.2), which is stable against inelastic decay in atom-dimer and dimer-dimer collisions (Petrov *et al.*, 2004). This stability originates from basically the same Pauli suppression effect that also affects three-body decay in an atomic Fermi gas. Such weakly bound molecules can be detected by converting them back to atoms or by direct absorption imaging (see Sec. V.B.1).

In a spin mixture of $^6$Li in the lowest two internal states, the route to molecular BEC is particularly simple (Jochim *et al.*, 2003b). Evaporative cooling toward BEC can be performed in an optical dipole trap at a constant magnetic field of about 764 G near the broad 834 G Feshbach resonance; here $a=+4500a_0$ and $E_b=k_B\times 1.5\ \mu$K. In the initial stage of evaporative cooling the gas is purely atomic and $a$ is the relevant scattering length for elastic collisions between the atoms in different spin states. With decreasing temperature the atom-molecule equilibrium (Sec. V.A.3) favors the formation of molecules and, in the final evaporation stage, a purely molecular sample is cooled down to BEC. The large atom-dimer and dimer-dimer scattering lengths of $1.2a$ and $0.6a$ along with strongly suppressed loss (Sec. V.B.3) facilitate an efficient evaporation process. In this way, molecular BECs are achieved with a condensate fraction exceeding 90%.

The experiments in $^{40}$K followed a different approach to achieve molecular BEC (Greiner *et al.*, 2003). For $^{40}$K the weakly bound dimers are less stable because of less favorable short-range three-body interaction properties. Therefore the sample is first cooled above the 202 G Feshbach resonance, where $a$ is large and negative, to achieve a deeply degenerate atomic Fermi gas. A sweep across the Feshbach resonance then converts the sample into a partially condensed cloud of molecules. Figure 29 shows the emergence of the molecular BEC in $^{40}$K.

The molecular BEC can be described in the mean-field approach outlined in Sec. IV.A.2 by simply replacing the atomic with the molecular mass ($m\to 2m$) and the atomic with the molecular scattering length ($a\to 0.6a$). The mean field of the molecular condensate was experimentally studied by Bartenstein *et al.* (2004b) and Bourdel *et al.* (2004). However, because of the large scattering length, molecular BECs show considerable beyond-mean-field effects (Altmeyer *et al.*, 2007).

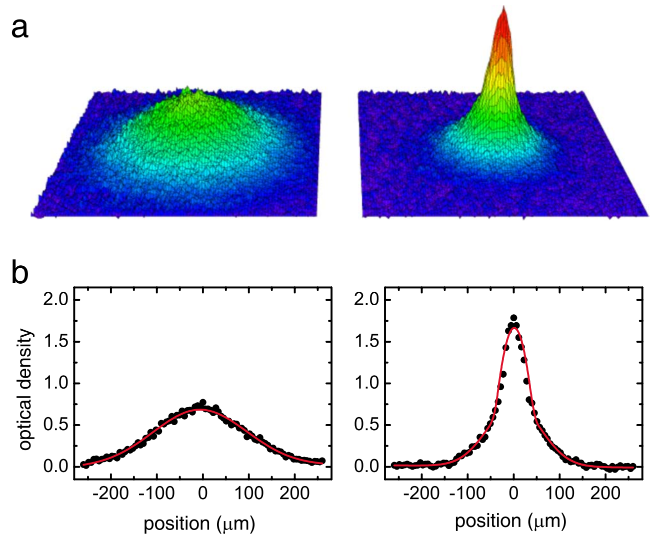


FIG. 29. (Color online) Emergence of a molecular BEC in an ultracold Fermi gas of $^{40}$K atoms, observed in time-of-flight absorption images. The density distribution on the left-hand side [upper graph, two-dimensional (2D) surface plot; lower graph, one-dimensional (1D) cross section] was taken for a weakly interacting Fermi gas which was cooled down to 19% of the Fermi temperature. After ramping across the Feshbach resonance no BEC was observed as the sample was too hot. The density distribution on the right-hand side was observed for a colder sample at 6% of the Fermi temperature. Here the ramp across the Feshbach resonance resulted in a bimodal distribution, revealing the presence of a molecular BEC with a condensate fraction of 12%. From Greiner *et al.*, 2003.

### 2. BEC-BCS crossover and fermion superfluidity

At a Feshbach resonance in a two-component Fermi gas, different regimes of fermion pairing and superfluidity can be experimentally realized. Pairing on the side with $a>0$ can be understood in terms of molecule formation, and superfluidity results from molecular Bose-Einstein condensation. On the other side of the resonance ($a<0$), pairing is a many-body effect and the ground state of the system at zero temperature is a fermionic superfluid. In the limit of weak interactions, this regime can be understood in the framework of the well-established BCS theory, developed in the 1950s to describe superconductivity. Both limits, BEC and BCS, are smoothly connected by a crossover through a regime where the gas is strongly interacting. This BEC-BCS crossover has attracted considerable attention in many-body quantum physics for more than two decades and has recently been reviewed by Chen *et al.* (2005), Giorgini *et al.* (2008), and Inguscio *et al.* (2008). A theoretical description of this challenging problem is very difficult and various approaches have been developed. With tunable Fermi gases, a unique testing ground has become available to quantitatively investigate the crossover problem.

The interaction regime can be characterized by a dimensionless parameter $1/k_Fa$, where $k_F$ is the Fermi wave number of a noninteracting gas, related to the Fermi energy by $E_F=\hbar^2k_F^2/(2m)$. For $1/k_Fa\gg 1$, the molecular BEC regime is realized. For $1/k_Fa\ll -1$, the system is in the BCS regime. In between ($1/|k_Fa|\lesssim 1$), the Fermi gas is strongly interacting. In the experiments, $E_F/k_B=1\ \mu$K gives a typical value for the Fermi energy and $1/k_F\approx 4000a_0$ sets the typical length scale. The realization of a strongly interacting gas thus requires $|a|\gtrsim 4000a_0$. which for the particularly broad $^6$Li resonance (Fig. 10) is obtained over a more than 100-G-wide magnetic field range.

A particularly interesting situation is the exact resonance case, where $1/k_Fa=0$. Here $a$ is no longer a relevant quantity to describe the problem and scattering is only limited by unitarity (Sec. II.A.2). Consequently, $k_F^{-1}$ and $E_F$ define the relevant scales for length and energy, and the Fermi gas acquires universal properties (Giorgini *et al.*, 2008; Inguscio *et al.*, 2008). For example, the size and shape of a harmonically trapped "universal Fermi gas" can be obtained as a rescaled version of a noninteracting Fermi gas.

Experimentally, various properties of strongly interacting Fermi gases have been explored in the BEC-BCS crossover (Inguscio *et al.*, 2008). All these experiments have been performed on two-component spin mixtures of $^6$Li near the 834 G resonance or of $^{40}$K near the 202 G resonance. In both cases, the resonances have entrance-channel dominated character, where the two-body interaction can be modeled in terms of a single scattering channel and universality applies (Sec. II.B.2). This condition is particularly well fulfilled for the $^6$Li resonance, where the resonance is exceptionally strong.

Regal *et al.* (2004) introduced fast magnetic-field sweeps to observe the condensed fraction of pairs in the crossover. Starting with an ultracold $^{40}$K Fermi gas in the strongly interacting regime, they performed *fast* Feshbach ramps into the BEC regime. The ramps were fast compared to the time scale of establishing a thermal atom-molecule equilibrium by collisions (see Sec. V.A.3). However, the Feshbach ramps were slow enough to adiabatically convert fermion pairs formed in the strongly interacting regime into molecules. After the ramp, the observed molecular condensate reflected the fermion condensate before the ramp. The fast-ramp method was applied by Zwierlein *et al.* (2004) to observe fermion condensates in $^6$Li.

For $^6$Li Bartenstein *et al.* (2004b) showed that *slow* Feshbach ramps allow conversion of the gas in a reversible way from the molecular BEC to the BCS regime. Here the gas adiabatically follows and stays in thermal equilibrium. They also observed *in situ* profiles of the trapped strongly interacting gas and measured its changing size for variable interaction strength.

Collective modes in the BEC-BCS crossover were studied in $^6$Li gases. Kinast *et al.* (2004) reported on ultraslow damping in a universal Fermi gas with resonant interactions, providing evidence for superfluidity. Bartenstein *et al.* (2004a) measured how the frequencies of collective modes in the crossover changed with variable interaction parameter $1/k_Fa$. They also observed a breakdown of hydrodynamic behavior on the BCS side of the resonance, which marks a transition from the superfluid to the normal phase. Precision measurements of collective modes also revealed beyond-mean-field effects in the molecular BEC regime (Altmeyer *et al.*, 2007).

Chin, Bartenstein, *et al.* (2004) performed spectroscopy on fermion pairs by using a radio-frequency technique. They measured the binding energy of the pairs in the crossover. They showed how an effective pairing gap continuously evolved from the molecular regime, where it simply reflects the dimer binding energy, into a many-body regime of pairing (Schunck *et al.*, 2008).

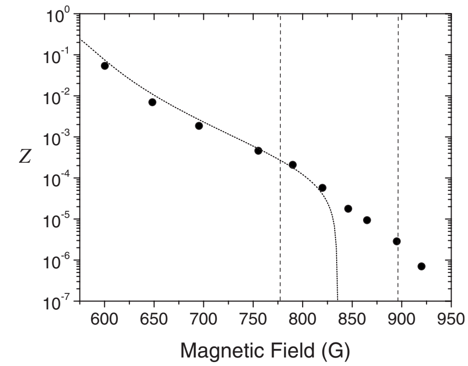


FIG. 30. Measurements of the closed channel fraction $Z$ for pairs in the BEC-BCS crossover. The experiment uses the 834 G resonance in $^6$Li and a photoassociation probe that only couples to closed channel singlet component. The vertical dashed lines indicate the boundaries of the strongly interacting regime, $k_F|a|>1$. The dotted line shows the result of a coupled-channel calculation for molecules (see Sec. II.C.5 and Fig. 16). Comparison with the experimental data shows that two-body physics describes the situation well up to close to the 834 G resonance. For higher fields, $Z$ shows strong many-body effects. Above the resonance, where two-body pairs cannot exist, the many-body system shows the closed channel admixture of the many-body pairs. From Partridge *et al.*, 2005.

Partridge *et al.* (2005) used an optical molecular-probe technique based on photoassociation to measure the closed channel contribution of pairs in the crossover. Their results, shown in Fig. 30, show that this fraction is very small in the strongly interacting regime. These observations strongly support single-channel descriptions for the crossover along with the concept of universality. The results also demonstrate that fermionic pairing reaches from the strongly interacting regime well into the weakly interacting BCS regime.

Superfluidity of a $^6$Li Fermi gas in the BEC-BCS crossover was observed by Zwierlein *et al.* (2005). They produced a rotating Fermi gas and observed the formation of vortex arrays. Here Feshbach tuning was applied not only to explore different regimes in the crossover but also to increase the vortex cores in the expanding Fermi gas after release from the trap; the latter was essential to observe the vortices by optical imaging.

Currently, there is considerable interest in exploring novel regimes of pairing and superfluidity. Partridge *et al.* (2006) and Zwierlein *et al.* (2006) performed experiments with unbalanced mixtures of two spin states, i.e., polarized Fermi gases. This led to deeper insight into phenomena such as phase separation (Partridge *et al.*, 2006; Shin *et al.*, 2008). Ultracold Fermi-Fermi mixtures of different species, such as $^6$Li and $^{40}$K, have recently become available (Taglieber *et al.*, 2008; Voigt *et al.*, 2008; Wille *et al.*, 2008), adding the mass ratio and independent control of the trapping potentials for both components to our tool box to explore the broad physics of strongly interacting fermions.

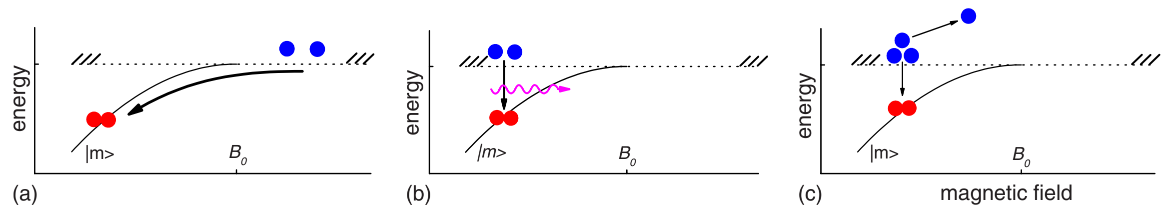


FIG. 31. (Color online) Illustration of experimental schemes to create ultracold molecules. The solid line marks the weakly bound molecular state $|m\rangle$, which dissociates into the continuum (indicated by the dotted line) at resonance $B=B_0$. In (a), the magnetic field is ramped across the resonance, which adiabatically converts two interacting atoms into one molecule; in (b), an oscillatory magnetic field drives the transition from the scattering state to the molecular state; and in (c), three-body recombination results in molecule formation.

## V. ULTRACOLD FESHBACH MOLECULES

Cold molecules are at the center of a rapidly developing research field (Doyle *et al.*, 2004; Hutson and Soldán, 2006), offering many new opportunities for cold chemistry, precision measurements, many-body physics, and quantum information. The coldest attainable molecules, at temperatures in the nanokelvin range, are created by Feshbach association in ultracold atomic gases. Here Feshbach resonances serve as the experimental key to couple pairs of colliding atoms into molecules.

In 2002, Donley *et al.* (2002) observed coherent oscillations between atom pairs and Feshbach molecules in a BEC of $^{85}$Rb atoms. The oscillation frequency reflected the small binding energy of the dimer in a weakly bound state and provided indirect evidence for the creation of molecules. In 2003, several groups reported on more direct observations of Feshbach molecules in Fermi gases of $^{40}$K (Regal *et al.*, 2003a) and $^{6}$Li (Cubizolles *et al.*, 2003; Jochim *et al.*, 2003a; Strecker *et al.*, 2003) and BECs of Cs (Herbig *et al.*, 2003), $^{87}$Rb (Dürr, Volz, Marte, and Rempe, 2004), and Na (Xu *et al.*, 2003). This rapid development culminated in the attainment of molecular BEC at the end of 2003 (Sec. IV.B.1) and has paved the way for numerous applications.

A comprehensive review of Feshbach molecules and their theoretical background has been given by Köhler *et al.* (2006). We do not consider optical methods of making molecules since this was recently reviewed by Jones *et al.* (2006). Here we discuss various formation methods based on magnetic Feshbach resonances (Sec. V.A) and the main properties of Feshbach molecules (Sec. V.B).

### A. Formation

Various schemes to create ultracold molecules near Feshbach resonances have been developed in the last few years, most of them relying on the application of time-varying magnetic fields. Section V.A.1 describes the use of magnetic field ramps, while Sec. V.A.2 discusses the application of oscillatory fields. These schemes have been applied to a variety of bosonic and fermionic atom gases. Section V.A.3 describes the formation of collisionally stable molecules of fermionic atoms through three-body recombination and thermalization.

Here we restrict our discussion to ultracold gases confined in macroscopic traps. The microscopic trapping sites of an optical lattice, where atom pairs can be tightly confined, constitute a special environment for molecule formation. This will be reviewed separately in Sec. VI.B.

#### 1. Feshbach ramps

Ramping an external magnetic field across a Feshbach resonance is the most commonly adopted scheme to form Feshbach molecules. This scheme, usually referred to as a Feshbach ramp, was proposed by Timmermans *et al.* (1999), van Abeelen and Verhaar (1999b), and Mies *et al.* (2000). In a simplified picture, shown in Fig. 31(a), the resonant coupling between the scattering state and the molecular state opens up a way to adiabatically convert interacting atom pairs into molecules. The atomic gas is prepared at a field $B$ away from resonance where the two atoms do not have a weakly bound state. In Fig. 31(a), this corresponds to $B>B_0$. The field is then ramped to a final $B<B_0$ to make a Feshbach molecule.

Regal *et al.* (2003a) created ultracold molecules in a degenerate Fermi gas of $^{40}$K, exploiting the resonance at 224 G in the *ac* channel. In the 10 G ramp across the resonance with a ramp speed of 25 G/ms, about 50% of the atoms were converted to molecules. The experimental signatures, shown in Fig. 32(a), were a disappearance of atoms when the field was ramped below 224 G and a recovery of the atoms when the field was ramped back. Since the Feshbach bound state exists below 224 G, their observation strongly suggests formation and dissociation of Feshbach molecules below and above 224 G, respectively. For the 202 G resonance in the *ab* channel of $^{40}$K, Hodby *et al.* (2005) reported conversion efficiencies of up to 80%. This resonance was also used for the formation of a molecular BEC (see Sec. IV.B.1).

Feshbach ramps were also applied to degenerate Fermi gases of $^{6}$Li in the lowest two spin states (*ab* channel) using both the narrow resonance at 543 G (Strecker *et al.*, 2003) and the broad resonance at 834 G (Cubizolles *et al.*, 2003). These two resonances in $^{6}$Li are discussed in Sec. II.B.5. Both experiments revealed a remarkable collisional stability of the molecules (see Sec. V.B.3).

In bosonic gases, an efficient atom-molecule conversion by a Feshbach ramp has to overcome inelastic col-

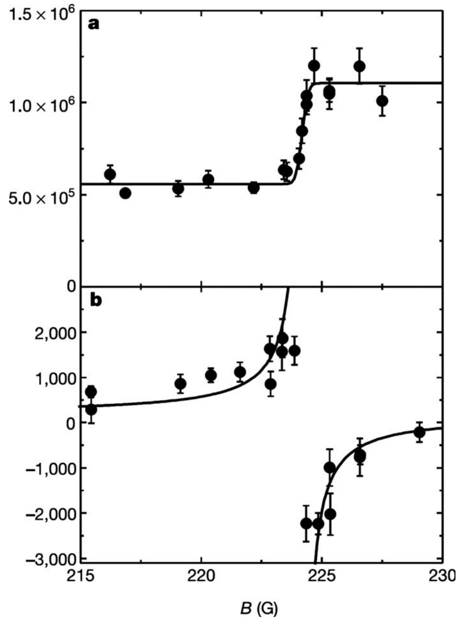


FIG. 32. Molecule formation in a $^{40}$K gas near the 224 G Feshbach resonance. (a) The number of atoms measured after a ramp across the resonance as a function of the final magnetic field shows the disappearance of atoms having formed molecules. (b) For comparison shows the magnetic field dependence of the $s$-wave scattering length in units of the Bohr radius, as measured by radio-frequency spectroscopy. From Regal *et al.*, 2003a.

lision loss during the ramp process (see Sec. V.B.3). In general, ramps applied to bosonic atom samples do not only create weakly bound Feshbach molecules, but they also lead to atom loss that cannot be recovered by a reverse field ramp. These atoms are lost presumably to deeply bound molecular states as a result of atom-molecule inelastic collisions. To optimize the Feshbach molecule fraction, which corresponds to the recoverable fraction, it is crucial to optimize the ramp speed. Furthermore, a fast separation of the molecules from the remaining atoms is essential. The latter can, for example, be achieved by Stern-Gerlach or optical methods.

Herbig *et al.* (2003) created a pure sample of about 3000 $g$-wave molecules from a BEC of $^{133}$Cs atoms by a Feshbach ramp across the narrow resonance at 20 G. The presence of an inhomogeneous magnetic field during the ramp facilitated an immediate Stern-Gerlach separation of the molecules from the atomic cloud. The Feshbach ramp removed about 60% of the atoms from the BEC, but only 20% were found in the weakly bound molecular state and thus could be recovered by a reverse field ramp. Expansion measurements on the $Cs_2$ cloud showed temperatures below 5 nK and suggested phase-space densities close to or exceeding unity. In later experiments on $^{133}$Cs, Chin *et al.* (2005), Mark, Kraemer, *et al.* (2007), and Knoop *et al.* (2008) produced Feshbach molecules in a variety of different internal states and partial waves including $s$-to $l$-wave ($\ell = 8$) states.

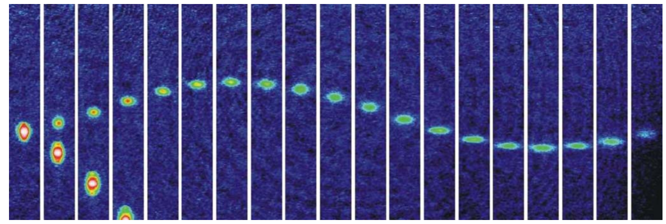

FIG. 33. (Color online) Motion of $^{87}Rb_2$ molecules in a magnetic field gradient. Right after the Feshbach ramp, the molecules are separated from the atoms because of the different magnetic moments. While the atom cloud leaves the observation region (see first four images) the molecules undergo an oscillatory motion, which is due to a changing magnetic moment caused by an avoiding level crossing in the molecular states. The images correspond to steps of 1 ms, and the field of view of each image is $0.24 \times 1.7$ mm. From Dürr, Volz, Marte, and Rempe, 2004.

Dürr, Volz, Marte, and Rempe (2004) applied a similar scheme to a $^{87}$Rb BEC and formed 7000 $s$-wave molecules near the 1007 G resonance with a 7% conversion efficiency. A magnetic gradient was applied right after the Feshbach ramp to separate atoms and molecules. The experiments showed remarkable oscillations of the molecular cloud in the gradient field (Fig. 33), which appear as a result of the changing magnetic moment near an avoided crossing between two molecular states. The creation of $^{87}$Rb Feshbach molecules has led to fascinating applications in optical lattices (see Sec. VI.B.1).

Xu *et al.* (2003) demonstrated molecule formation with a 4% conversion efficiency in a large BEC of $^{23}$Na atoms by a Feshbach ramp across the 907 G resonance. A large number of more than $10^5$ Feshbach molecules were observed. Expansion measurements on the $Na_2$ cloud showed that it was in the quantum-degenerate regime. By diffraction off an optical standing wave, Abo-Shaeer *et al.* (2005) demonstrated the matter-wave coherence of $Na_2$ molecules.

Hodby *et al.* (2005) presented a model of the atom-molecule conversion efficiency that is valid for both near-degenerate fermionic and bosonic atoms. Figure 34 shows a comparison of this model with data from experiments on $^{40}$K and $^{85}$Rb. The atom-molecule conversion efficiency follows a Landau-Zener-like behavior

$$\frac{P}{P_{\max}} = 1 - \exp\left( -\alpha n \frac{\hbar}{m} \left| \frac{\Delta a_{\rm bg}}{\dot{B}} \right| \right), \tag{61}$$

where $P_{\max}$ is the maximum conversion efficiency, solely determined by the phase-space density of the atomic cloud. This expression reveals a simple dependence on the resonance parameters $\Delta$ and $a_{\rm bg}$, the atomic number density $n$, and the ramp speed $\dot{B}$; the dimensionless prefactor $\alpha$ is discussed by Köhler *et al.* (2006).

Improved conversion techniques have been reported for atomic BECs. For the case of the narrow 20 G $g$-wave resonance of $^{133}$Cs, Mark *et al.* (2005) successfully converted 30% of the atoms into Feshbach mol-

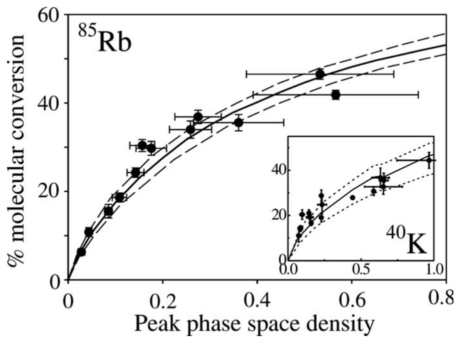


FIG. 34. Illustration of the dependence of the atom-molecule conversion efficiency on the atomic phase-space density. The main figure shows the results obtained in a near-degenerate bosonic gas of $^{85}$Rb atoms, while the inset shows corresponding results on a fermionic gas of $^{40}$K atoms. The lines refer to a theoretical model that is based on the phase-space overlap of atom pairs in the trapped gases. From Hodby et al., 2005.

ecules. Their scheme relied on fast switching of the magnetic field from 21 G right on the resonance, followed by a hold time of ~10 ms and a further switch to 18 G. This scheme was found to be superior to using an optimized linear ramp.

Feshbach ramps have also been applied to create $p$-wave molecules in ultracold Fermi gases. Formation of $p$-wave molecules in a $^6$Li gas was reported by Zhang et al. (2004) based on the 185 G resonance in the $ab$ channel. Fuchs et al. (2008) measured the binding energies of such $p$-wave Feshbach molecules in three channels ($aa$, $ab$, and $bb$) using an oscillating magnetic field (see Sec. III.A.5). Inada et al. (2008) studied the collisional properties of these molecules in all three channels. Gaebler et al. (2007) created $p$-wave molecules in a $^{40}$K gas by fast switching of the magnetic field to the $p$-wave Feshbach resonances at 198.4 and 198.8 G (both in the $bb$ channel) and studied the lifetimes of the molecules.

Similarly, Feshbach ramps have also been applied to ultracold atomic mixtures to create heteronuclear molecules, such as $^{40}$K $^{87}$Rb (Ni et al., 2008) and $^6$Li $^{40}$K (Voigt et al., 2008). An isotopic rubidium mixture was used to associate $^{85}$Rb $^{87}$Rb molecules by Papp and Wieman (2006). A variety of other heteronuclear molecule systems is currently under investigation in different laboratories. Feshbach ramps have become a standard approach to create ultracold molecules and serve as a starting point to investigate the dynamics and the interaction properties of Feshbach molecules.

### 2. Oscillatory fields

Another powerful method to produce ultracold Feshbach molecules is based on a modulation of the magnetic field strength (Thompson et al., 2005b; Hanna et al., 2007). The oscillating field induces a stimulated transition of two colliding atoms into a bound molecular state [see Fig. 31(b)]. Heating and atom loss are reduced since association occurs at a bias field $B$ away from the resonance position $B_0$. For a $^{85}$Rb BEC near the 155 G resonance, Thompson et al. (2005b) reported on high conversion efficiencies for molecules with binding energies on the order of 10 kHz; the molecule formation was inferred from the observation of a resonant loss signal. Lange et al. (2009) used the same method to explore weakly bound molecular states of Cs atoms in the $aa$ channel in an energy range of up to 300 kHz.

In a $^{40}$K spin mixture, $p$-wave molecules were produced with an oscillating magnetic field near the 198 G resonance doublet in the $bb$ channel (Gaebler et al., 2007). The method was also applied to produce heteronuclear $s$-wave molecules in mixtures of the two Rb isotopes (Papp and Wieman, 2006) and of $^{41}$K and $^{87}$Rb atoms (Weber et al., 2008).

In contrast to the magnetic field modulation method, radio-frequency transitions in the range of tens of MHz that involve a change of spin channel can also be used to associate two atoms to make a Feshbach molecule. This is the inverse of the dissociation process described in Sec. III.A.5. In this way Klempt et al. (2008) and Zirbel, Ni, Ospelkaus, Nicholson, et al. (2008) achieved association of $^{87}$Rb and $^{40}$K in a dipole trap. Similar association experiments in an optical lattice are described in Sec. VI.B.1.

### 3. Atom-molecule thermalization

A particular situation for molecule formation arises in a spin mixture of $^6$Li near the 834 G Feshbach resonance. At the low-field side of the resonance there is a broad field range, where the $s$-wave scattering length is large and positive. Here a weakly bound state exists with a pronounced halo character. The molecular state shows an extraordinary stability against inelastic decay, which opened the way to efficiently create molecular BECs by straightforward evaporative cooling at a constant magnetic field near 764 G (Jochim et al., 2003b; Zwierlein et al., 2003).

The formation of molecules in this region can be understood in terms of a chemical atom-molecule equilibrium (Chin and Grimm, 2004; Kokkelmans et al., 2004), where exoergic three-body recombination events compete with endoergic two-body dissociation processes. From a balance of these processes one can intuitively understand that molecule formation is favored at low temperatures and high number densities, i.e., at high phase-space densities. Indeed, for a nondegenerate gas, the atom-molecule equilibrium follows a simple relation (Chin and Grimm, 2004)

$$\phi_{\mathrm{mol}} = \phi_{\mathrm{at}}^2 \exp(E_b/k_B T), \quad (62)$$

where $\phi_{\mathrm{mol}}$ and $\phi_{\mathrm{at}}$ denote the molecular and atomic phase-space densities, respectively. The Boltzmann factor, determined by the ratio of the molecular binding energy $E_b$ and the thermal energy $k_BT$, enhances the fraction of molecules and can partially compensate for a low atomic phase-space density.

The thermal atom-molecule equilibrium was experimentally investigated by Jochim et al. (2003a) in a non-

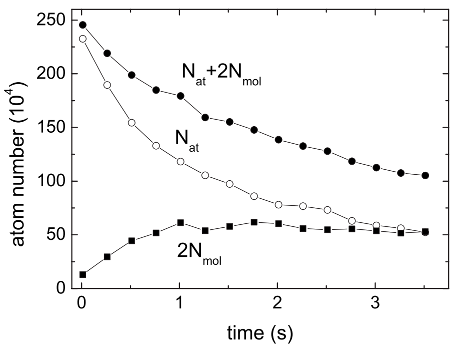


FIG. 35. An ultracold $^6$Li gas approaches a chemical atom-molecule equilibrium on the molecular side of the 834 G Feshbach resonance. The experiment starts with a nondegenerate purely atomic gas at a temperature of 2.5 $\mu$K and a peak atomic phase-space density of 0.04. The magnetic field is set to 690 G, where the molecular binding energy corresponds to 15 $\mu$K. $N_{at}$ and $N_{mol}$ denote the number of unbound atoms and the number of molecules, respectively. The total number of unbound and bound atoms $2N_{mol}+N_{at}$ slowly decreases because inelastic loss is not fully suppressed. From Jochim *et al.*, 2003a.

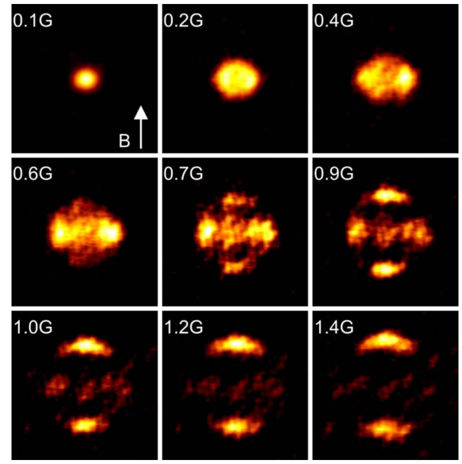


FIG. 36. (Color online) Dissociation patterns of $^{87}Rb_2$ molecules, showing the interference of *s*- and *d*-partial waves. At small magnetic field offsets $B-B_0$ (values given in the upper left corners), the *s*-wave pattern dominates; at large offsets, *d* waves are strongly enhanced due to a *d*-wave shape resonance. From Volz *et al.*, 2005.

degenerate gas of $^6$Li atoms. Figure 35 shows how the initially pure atomic gas tends to an atom-molecule equilibrium. The observation that more than 50% of the atoms form molecules at a phase-space density of 0.04 highlights the role of the Boltzmann factor. The chemical atom-molecule equilibrium also played an essential role in the experiment by Cubizolles *et al.* (2003), where a slow Feshbach ramp, which kept the sample in thermal equilibrium, led to a conversion efficiency of 85%.

### B. Properties

#### 1. Dissociation and detection

A general way to detect Feshbach molecules is their controlled dissociation through reverse magnetic field sweeps, followed by imaging of the resulting cloud of atoms. If the image is taken immediately after the forced dissociation, it reflects the spatial distribution of the molecules before the onset of dissociation. However, if the image is taken after a certain time of flight, it will be strongly affected by a release of kinetic energy. The image then contains additional information on the dissociation process.

A reverse Feshbach ramp brings the molecule into a quasibound state above the dissociation threshold, from which it decays into two atoms in the continuum. The decay rate $\Gamma(E)/\hbar$ depends on the energy $E$ above threshold and can be calculated from Eqs. (14), (17), and (22),

$$\Gamma(E) = 2ka_{bg}\delta\mu\Delta = 2k\bar{a}\bar{E}s_{res}. \tag{63}$$

Mukaiyama *et al.* (2004) gave the energy spectrum of hot atoms using this Fermi's golden rule expression for a linear ramp and showed that it agreed well with measurements with $^{23}Na_2$ Feshbach molecules. Góral *et al.* (2004) verified the golden rule theory with a full quantum dynamics calculation of Feshbach molecule dissociation.

The mean kinetic energy released in a reverse Feshbach ramp corresponds to the typical energy that the molecules can reach in the quasibound level before the dissociative decay takes place. In experiments on $^{87}Rb_2$, Dürr, Volz, and Rempe (2004) studied the dependence of the energy release on the ramp rate and on the resonance width. They demonstrated kinetic energy measurements after reverse Feshbach ramps as a powerful indirect tool to determine the widths of weak resonances with $\Delta$ in the mG range, where direct methods are impractical. They also demonstrated the production of a monoenergetic spherical wave of atoms by rapidly switching the magnetic field instead of ramping it.

The dissociation properties of Feshbach molecules can provide additional spectroscopic information. Volz *et al.* (2005) observed interesting dissociation patterns of $^{87}Rb_2$ when the molecular state was brought high above the threshold with fast jumps of the magnetic field. The patterns, shown in Fig. 36, reveal a *d*-wave shape resonance. The dissociation of $^{133}Cs_2$ molecules in *l*-wave states was observed by Mark, Kraemer, *et al.* (2007). The dissociation pattern showed a strikingly different behavior from molecules in a *g*-wave state and allowed to clearly distinguish between these two types of molecules.

We note that direct imaging of Feshbach molecules is not feasible in most situations because of the absence of cycling optical transitions. An exception, however, is the direct imaging of atoms in halo states as demonstrated for $^6$Li (Zwierlein *et al.*, 2003; Bartenstein *et al.*, 2004b). In this special case, the extremely weakly bound dimer absorbs resonant light essentially like free atoms.

### 2. Halo dimers

Broad entrance-channel dominated *s*-wave resonances feature a considerable region where Feshbach molecules acquire universal properties [see Sec. II and Köhler *et al.* (2006)]. "Universality" means that details of the interaction become irrelevant and that all properties of the dimer are characterized by a single parameter, the *s*-wave scattering length $a$ or alternatively the binding energy $E_b = \hbar^2/ma^2$. The reason for this simplification is the fact that the wave function extends far out of the classical interaction range of the potential. States of this kind have been coined "quantum halos." They have attracted considerable attention in nuclear physics and, more recently, in molecular physics and have been reviewed by Jensen *et al.* (2004). An early example is the deuteron, where the neutron and proton are likely to be found outside of the classically allowed region. Before the advent of Feshbach molecules, the most extended halo system experimentally accessible was the helium dimer ($^4He_2$), which is about ten times larger than typical diatomic molecules. An extreme example is given by Bose-condensed $^6Li_2$ Feshbach dimers with a size of $a/2 \simeq 2000a_0$, which exceeds the van der Waals length $R_{vdW} \simeq 30a_0$ by almost two orders of magnitude.

First experiments on halo dimers have been conducted with bosonic $^{85}$Rb (Donley *et al.*, 2002) and $^{133}$Cs (Mark, Ferlaino, *et al.*, 2007) and fermionic $^{40}$K and $^6$Li (see Sec. IV.B.1). For $^{85}$Rb, the dimers are not formed from atoms in the lowest internal states and thus have open decay channels. This leads to spontaneous dissociation without the presence of other atoms or molecules. Thompson *et al.* (2005a) observed an $a^{-3}$ scaling of the dissociation rate, which can be understood as a direct consequence of universality through wave-function overlap arguments (Köhler *et al.*, 2005). For halo dimers of $^{133}Cs_2$ created from atoms in their lowest internal states there are no open dissociation channels. These molecules cannot decay spontaneously but decay through collisions with other atoms or molecules (Ferlaino *et al.*, 2008; Knoop *et al.*, 2009).

A future promising direction with Feshbach molecules in halo states is the experimental investigation of universal few-body physics (see Sec. VI.C).

### 3. Collision properties

Fast collisional loss is usually observed in trapped samples of ultracold molecules. This has been seen in experiments with bosonic $^{23}Na_2$ (Mukaiyama *et al.*, 2004), $^{87}Rb_2$ (Wynar *et al.*, 2000; Syassen *et al.*, 2006), and $^{133}Cs_2$ (Chin *et al.*, 2005). Zirbel, Ni, Ospelkaus, Nicholson, *et al.* (2008) measured large rate coefficients for fermionic $^{40}$K $^{87}$Rb Feshbach molecules due to collisions with $^{87}$Rb or $^{40}$K. Both atom-dimer and dimer-dimer collisions are generally found to cause strong inelastic loss, as shown by the example in Fig. 37. Vibrational relaxation is the dominant mechanism, which leads to large loss rate coefficients of the order of $10^{-10}$ cm$^3$/s. Rate coefficients of such magnitude result in molecular lifetimes on the order of a few ms or less for density characteristic of ultracold gases. Rearrangement reactions, such as trimer formation, may also play a significant role in limiting molecular lifetimes.

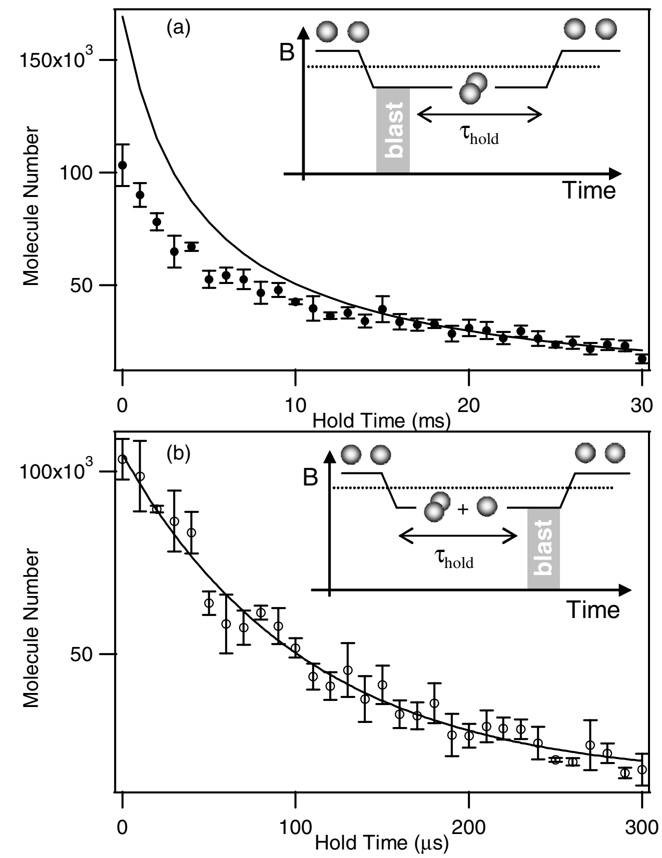


FIG. 37. Fast collisional decay of $^{23}Na_2$ Feshbach molecules. The molecules are trapped (a) alone or (b) together with atoms. From Mukaiyama *et al.*, 2004.

Inelastic collision rates of Feshbach molecules in the very highest bound state, when they are not universal halo states, are not significantly different from rates for more deeply bound states, for which fast inelastic loss has been observed (Staanum *et al.*, 2006; Zahzam *et al.*, 2006) and predicted (Quéméner *et al.*, 2005; Cvitas *et al.*, 2007). Hudson *et al.* (2008) measured large inelastic collision rate coefficients for vibrationally excited triplet $^{87}$Rb $^{133}$Cs molecules colliding with $^{133}$Cs or $^{87}$Rb atoms. They also used a simple model to help understand why such large rate constants are typical for atom-molecule vibrational relaxation. Assuming a probability near unity for inelastic loss when the collision partners approach one another in the short-range region of chemical bonding, the overall collision rate coefficient is then determined from the threshold scattering of the long-range van der Waals potential. In effect, the rate constant is given by Eq. (10), where the length $b$ turns out to be similar in magnitude to the van der Waals length $R_{vdW}$. Such a simple model gives the typical order of magnitude of $10^{-10}$ cm$^3$/s for the vibrational relaxation rate constant, nearly independent of the vibrational level, found for the $^{87}$Rb or $^{133}$Cs system.

Halo molecules comprised of two unlike fermions bound in an $s$-wave state offer an exception to the rule of fast inelastic dimer-dimer and atom-dimer collisions. This has allowed stable molecular samples and even molecular Bose-Einstein condensation (see Sec. IV.B). Petrov *et al.* (2004) showed that a combination of two effects explains this stability. The first effect is a small wave-function overlap of a halo dimer with more deeply bound dimer states, and the second one is Pauli suppression in the few-body process. For inelastic dimer-dimer collisions, Petrov *et al.* (2004) predicted the rate coefficient for inelastic loss to scale as $(a/R_{\mathrm{vdW}})^{-2.55}$ whereas for the elastic part they obtained a dimer-dimer scattering length of $0.6a$. For the atom-dimer interaction, the predicted scaling of inelastic loss is $(a/R_{\mathrm{vdW}})^{-3.33}$ and the scattering length is $1.2a$.

An interesting case is the observation of stable $^{6}\mathrm{Li}_2$ molecules created near the closed-channel dominated resonance at 543 G (Strecker *et al.*, 2003). These are not halo molecules and would be expected to have a large collisional loss rate coefficient similar to molecules comprised of bosons. The collision properties of these molecules await detailed investigation.

A possible way to overcome harmful inelastic collisional loss is the application of an optical lattice (Thalhammer *et al.*, 2006). Here a pair of atoms or a single molecule can be trapped in an individual lattice site, which offers shielding from collisions with other molecules or atoms. Many experiments on ultracold molecules are now performed with Feshbach resonances and molecules in an optical lattice (see discussion in Sec. VI.B). Another way to prevent inelastic collisions of ultracold molecules is to transfer them to their lowest energy ground state, where they do not undergo vibrational, rotational, or spin relaxation. However, reactive collisions may still be possible.

#### 4. Internal state transfer

A Feshbach resonance can serve as an "entrance gate" into the rich variety of molecular states below threshold, allowing preservation of the ultralow temperature of the atomic gas that is used as a starting point. The magnetic association technique (Sec. V.A.1) produces a molecule in a specific weakly bound molecular state, i.e., the particular molecular state that represents the closed scattering channel of the resonance. This leads to the question how a Feshbach molecule can be transferred to other states with specific properties of interest or, ultimately, to the absolute rovibrational ground state. Various methods have been developed for a controlled internal state transfer based on magnetic field ramps, radio-frequency or microwave radiation, or optical Raman excitations.

When a Feshbach ramp after initially associating the molecules is continued over a wider magnetic field range, the molecule will perform a passage through many level crossings (see, e.g., Fig. 14). The ramp speed controls whether crossings are traversed diabatically (fast ramp) or whether they are followed adiabatically

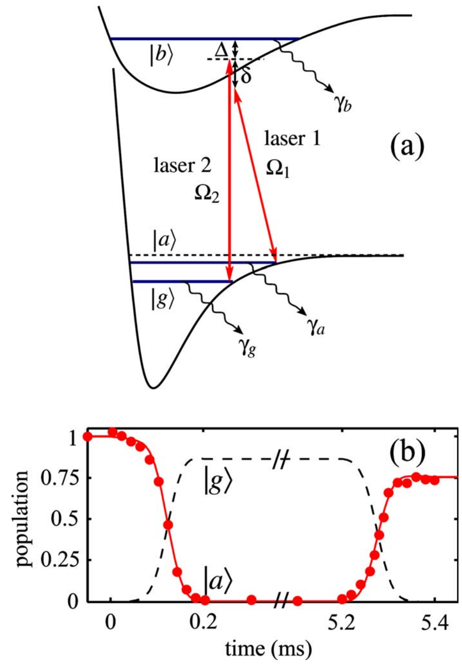


FIG. 38. (Color online) STIRAP with Feshbach molecules. (a) After creation of Feshbach molecules in a weakly bound state $|a\rangle$, a two-photon transition is used to transfer the molecules into a more deeply bound state $|g\rangle$. In the counterintuitive pulse sequence of STIRAP, laser field 2 is switched on before laser field 1, and the molecule is always kept in a dark superposition state of $|a\rangle$ and $|g\rangle$ during the transfer sequence. This suppresses the unwanted electronic excitation of state $|b\rangle$ and leads to a very high transfer efficiency. The measurements shown in (b) refer to an experiment in $^{87}\mathrm{Rb}_2$, where $|a\rangle$ and $|g\rangle$ correspond to the last and second-to-last bound vibrational levels. The data show the measured population in $|a\rangle$ during a 0.2 ms transfer sequence and a reverse transfer sequence after a 5 s hold time in state $|g\rangle$. The observed efficiency of 75% for a double passage corresponds to single-passage transfer efficiency of 87%. Adapted from Winkler *et al.*, 2007.

(slow ramp). Mark, Ferlaino, *et al.* (2007) demonstrated the controlled transfer of $^{133}\mathrm{Cs}_2$ molecules into different states by elaborate magnetic field ramps. In this way, they could populate various states from $s$ up to $l$ waves with binding energies of up to ~10 MHz. In practice, finite ramp speeds limit this method to rather weak crossings with energy splittings of up to typically 200 kHz. Lang, van der Straten, *et al.* (2008) showed how this problem can be overcome with the help of radio-frequency excitation. They demonstrated the transfer of $^{87}\mathrm{Rb}_2$ molecules over nine level crossings when the magnetic field was ramped down from the 1007 G resonance to zero field in 100 ms. This produced molecules having a binding energy $E_b = h\times 3.6$ GHz with a total transfer efficiency of about 50%.

More deeply bound states can be reached by two-photon Raman transitions, as implemented in a very efficient way by stimulated Raman adiabatic passage (STIRAP) (Bergmann *et al.*, 1998). Figure 38 shows STIRAP between the two highest vibrational levels in $^{87}\mathrm{Rb}_2$ with binding energies corresponding to 24 and

637 MHz, as demonstrated in a proof-of-principle experiment by Winkler *et al.* (2007). The experiment also highlighted the potential of the approach to combine Feshbach association with stimulated Raman optical transitions, as originally suggested by Kokkelmans *et al.*, (2001) to create deeply bound molecules.

In 2008 experimental progress was made in applications of STIRAP to transfer both homonuclear and heteronuclear Feshbach molecules into deeply bound states. Danzl *et al.* (2008) explored $^{133}Cs_2$ molecules and demonstrated large binding energies corresponding to 31.8 THz. Lang, Winkler, *et al.* (2008) reached the rovibrational ground state in the triplet potential of $^{87}Rb_2$, the binding energy of which corresponds to 7.0 THz. The heteronuclear case was successfully explored with $^{40}K^{87}Rb$. Initial experiments by Ospelkaus *et al.* (2008) demonstrated the transfer to states with a binding energy corresponding to 10.5 GHz. Only shortly afterward, the same group (Ni *et al.*, 2008) demonstrated polar molecules in both the triplet and singlet rovibrational ground states, where the binding energies correspond to 7.2 and 125 THz, respectively. These experiments opened up a promising new research field related to the exciting interaction properties of ground-state molecular quantum gases.

All the above methods for controlled state transfer rely on coherent processes. Therefore they can also be applied to produce coherent superpositions of molecular states. This can, for example, be used for precise interferometric measurements of the molecular structure. Mark, Kraemer, *et al.* (2007) and Lang, van der Straten, *et al.* (2008) investigated molecular level crossings in this way. Using STIRAP, Winkler *et al.* (2007) created quantum superpositions between neighboring vibrational states and tested their coherence interferometrically.

## VI. RELATED TOPICS

### A. Optical Feshbach resonances

Magnetic fields have proven to be a powerful tool to change the interaction strength or scattering length between ultracold atoms. As discussed in this review this has been made possible by the presence of a molecular bound state that is resonantly coupled to the colliding atom pair. The width of the resonance [$\Delta$ in Eq. (1)], however, is governed by the interatomic forces between the two atoms. Optical Feshbach resonances promise control of both the resonance location and its width.

#### 1. Analogies

Figure 39 shows a schematic diagram of an optical Feshbach resonance. As first proposed by Fedichev, Kagan, *et al.* (1996) laser light nearly resonant with a transition from a colliding atom pair and a rovibrational level of an excited electronic state induces a Feshbach resonance and modifies the scattering length of the two atoms. Excited electronic states dissociate to one ground and one electronically excited atom for large interatomic separations. For many kinds of atoms the photon needed to reach such states is in the visible or optical domain and, hence, the term optical Feshbach resonance has been adopted.

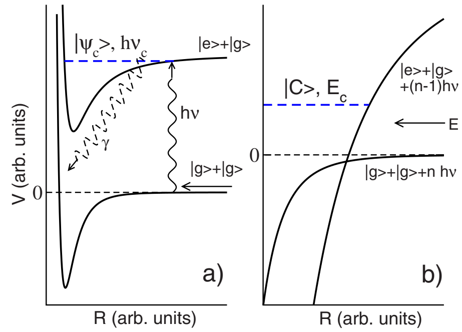


FIG. 39. (Color online) Schematic of an optical Feshbach resonance. (a) Two colliding ground-state atoms $|g\rangle$ are coupled through a laser at frequency $\nu$ to a vibrational level $|\psi_c\rangle$ of an excited electronic state that dissociates to one excited-state $|e\rangle$ and one ground-state $|g\rangle$ atom. The energy $h\nu_c$ is the energy of the vibrational level relative to two colliding atoms at zero collision energy. The excited bound state $|\psi_c\rangle$ irreversibly decays with an (energy) width $\gamma$. (b) The dressed state picture corresponding to (a). The initial state is an atom pair with $n$ photons and the closed channel state $|C\rangle$ represents $|\psi_c\rangle$ with $n-1$ photons. The atom pair has a relative kinetic energy $E$ and $E_c = h\nu_c - h\nu$. In the dressed state picture the ground and excited interatomic potentials cross at a point called the Condon point.

The location and strength of an optical Feshbach resonance are determined by the laser frequency $\nu$ and intensity $I$, respectively. Both can be controlled experimentally. There is, however, a crucial difference between magnetic and optical Feshbach resonances. For optical Feshbach resonances the resonant state has a finite energy width $\gamma$ and thus lifetime $\hbar/\gamma$ due to spontaneous emission. Hence the scattering length becomes a complex number.

Note that by changing the laser frequency and simultaneously detecting the population in the excited electronic potentials the rovibrational level structure of these potentials can be studied. This is called ultracold photoassociative spectroscopy and has been reviewed by Jones *et al.* (2006).

Bohn and Julienne (1996, 1999) obtained expressions for the complex scattering length in Eqs. (24) and (25). Resonances are characterized by a width $\Gamma(E)$ and shift $h\delta\nu_c$, where $E_0 = h\nu_c - h\nu - h\delta\nu_c$. The width is

$$\Gamma(E) = 2\pi|\langle C|\vec{d}\cdot\vec{\mathcal{E}}|E\rangle|^2, \tag{64}$$

where $\vec{\mathcal{E}}$ is the electric field of the laser and $\vec{d}$ is the molecular electronic transition dipole moment. Both the width and the shift of the resonance are proportional to $I$. As in magnetic resonances $|E\rangle$ is the scattering wave function at collision energy $E$ in the entrance channel.

Figure 6 in Sec. II.A.3 shows the real and imaginary parts of the scattering length $a - ib$ for an optical Feshbach resonance. The numbers are based on an analysis of the strength and lifetime of an experimentally observed optical Feshbach resonance in $^{87}$Rb (Theis *et al.*, 2004). For the intensity used in the figure the optical length $a_{\mathrm{res}}$ defined by Eq. (26) is 5.47 nm and $\Gamma_0/h$ =21 MHz. That is, $a_{\mathrm{res}} \approx a_{\mathrm{bg}}$ and $\Gamma_0 \approx \gamma$. Since $ka_{\mathrm{bg}} \ll 1$, the width $\Gamma(E) \ll \gamma$ so that there is negligible power broadening. Unlike for a magnetic Feshbach resonance, the real part of the scattering length is now finite for any detuning with a peak to peak variation of $2a_{\mathrm{res}}$. The length $b$ peaks at zero detuning. The maximum value is $2a_{\mathrm{res}}$ and the full width at half maximum is $\gamma$.

In order for an optical Feshbach resonance to be practical it is necessary that the change in the real part of the scattering length $a-a_{\mathrm{bg}}$ is large compared to $b$. This requires that the detuning $h\nu - h\nu_c$ is large compared to $\gamma$. On the other hand, we would also like to ensure that $a-a_{\mathrm{bg}}$ is at least on the order of $a_{\mathrm{bg}}$ at such a detuning. In order to satisfy these requirements simultaneously we need $a_{\mathrm{res}} \gg a_{\mathrm{bg}}$ or equivalently $\Gamma_0 \gg \gamma$. For the parameters used in Fig. 6 this is not true. Section VI.A.3 discusses how for alkaline-earth atoms it is possible to satisfy $a_{\mathrm{res}} \gg a_{\mathrm{bg}}$.

By adding extra laser fields at different frequencies the scattering length can be further manipulated. Of particular interest is the case where a second field is nearly resonant with the excited bound state $|\psi_c\rangle$ and a second molecular bound state. If this second bound state is in the electronic ground state, then the situation corresponds to a Raman transition. The analytic expression for the scattering length (Bohn and Julienne, 1999; Thalhammer *et al.*, 2005) is

$$a - ib = a_{\mathrm{bg}} + \frac{1}{2k}\frac{\Gamma(E)}{h\nu - h\nu_0 + \Omega^2/\Delta_2 + i(\gamma/2)}, \tag{65}$$

where $a_{\mathrm{bg}}$, $\Gamma$, and $\gamma$ are defined as before and $h\nu_0 = h\nu_c + h\delta\nu_c$. The two-photon detuning $\Delta_2$ is zero when the absolute value of the frequency difference of the two lasers equals the absolute value of binding energy of the ground bound state relative to two free atoms at rest. It is positive when the absolute value of the frequency difference is larger than the absolute value of the binding energy. The quantity $\Omega$ is the coupling matrix element between the bound levels in the ground and excited states and is proportional to the square root of the intensity of the second laser.

### 2. Observations in alkali systems

In a magneto-optical trap filled with cold ($<1$ mK) atomic sodium Fatemi *et al.* (2000) confirmed the predictions of Fedichev, Kagan, *et al.* (1996). They observed the changing scattering length by detecting the corresponding change in the scattering wave function. Weak detection lasers, with frequencies that differ from those used for the optical Feshbach resonance, induce a molecular ion signal that probes the change in the scattering wave function. For the molecular level used in the experiment Fatemi *et al.* (2000) were able to deduce the strength of the resonance as well as the light shift $\delta\nu_c$.

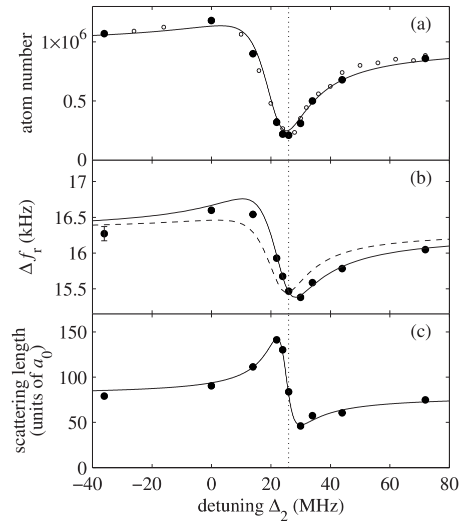


FIG. 40. Optical Feshbach resonance using a two-color Raman transition in an $^{87}$Rb BEC. (a) The measured atom number after a 100 $\mu$s Raman pulse as a function of the two-photon detuning $\Delta_2$. (b) The measured Bragg resonance frequency. (c) The scattering length, as determined from (a) and (b). The open and filled circles correspond to the data. As indicated by the error bar in (b) the frequency uncertainty in the Bragg spectroscopy is smaller than 100 Hz. The solid lines have been obtained from a fit to Eq. (65) adapted to include the finite linewidth of the ground-bound state. The dashed line in (b) shows the expected signal if there was only loss in atom number but no change in scattering length. The vertical line indicates the location of maximal loss in (a) and helps us to compare the relative positions of the three curves. From Thalhammer *et al.* (2005).

They found an $a_{\mathrm{res}}$ of around 2 nm and $\Gamma_0/h$ of around 20 MHz for the maximum reported laser intensity of $I = 100\ \mathrm{W/cm^2}$. For Na the background scattering length is $a_{\mathrm{bg}} = 2.8$ nm.

Theis *et al.* (2004) tuned the scattering length by optical means in a Bose-Einstein condensate. In a $^{87}$Rb condensate they were able to change the scattering length over one order of magnitude from 0.5 to 10 nm. The parameters of the optical resonance are given in the caption of Fig. 6. The scattering length was measured using Bragg spectroscopy, where a change in condensate mean-field energy proportional to the scattering length is measured by a change in the frequency that determines the Bragg condition.

Thalhammer *et al.* (2005) modified the scattering length by a two-color Raman transition. As from Theis *et al.* (2004) the change in scattering length was observed in an $^{87}$Rb condensate and detected by Bragg spectroscopy. In fitting to Eq. (65) a complication arose. Thalhammer *et al.* (2005) could only explain their observations if they assumed that the target ground state had a finite linewidth. It turned out that, even though this state cannot be lost by spontaneous emission, it can absorb a photon from the (strong) laser that photoassociates the scattering atom pair. This process gave rise to a linewidth of 2 MHz. The results are shown in Fig. 40.

#### 3. Prospects in alkaline-earth systems

The scattering length so far has been experimentally modified by optical means in ultracold alkali-metal atom collisions. In these experiments the optical length $a_{\mathrm{res}}$ was of the same order of magnitude as the background scattering length $a_{\mathrm{bg}}$ so that changes in scattering length were accompanied by large atom losses. Ciuryło *et al.* (2005) showed that optical Feshbach resonances in ultracold alkaline-earth atom collisions can have $a_{\mathrm{res}} \gg a_{\mathrm{bg}}$. The presence of intercombination lines in alkaline-earth systems make this possible. Atomic intercombination lines are transitions between the ground ${}^1S_0$ state and the excited ${}^3P_1$ state. The transition is only weakly allowed by virtue of relativistic mixing with the ${}^1P_1$ state. For example, for Sr isotopes $\gamma/h = 7.5$ kHz is much smaller than for alkali atoms.

When $\gamma$ is small, it is possible to use excited bound levels that are very close to the excited-state dissociation threshold while simultaneously maintaining the large detunings that are necessary to suppress losses. Using levels close to threshold allows a very large value of the ratio $\Gamma_0/\gamma$, and consequently $a_{\mathrm{res}}$ can be orders of magnitude larger than $a_{\mathrm{bg}}$. Ciuryło *et al.* (2005) illustrated this by model calculations of optical lengths of ultracold calcium, for which $\gamma/h = 0.7$ kHz. Using a model that assumes a level with a binding energy on the order of 100 MHz, they predicted that $a_{\mathrm{res}}$ could be as large as 100 nm at the relatively low intensity of $I = 1\ \mathrm{W/cm^2}$.

Zelevinsky *et al.* (2006) obtained photoassociation spectra near the intercombination line of $^{88}$Sr and measured the strength of various transitions. They found that the last bound state of the excited potential had an optical length $a_{\mathrm{res}} = 24\ \mu\mathrm{m}$ at $I = 1\ \mathrm{W/cm^2}$. The very large value of $a_{\mathrm{res}}$ implies that practical changes in the scattering length should be feasible in this species. Similar photoassociation spectra have been observed for two different isotopes of ytterbium (Tojo *et al.*, 2006), which has an electronic structure like that of the alkaline earth atoms. Optical control of both bosonic and fermionic isotopic species may become possible with alkaline earth or Yb atoms. Enomoto *et al.* (2008) demonstrated optically induced changes in scattering length for $^{172}$Yb and $^{176}$Yb.

### B. Feshbach resonances in optical lattices

Ultracold atoms in optical lattices are of great interest because of the exciting prospects to simulate a variety of condensed matter phenomena, to realize large scale quantum information processing (Bloch, 2005), and to form ultracold molecules in individual lattice sites to avoid detrimental collision instability. In all these research directions, Feshbach resonances provide excellent tools to control the interaction of the constituent atoms and to explore the transition between different quantum regimes and quantum phases. In the following sections we review atom-atom scattering in optical lattices and describe the role of Feshbach resonances therein.

Optical lattices are realized by standing-wave laser fields, which result in spatially periodic potentials for the atoms. The atoms are confined in the individual potential minima or sites of the lattice potential. One-, two-, and three-dimensional lattices can be created in this way. In experiments with three-dimensional configurations the optical lattice can be filled with only one or two atoms per site.

SectionVI.B.1 discusses that when two atoms are held in a single lattice site a Feshbach resonance can be used to efficiently produce stable molecules. One advantage of lattice confinement is that such molecules are protected from harmful collisional losses with a third body. Section VI.B.2 discusses the possibility that confinement in one spatial direction can induce resonant behavior in scattering along the remaining directions. Finally, Sec. VI.B.3 describes uses of Feshbach resonances in optical lattices where tunneling between lattices sites is important.

#### 1. Atom pairs and molecules

When an atom pair is trapped in a single site of a three-dimensional optical lattice the motion is fully quantized. For deep optical lattices the confining potential is harmonic, and the center of mass and relative motion of the atom pair separate. In other words the six-dimensional wave function of the two atoms becomes a product of a center of mass and relative wave function. The center-of-mass motion is harmonic and is solved trivially. The relative motion is determined by a potential that is the sum of the atom-atom interaction potentials and a harmonic potential.

The atom-atom interactions between alkali-metal atoms are independent of the relative orientation of the atoms when very weak spin-dependent interactions $V_{\mathrm{ss}}$ are ignored. Consequently, for a spherically symmetric harmonic trapping potential the three-dimensional relative motion can be further simplified. The angular motion can be solved analytically and only a radial Schrödinger equation for the atom-atom interaction potential plus $\mu\omega^2R^2/2$ needs to be solved. Here $\mu$ is the reduced mass and $\omega$ is the oscillation frequency in the trap.

Figure 41 shows eigenenergies for two Na atoms with zero relative orbital angular momentum ($\ell = 0$) in a spherically symmetric harmonic trap as a function of magnetic field (Tiesinga *et al.*, 2000). The atoms are in their lowest hyperfine state and the energies are obtained from coupled-channel calculations. For these atomic states there is a Feshbach resonance near 910 G (91 mT). The zero of the vertical axis corresponds to zero relative kinetic energy in the absence of a trapping potential. Hence, positive energies correspond to atoms in the trap and negative energies correspond to molecules bound in the atom-atom interaction potential. Avoided crossings between the closed

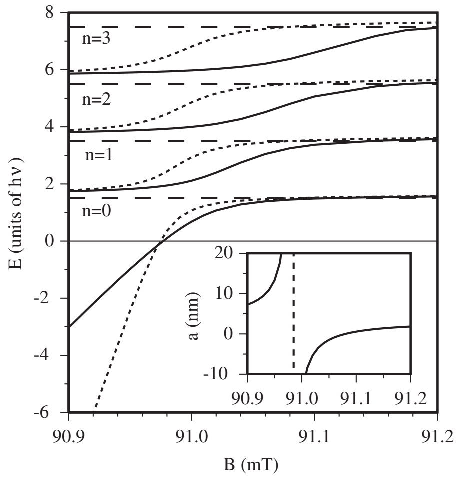


FIG. 41. The energy in the relative motion of two trapped interacting Na atoms in their lowest hyperfine state $|a\rangle$ as a function of magnetic field. The trapping frequency $\nu=\omega/2\pi$ is 1 MHz. The full lines correspond to energies obtained from exact numerical calculations. The dotted lines correspond to eigenenergies for trapped Na atoms interacting via a regularized delta-function potential with a magnetic field dependent scattering length given by the inset. This inset shows the exact scattering length for two freely scattering $|a\rangle$ states near a Feshbach resonance. In the theoretical model $B_0=90.985$ mT, whereas experimentally $B_0=90.7$ mT (see Sec. III.B.2). The long-dashed lines correspond to energies of the $\ell=0$, $n=0$, 1, 2, and 3 harmonic oscillator states. From Tiesinga *et al.*, 2000.

channel Feshbach state and the trap levels are clearly visible.

An analytic solution for two interacting atoms trapped in a harmonic trap was found by Busch *et al.* (1998). The atom-atom interaction was modeled by a so-called regularized delta-function potential $(4\pi\hbar^2/2\mu)a\delta(\vec{R})(d/dR)R$, where $a$ is the scattering length. This approximation of the actual interaction potential is valid in the Wigner threshold regime. In particular, they showed that the eigenenergies for the relative motion are given by

$$\frac{a}{\sigma}=\frac{\Gamma(-E/2+1/4)}{2\Gamma(-E/2+3/4)}, \tag{66}$$

where $\Gamma$ is the gamma function, the energy $E$ is in units of $\hbar\omega$, and $\sigma=\sqrt{\hbar/\mu\omega}$ is the harmonic oscillator length for the relative motion.

Near a magnetic Feshbach resonance the scattering length is a rapidly changing function of $B$ as, for example, shown in the inset of Fig. 41. The dotted lines in Fig. 41 are the eigenenergies found from combining Eq. (66) and the $a(B)$ for the resonance. The exact and model calculations do not agree where the scattering length is large. As shown by Blume and Greene (2002) and Bolda *et al.* (2003) this is due to the breakdown of the Wigner threshold regime at the finite zero-point energy of the atoms near the resonance. Blume and Greene (2002) introduced an energy-dependent scattering length based on the effective range theory. Bolda *et al.* (2002) found that an energy-dependent regularized delta-function potential reproduces well the exact results in Fig. 41.

Dickerscheid *et al.* (2005) and Gubbels *et al.* (2006) developed an analytic approach extending the theory of Busch *et al.* (1998) to the states of two trapped atoms in a single lattice site that interact strongly through a Feshbach resonance. They applied their two-body theory to the broad $^6$Li resonance near 834 G. They also showed how to incorporate this theory into a many-body Hubbard model that treats the tunneling of atoms between lattice sites.

Mies *et al.* (2000) theoretically showed that by varying the magnetic field in time two atoms in a single lattice site can be converted into a molecule with near 100% efficiency. The idea is to prepare the atoms in the lowest trap level at a magnetic field where the Feshbach state has a higher energy. In Fig. 41 this corresponds to the nominally $n=0$ state at, for example, $B=912$ G. The magnetic field is then varied. If the ramp is sufficiently slow, the atom pair will be adiabatically converted into a molecule. Mies *et al.* (2000) also showed that this process can be described by a Landau-Zener curve crossing model. A more recent derivation is given by Julienne *et al.* (2004).

Widera *et al.* (2004) used a magnetic Feshbach resonance to entangle two $^{87}$Rb atoms in a site of an optical lattice. In a Ramsey-type interferometer a sequence of microwave pulses manipulates and controls the superposition between the $|0\rangle\equiv|F=1,m_F=1|$ and $|1\rangle\equiv|F=2,m_F=-1\rangle$ hyperfine states of each $^{87}$Rb atom. Initially the atoms are in state $|0\rangle$. The population in the two hyperfine states after the pulses will depend on the atom-atom interaction, which entangles the two atoms. By controlling the scattering length with the magnetic field and the hold time between the pulses, Widera *et al.* (2004) were able to create maximally entangled Bell states.

Stöferle *et al.* (2006) spectroscopically mapped the avoided crossing between the Feshbach and the lowest harmonic oscillator state as a function a magnetic field. They prepared fermionic $^{40}$K atoms in a three-dimensional optical lattice configured such that the bottom of the lattice sites is spherically symmetric. The two atoms in each lattice site are in different hyperfine states. They confirmed that the model of trapped atoms interacting via an energy-dependent delta-function potential agrees with the experimental observations.

Thalhammer *et al.* (2006) showed in an experiment with $^{87}$Rb in its lowest hyperfine state that the Landau-Zener model for a time-dependent sweep of the magnetic field through the Feshbach resonance, as developed by Mies *et al.* (2000) and Julienne *et al.* (2004) is valid. The Feshbach resonance near 1007 G was used. In the experiment the ramp speed $dB/dt$ was varied over four orders of magnitude and for the slowest ramp speed of $2\times10^3$ G/s a 95% conversion efficiency was observed. The experiment demonstrated a dramatic increase in the lifetime of the trapped molecules, where

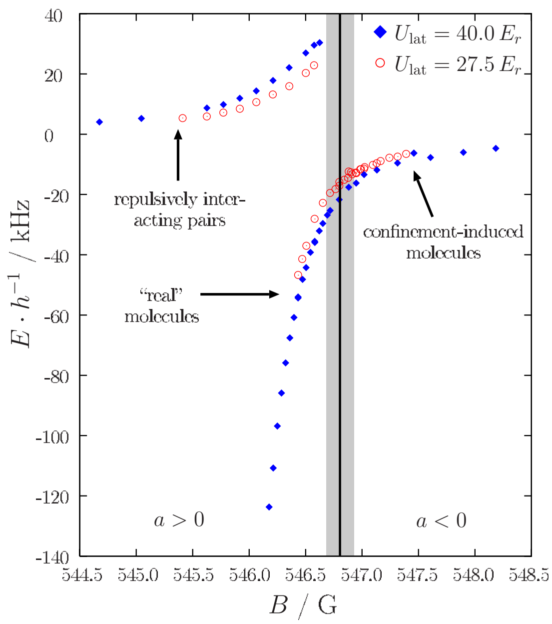


FIG. 42. (Color online) Energy of heteronuclear $^{40}$K-$^{87}$Rb molecules vs $B$ in an optical lattice for two different lattice depths $U_{\rm lat}$ in units of the $^{87}$Rb recoil energy $E_r = \hbar^2 k^2 / 2m_{\rm Rb}$ ($E_r/h \approx 3.7$ kHz). The center of the Feshbach resonance is located at $B_0 = 546.8(1)$ G. The zero of energy corresponds to two atoms in the lattice cell with $B$ far from $B_0$. Molecules which are stable in free space are observed for $B < B_0$ where $a > 0$. Confinement-induced molecules are observed for $B > B_0$ where $a < 0$ and no threshold bound state exists in free space. In addition, repulsively interacting pairs are observed for $B < B_0$. From Ospelkaus, Ospelkaus, Humbert, Ernst, *et al.*, 2006.

the lattice protected them from harmful collisions. Molecular lifetimes up to 700 ms were observed.

Ospelkaus, Ospelkaus, Humbert, Ernst, *et al.* (2006) were able to make heteronuclear molecules by associating atoms of two different species, $^{40}$K and $^{87}$Rb, trapped on the same lattice site. They used a rf association technique both to form the molecule and to measure its binding energy. Figure 42 shows the energy of the near-threshold states of the atom pair as a function of $B$ and illustrates an avoided crossing similar to that shown in Fig. 41. Deuretzbacher *et al.* (2008) developed a theoretical model to account for anharmonic corrections, which couple center-of-mass and relative motion of the atoms in the trap.

### 2. Reduced dimensional scattering

Optical lattices that confine atoms in only one or two directions in combination with magnetic Feshbach resonances lead to controllable quasi-2D or quasi-1D scattering, respectively. Yurovsky *et al.* (2008) recently reviewed such reduced dimensional scattering. By integrating out the confined spatial direction, effective one- and two-dimensional atom-atom potentials can be derived. Their strength is related to the magnetic-field dependent scattering length for free scattering.

Olshanii (1998) and Bergeman *et al.* (2003) derived the effective atom-atom potential for quasi-one-dimensional scattering. As for Busch *et al.* (1998) the starting point is a regularized three-dimensional delta-function potential for the atom-atom interaction potential. The trapping potential along the two confined dimensions is the same and harmonic with frequency $\omega_\perp$. They found that for an atom pair in the lowest harmonic oscillator state of the confined directions the atoms interact via a one-dimensional delta-function potential $g_{1\rm D}\delta(z)$, with coupling constant

$$g_{1\rm D} = 2\frac{\hbar^2}{\mu}\frac{a}{\sigma_\perp^2}\frac{1}{1 - Ca/\sigma_\perp},$$

where $C = 1.4602\ldots$ and $\sigma_\perp = \sqrt{\hbar/\mu\omega_\perp}$. The coupling constant is singular when $a = \sigma_\perp / C$ and approaches the negative finite value $g_\infty = -2\hbar^2/\mu C \sigma_\perp$ for $a \to \pm\infty$. Olshanii (1998) called the singularity a confinement-induced resonance. In practice, the resonance condition can be fulfilled by changing $a$ with a magnetic Feshbach resonance. For fermionic atoms in quasi-one-dimensional confinement the effective atom-atom potential has been derived by Granger and Blume (2004).

Petrov *et al.* (2000) and Petrov and Shlyapnikov (2001) derived a similar coupling constant for one-dimensional confinement or two-dimensional scattering. In this case the resonance location not only depends on $a$ but also logarithmically on the relative wave number between the atoms along the two free spatial directions. Naidon *et al.* (2007) described how these reduced dimensional treatments can be extended to much tighter confinements than previously thought and made more accurate using the energy-dependent scattering length of Blume and Greene (2002) with the effective range expansion for the scattering phase.

Moritz *et al.* (2005) presented experimental evidence for a confinement-induced bound state in a one-dimensional system. They confirmed the existence of the bound state of the one-dimensional Hamiltonian $H_{1\rm D} = -(\hbar^2/2\mu)d^2/dz^2 + g_{1\rm D}\delta(z)$ by changing both $a$ and $\omega_\perp$. The experiment was performed by employing an array of 1D tubes, each containing about 300 $^{40}$K atoms, equally divided between the $|f=9/2, m=-9/2\rangle$ and $|f=9/2, m=-7/2\rangle$ hyperfine states, which were held in a two-dimensional harmonic trap with frequency $\omega_\perp/(2\pi) = 69$ kHz. The scattering length for the collision between these two hyperfine states was varied using the magnetic Feshbach resonance at $B_0 = 202$ G. Figure 43 shows that the measured energy of the tightly confined atom pair varies as predicted by theory. Confinement-induced molecules exist in reduced dimension for $B > B_0$, where they do not exist in free space. Dickerscheid and Stoof (2005) developed an analytical nonperturbative two-channel theory of the binding energy that is in excellent agreement with the data.

Günter *et al.* (2005) prepared fermionic $^{40}$K atoms in a single hyperfine state and held in either a one- or two-dimensional optical lattice. By virtue of Fermi statistics the atoms can only collide via odd partial waves, which

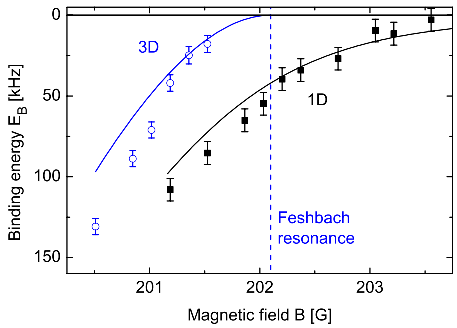


FIG. 43. (Color online) Measured molecular bound state binding energy vs magnetic field $B$ near the 202.1 G resonance between the two lowest spin states of $^{40}$K. The upper curve labeled 3D is for a free space gas, whereas the lower curve labeled 1D is for a quasi-1D gas with tight confinement in two dimensions. The points show measured binding energies and the lines show theoretical predictions. From Moritz *et al.*, 2005.

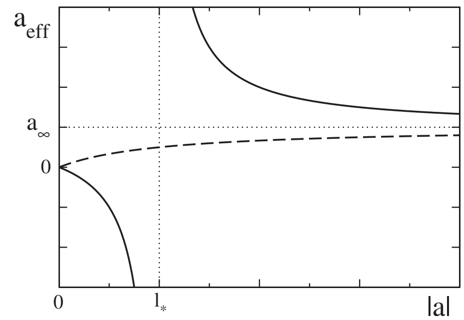


FIG. 44. The dependence of the effective scattering length $a_{\text{eff}}$ on the absolute value of the microscopic scattering length $|a|$. The dashed line corresponds to a repulsive interaction potential ($a>0$). The solid line corresponds to an attractive potential ($a<0$) with a geometric resonance at $|a|=l_*$. From Fedichev *et al.*, 2004.

for ultracold collision energies have very small cross sections. One might expect the atomic gas to be a noninteracting Fermi gas. Nevertheless, Günter *et al.* (2005) could observe a Feshbach resonance in the $p$-wave collision by the losses it induced. The losses were even sensitive to the orientation of the magnetic field relative to the principal axis of the trap. Moreover, they showed that the magnetic field location of the resonance is modified by the confinement.

### 3. Scattering in shallow lattices

Sections VI.B.1 and VI.B.2 discussed deep optical lattices where the tunneling between lattices sites could safely be neglected. For weaker optical lattices, atoms tunnel from site to site and then interact with all other atoms. This leads to many-body systems that can be described by either a mean-field Gross-Pitaevskii equation or a Bose- or Fermi-Hubbard Hamiltonian (Bloch, 2005). The presence of Feshbach resonances has added and continues to add new twists to these kinds of Hamiltonians.

We discuss the more simple situation where only two atoms scatter in an optical lattice. Fedichev *et al.* (2004) studied the case of two atoms scattering in a weak three-dimensional optical lattice of cubic symmetry and interacting with the regularized delta-function potential. They predicted the presence of a geometrical resonance in the 3D lattice based on a derivation of an effective atom-atom interaction between the atoms, which by virtue of the periodic potential have an effective mass $m^*$ that is much larger than their atomic mass $m$. Figure 44 shows the results of their calculation. The resonance occurs at a scattering length $a=l_* \equiv -[\pi/(2\ln 2)](m/m^*)(\sigma/d)^2\sigma$, where $\sigma$ is the atomic harmonic oscillator length for motion in a single lattice site and $d$ is the lattice period. Note that, in practice, $l_* \ll \sigma$. Orso *et al.* (2005) presented a similar analysis for a one-dimensional optical lattice. Grupp *et al.* (2007) studied the effect of a very-narrow Feshbach resonance in scattering in an one-dimensional lattice.

Nygaard *et al.* (2008a) investigated the effect of tuning a narrow Feshbach resonance across the Bloch band of a one-dimensional optical lattice for the case when the resonance width is small compared to the width of the band, such as the 414 G $^{87}$Rb resonance studied by Syassen *et al.* (2007). They investigated the changes in scattering and bound states due to the band structure in the periodic structure and characterized the time-dependent dynamics of sweeping the resonance across the band. Nygaard *et al.* (2008b) extended this work, developed the concept of a generalized scattering length at the band edges, and showed the existence of a "universal" bound state near the top and bottom band edges at the field strength where the resonance emerges from the band.

## C. Efimov states and universal few-body physics

Feshbach resonances provide experimental access to systems with very large values of the scattering length. Such systems are governed by universal physics; i.e., their low-energy observables are independent of details of the interaction (Braaten and Hammer, 2006). Universality appears as a consequence of the quantum halo character of the wave function carrying its dominant part far out of the classically allowed region. In this case, details of the interaction potential become irrelevant and the system can be described by a few global parameters. Halo dimers (Sec. V.B.2) are the most simple example. For addressing universal physics with ultracold gases, Feshbach resonances that are strongly entrance channel dominated ($s_{\text{res}} \gg 1$) are of particular interest, as they allow a description in terms of a single-channel model with a large range of universal behavior (see discussion in Secs. II.B.2 and II.C.5).

### 1. Efimov's scenario

Efimov quantum states in a system of three identical bosons (Efimov, 1970, 1971) are a paradigm for universal

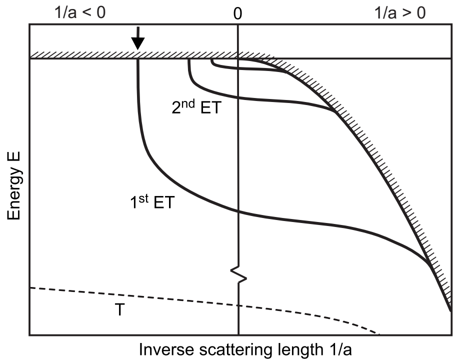


FIG. 45. Efimov's scenario: appearance of an infinite series of weakly bound Efimov trimer (ET) states for resonant two-body interaction. The binding energy is plotted as a function of the inverse two-body scattering length $1/a$. The shaded region indicates the scattering continuum for three atoms ($a<0$) and for an atom and a dimer ($a>0$). The arrow marks the intersection of the first Efimov trimer with the three-atom threshold. To illustrate the series of Efimov states, the universal scaling factor is artificially reduced from 22.7 to 2. For comparison, the dashed line indicates a more tightly bound non-Efimov trimer ($T$) which does not cross the scattering continuum. From Kraemer *et al.*, 2006.

few-body physics. These states have attracted considerable interest, fueled by their bizarre and counterintuitive properties and by the fact that they had been elusive to experimentalists for more than 35 years. In 2006, Kraemer *et al.* (2006) reported on experimental evidence for Efimov states in an ultracold gas of cesium atoms. By Feshbach tuning they could identify a pronounced three-body resonance, which occurs as a fingerprint of an Efimov state at the three-body scattering threshold. Three years later, Knoop *et al.* (2009) presented additional evidence for Efimov-like trimer states, reporting on the observation of a decay resonance in atom-dimer scattering.

Efimov's scenario is shown in Fig. 45, showing the energy spectrum of the three-body system as a function of the inverse scattering length $1/a$. For $a<0$, the natural zero of energy is the three-body dissociation threshold for three atoms at rest. States below are trimer states and states above are continuum states of three free atoms. For $a>0$, the dissociation threshold is given by $-E_b=-\hbar^2/ma^2$, where $E_b$ is the universal binding energy of the weakly bound halo dimer; at this threshold a trimer dissociates into a dimer and an atom. All states below threshold are necessarily three-body bound states. Efimov predicted that in the limit $a\rightarrow\pm\infty$ there would be an infinite sequence of weakly bound trimer states with a universal scaling behavior. Each successive Efimov state is larger in size by a universal scaling factor $e^{\pi/s_0}\approx 22.7$ ($s_0=1.006\,24$) and has a weaker binding energy by a factor of $(22.7)^2\approx 515$.

Efimov states exist on both sides of a resonance, and Fig. 45 shows the adiabatic connection between both sides. For $a>0$, an Efimov state near the atom-dimer dissociation threshold can be regarded as a weakly bound state of an atom and a dimer with a size set not by $a$ but by the even larger atom-dimer scattering length (Braaten and Hammer, 2006). For $a<0$, Efimov states are "Borromean" states (Jensen *et al.*, 2004), which means that a weakly bound three-body state exists in the absence of a weakly bound two-body state. This property that three quantum objects stay together without pairwise binding is part of the bizarre nature of Efimov states.

Resonant scattering phenomena arise as a natural consequence of this scenario (Efimov, 1979), and they are closely related to the basic idea of a Feshbach resonance. When an Efimov state intersects with the continuum threshold for $a<0$, three free atoms resonantly couple to a trimer. This results in a "triatomic Efimov resonance." When an Efimov state intersects with the atom-dimer threshold for $a>0$, the result is an "atom-dimer Efimov resonance" (Nielsen *et al.*, 2002).

### 2. Observations in ultracold cesium

In an ultracold atomic gas with resonant interactions, Efimov physics manifests itself in three-body decay properties (Esry *et al.*, 1999; Nielsen and Macek, 1999; Bedaque *et al.*, 2000; Braaten and Hammer, 2001, 2006). The three-body loss coefficient $L_3$ (Sec. III.A.2) can be conveniently expressed in the form $L_3=3C(a)\hbar a^4/m$, which separates an overall $a^4$ scaling from an additional dependence $C(a)$. Efimov physics is reflected in a logarithmically periodic behavior $C(22.7a)=C(a)$, corresponding to the scaling of the infinite series of weakly bound trimer states. A triatomic Efimov resonance leads to giant recombination loss (Esry *et al.*, 1999; Braaten and Hammer, 2001) as the resonant coupling of three atoms to an Efimov state opens up fast decay channels into deeply bound dimer states plus a free atom.

Kraemer *et al.* (2006) observed a triatomic Efimov resonance in an ultracold thermal gas of Cs atoms. They made use of the strong variation in the low-field region (Fig. 22). This tunability results from a strongly entrance channel dominated resonance at $-12$ G with $s_{\mathrm{res}}=566$ (see the Appendix), which provides a broad range of universal behavior. By applying magnetic fields between 0 and 150 G, Kraemer *et al.* (2006) varied the $s$-wave scattering length $a$ between $-2500a_0$ and $1600a_0$, large enough to study the universal regime, which requires $|a|\gg R_{\mathrm{vdW}}\simeq 100a_0$. The occurrence of one triatomic Efimov resonance could be expected in the accessible negative-$a$ region. The position, however, could not be predicted from knowledge of the scattering length alone as, for a three-body process, a second parameter is required to characterize the universal properties (Braaten and Hammer, 2006).

Figure 46 shows the results of Kraemer *et al.* (2006). The three-body loss resonance was found at a magnetic field of 7.5 G, corresponding to a scattering length of $-850a_0$. The behavior of loss at temperatures around 10 nK closely resembles the theoretical predictions of Esry *et al.* (1999), who numerically solved the three-body Schrödinger equation for a generic two-body model potential. The observed behavior is also well fit with a uni-

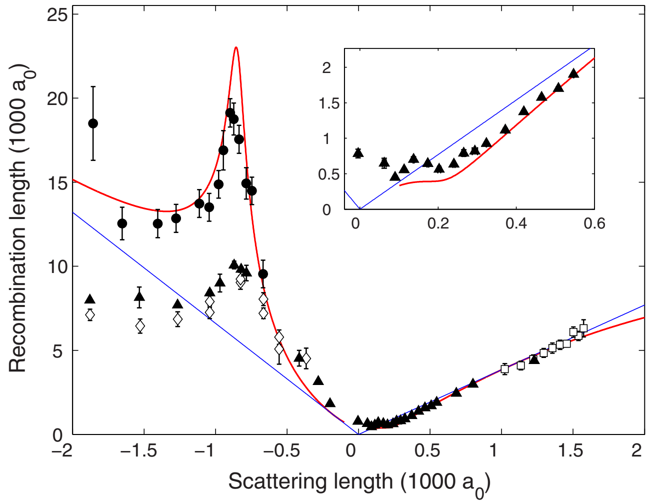


FIG. 46. (Color online) Observation of an Efimov resonance in three-body decay of an ultracold gas of cesium atoms. The data are presented in terms of a recombination length $\rho_3 = [(2m/\sqrt{3}\hbar)L_3]^{1/4}$ (Esry *et al.*, 1999). The general $a^4$ scaling of $L_3$ corresponds to a linear behavior in $\rho_3(a)$ (straight lines). The filled circles represent measurements taken at temperatures around 10 nK, whereas the filled triangles and open diamonds refer to measurements in the range of 200–250 nK. The solid line is a fit to the low-temperature data based on effective-field theory (Braaten and Hammer, 2006). The inset shows an expanded view of the region of positive scattering lengths up to $600a_0$. From Kraemer *et al.*, 2006.

versal analytic expression obtained in the framework of effective-field theory (Braaten and Hammer, 2006). Experimental data taken at higher temperatures demonstrated the unitarity limitation of three-body loss (D'Incao *et al.*, 2004) and showed how the Efimov resonance evolved into a triatomic continuum resonance (Bringas *et al.*, 2004).

For positive scattering lengths, theory predicts a variation of $C(a)$ between very small values and a maximum of about 70 (Esry *et al.*, 1999; Nielsen and Macek, 1999; Bedaque *et al.*, 2000). The results in Fig. 46 are consistent with the upper loss limit, represented by the straight line for $a>0$. For $a$ below $600a_0$, the experimentally determined recombination length significantly drops below this limit, as seen in the inset of the figure. Further measurements by Kraemer *et al.* (2006) revealed the existence of a loss minimum at $B=21$ G, where $a=+210a_0$. It is interesting to note that earlier experiments by the same group (Kraemer *et al.*, 2004) had identified 21 G as an optimum magnetic field for evaporative cooling of cesium and attainment of BEC (see Sec. IV.A.1). The nature of the minimum may be interpreted in the framework of universal physics, following theoretical predictions of an interference effect between two different recombination pathways (Esry *et al.*, 1999; Nielsen and Macek, 1999). However, as the minimum occurs at a scattering length which is only a factor of 2 larger than $R_{\mathrm{vdW}} \simeq 100a_0$ (Table I) the application of universal theory to describe this feature is questionable. Massignan and Stoof (2008) presented an alternative theoretical approach, which reproduced both this minimum and the maximum observed for negative $a$ on the basis of the two-body physics of the particular Feshbach resonance.

In a pure sample of trapped atoms, as discussed so far, three-body recombination is the only probe for Efimov physics. Mixtures of atoms and dimers can provide complementary information on Efimov states through resonances in inelastic atom-dimer collisions (Nielsen *et al.*, 2002; Braaten and Hammer, 2007). In a recent experiment, Knoop *et al.* (2009) prepared an optically trapped mixture of Cs atoms and $\mathrm{Cs}_2$ halo dimers. Their measurements revealed an atom-dimer scattering resonance, which is centered at a large value of the two-body scattering length, $a \simeq +390a_0$, at a magnetic field of 25 G. This observation provides strong evidence for a trimer state approaching the atom-dimer threshold. The situation is close to the atom-dimer resonance in Efimov's scenario, but it probably remains a semantic question whether, at $a \simeq 4R_{\mathrm{vdW}}$, the underlying trimer state may be called an Efimov state.

In the Cs experiments described in this section, the Efimov state that causes the observed triatomic resonance at 7.5 G does not connect to the state that causes the atom-dimer resonance at 25 G when the magnetic field is varied. This is because these two cases are separated by a zero crossing in the scattering length (Fig. 22) and not by the pole as in Efimov's scenario in Fig. 45. A universal relation between these regimes may nevertheless exist (Kraemer *et al.*, 2006). Lee *et al.* (2007) provided a further interpretation of these observations in terms of the underlying $\mathrm{Cs}_3$ states and pointed out the analogies to trimer states of helium (Schöllkopf and Toennies, 1994).

**3. Prospects in few-body physics**

Ultracold gases with resonantly tuned interactions offer many opportunities to study universal Efimov-related few-body physics. Cesium alone has much more to offer than the experiments could explore so far. Moreover, several other systems with broad Feshbach resonances promise new insight into this field.

In cesium, a predicted broad Feshbach resonance near 800 G (Lee *et al.*, 2007) in the *aa* channel offers similar properties as the low-field region explored in previous experiments but overcomes the disadvantage that only the tail of the resonance is accessible at low fields. The broad 155 G resonance in $^{85}$Rb (Sec. III.B.4) might be another interesting candidate, but experiments may suffer from strong two-body decay which is absent for the discussed cesium resonances. A further interesting candidate is the 402 G resonance in $^{39}$K (Sec. III.B.3): Zaccanti *et al.* (2008) studied three-body decay near this resonance and found features strongly indicative of Efimov physics.

Many more opportunities for studying Efimov-related physics in ultracold gases with resonant interactions are offered by mixtures of different spin states or different species. In $^6$Li, all three combinations of the lowest three spin states (channels *ab*, *ac*, and *bc*) have broad Feshbach resonances (Bartenstein *et al.*, 2005) that overlap in a magnetic-field range between 650 and 850 G. For such a three-component fermionic spin mixture Luu and Schwenk (2007) predicted a novel Borromean three-body state. Ottenstein *et al.* (2008) and Huckans *et al.* (2009) experimentally investigated the stability of a $^6$Li three-component spin mixture and found evidence for a three-body resonance at 130 G. Its interpretation in terms of coupling to a three-body bound state is supported by several theoretical studies (Braaten *et al.*, 2009; Floerchinger *et al.*, 2009; Naidon and Ueda, 2009). A particularly interesting situation arises in mixtures of atoms with different masses. With increasing mass ratio the Efimov factor substantially decreases from its value of 22.7 at equal masses to values as low as 4.9 for the mass ratio of $^{133}$Cs combined with $^6$Li. D'Incao and Esry (2006) pointed out that this will substantially enhance the observability of the Efimov effect in terms of the logarithmically periodic variation of the three-body loss coefficient with increasing two-body scattering length.

Four-body processes at large values of the *s*-wave scattering length $a$ represent a logical next step in understanding universal few-body physics. Theoretical studies (Hammer and Platter, 2007; von Stecher *et al.*, 2009; Wang and Esry, 2009) predicted the existence of universal four-body states and considered the process of atomic four-body recombination. A first experimental step into this field was made by Ferlaino *et al.* (2008), who studied collisions of $Cs_2$ halo dimers at large positive $a$. They observed a loss minimum in the same region where atom-dimer scattering shows a maximum ($a \simeq 500a_0$ at 30 G), which may be related to a universal connection between four- and three-body physics (Hammer and Platter, 2007; von Stecher *et al.*, 2009).

Optical lattices have proven a powerful tool for the manipulation of ultracold Feshbach molecules (see Sec. VI.B.1) and may also open up new possibilities for the creation of Efimov trimers and, more generally, for the controlled production of few-body quantum states (Stoll and Köhler, 2005; Luu and Schwenk, 2007).

### D. Molecular resonances and cold chemistry

While we have reviewed the formation of cold molecules from ultracold atoms, parallel progress has been made by other techniques for preparing samples of cold molecules that extend the range far beyond alkali-metal species. These advances have been made possible by Stark deceleration of molecules such as $ND_3$, OH, and formaldehyde (van de Meerakker *et al.*, 2006) van de Meerakker, Vanhaecke, and Meijer or by buffer gas cooling with liquid helium (DeCarvalho *et al.*, 1999). In contrast to the association of cold atoms to make Feshbach molecules, which have a high level of vibrational excitation, these methods can produce cold molecules in the rotational and vibrational ground states. See Doyle *et al.* (2004), Krems (2005), and Hutson and Soldán (2007) for overviews of the issues involved in trapping, cooling, and colliding such molecules.

Resonances will play a prominent role in atom-molecule and molecule-molecule collisions. The complexity of these systems will increase the number of closed channels and lead to numerous resonances with diverse properties. Their presence will make it possible to change molecular scattering properties as well as to create more complex molecules. Both static magnetic and electric fields can be used to tune the molecule-molecule resonance and provide control over collisions, as many molecules not only have a magnetic moment but an electric dipole moment as well. Here we review some of this work.

Forrey *et al.* (1998) pointed out that Feshbach resonances occur in ultracold atom-diatom scattering, giving an example from collisions of $H_2$ with He. The effect of resonance states in chemical reactions has been studied by Balakrishnan and Dalgarno (2001) for $F+H_2 \to FH + H$ and by Weck and Balakrishnan (2005) for $Li+HF \to H+LiF$ reactions. Recent coupled-channel models of Rb+OH (Lara *et al.*, 2007) and He+NH (González-Martinez and Hutson, 2007) collisions have been developed to give a realistic assessment of atom-molecule scattering. The latter study demonstrated the effect of magnetic tuning of a decaying resonance across a threshold using the resonance length formalism described in Sec. II.A.3.

Bohn *et al.* (2002) realized that, unlike for atomic systems where Feshbach resonances originate from the hyperfine structure of the atoms, for molecules the resonances can also be due to rotational states. For many molecules the rotational spacing for low-lying rotational levels is of the same order of magnitude as hyperfine interactions in atoms. Based on the rotational splittings and a potential energy surface Bohn *et al.* (2002) estimated the mean spacing and widths of the resonances and found for collisions between oxygen molecules as many as 30 resonances for collision energies below $E/k_B = 1$ K.

Chin *et al.* (2005) observed magnetic Feshbach-like resonances between two weakly bound $^{133}Cs_2$ molecules that temporarily form a tetramer during a collision. Their data are shown in Fig. 47. The $^{133}Cs_2$ molecules in this experiment are bound by no more than $E/h = 5$ MHz and have a temperature and peak density of 250 nK and $5\times 10^{10}$ cm$^{-3}$, respectively. As the magnetic field is varied near $B = 13$ G the lifetime of the molecules rapidly changes, indicating two resonances.

Heteronuclear molecules can be manipulated by static electric fields in addition to magnetic fields. The electric field Stark shifts the rotational levels of the molecule. These level shifts can then give rise to electric Feshbach resonances (Avdeenkov and Bohn, 2002). In atoms the levels can also be sufficiently Stark shifted to induce collisional resonances but rather large fields are required (Marinescu and You, 1998).

Figure 48 shows the results of a calculation on reaction rate coefficients of formaldehyde $H_2CO$ reacting with OH to yield HCO and $H_2O$ (Hudson *et al.*, 2006). Both $H_2CO$ and OH are in their lowest vibrational state

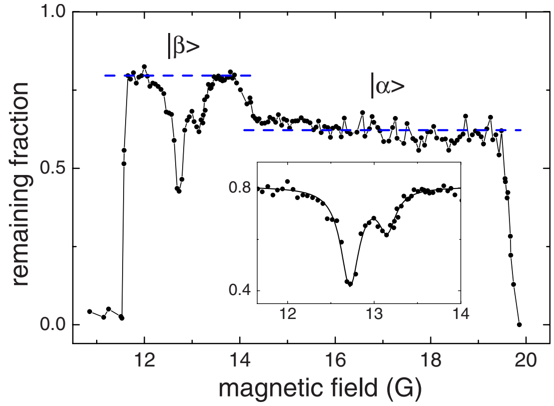


FIG. 47. (Color online) Observation of Feshbach-like resonances in the collisions of $^{133}Cs_2$ molecules. The number of remaining $^{133}$Cs molecules after fixed storage time in an optical trap as a function of external magnetic field. The two features near 13 G shown magnified in the inset have been interpreted as tetramer resonances. From Chin *et al.*, 2005.

of their ground electronic configuration. Multiple resonances occur for electric fields up to 2 kV/cm. Recently Tscherbul and Krems (2008) studied reaction rates of LiF with H in the presence of electric fields.

We can expect atom-molecule and molecule-molecule collisions to exhibit a rich variety of resonance phenomena in elastic, inelastic, and reactive collisions. Such phenomena are likely to become progressively more important to understand as sources of trap loss and for coherent control of molecular ensembles.


## ACKNOWLEDGMENTS

Over the past decade, many people have contributed to advancing our knowledge on Feshbach resonances in ultracold gases. For valuable discussions and insights related to this exciting field, we particularly acknowledge B. Esry, F. Ferlaino, C. Greene, J. Hecker Denschlag, J. Hutson, S. Knoop, H.-C. Nägerl, W. Phillips, F. Schreck, and G. Shlyapnikov. We thank E. Braaten, S. Dürr, T. Esslinger, M. Gustavsson, W. Ketterle, L. Khaykovich, S. Kokkelmans, H. Moritz, T. Pfau, H. Stoof, B. Verhaar, J. Walraven, M. Zaccanti, C. Zimmermann, and in particular, S. Jochim and I. Spielman for helpful comments on the paper. C.C. acknowledges support from NSF No. PHY-0747907 and NSF-MRSEC DMR-0213745 and USARO No. W911NF0710576 with funds from the DARPA OLE Program. R.G. thanks the Austrian Science Fund FWF and the Austrian Science ministry BMWF for support. P.J. and E.T. acknowledge support by the Office of Naval Research (ONR).


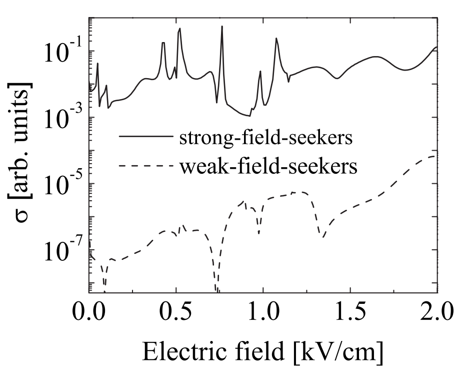


FIG. 48. Calculated chemical reaction cross section of $H_2CO + OH \rightarrow HCO + H_2O$ at a collision energy of $E/k_B=1$ mK as a function of applied electric field. Strong- (weak-) field seekers correspond to states of $H_2CO$ and OH that can be held in an electric trap where the center of the trap has the largest (smallest) electric field strength, respectively. From Hudson *et al.*, 2006.

## APPENDIX: TABLES OF SELECTED RESONANCES

Table IV lists positions and properties of selected resonances for various species. The data are a combination of experimentally determined as well as theoretically derived values. Most of the magnetic field locations are experimentally determined. Most of the widths $\Delta$ and background scattering lengths $a_{bg}$ are determined from theoretical calculations. Where unavailable we calculated values based on the best Born-Oppenheimer potentials obtained from the literature. For a complete list as well as error bars on the resonance locations the reader is referred to the literature. The notation defined in Secs. II.A.3 and II.B.4 has been used in the table.

Table IV shows a richness in the kinds of resonances available for magnetic field values that are relatively easily created in laboratories. Some of the resonances are very narrow with $\Delta$ on the order of a mG. Others are very broad with $\Delta$ larger than 100 G. The background scattering length can be either negative or positive, its absolute value ranging from a few tens to several thousands Bohr radii. The magnetic moment of the resonance state is always on the order of the Bohr magneton, which reflects the form of the Zeeman interaction. The partial wave of the resonance states ranges from zero to four ($\ell_c=0,\dots,4$). Finally, the resonances are characterized in terms of their background scattering

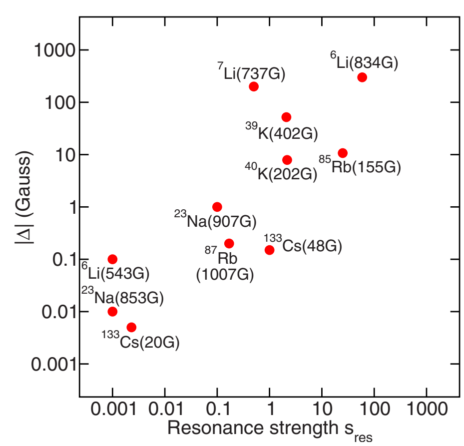


FIG. 49. (Color online) Overview of selected Feshbach resonances in terms of widths $\Delta$ and strengths $s_{res}$.

TABLE IV. Properties of selected Feshbach resonances. The first column describes the atomic species and isotope. The next three columns characterize the scattering and resonance states, which include the incoming scattering channel (ch.), partial wave $\ell$, and the angular momentum of the resonance state $\ell_c$. This is followed by the resonance location $B_0$, the width $\Delta$, the background scattering length $a_{bg}$, the differential magnetic moment $\delta\mu$, the dimensionless resonance strength $s_{res}$, the background scattering length in van der Waals units $r_{bg}=a_{bg}/\bar{a}$, and the bound state parameter $\zeta$ from Eq. (52). Here $a_0$ is the Bohr radius and $\mu_B$ is the Bohr magneton. Definitions are given in Sec. II. The last column gives the source. A string "na" indicates that the corresponding property is not defined. For example $a_{bg}$ is not defined for $p$-wave scattering.

| Atom | ch. | $\ell$ | $\ell_c$ | $B_0$ (G) | $\Delta$ (G) | $a_{bg}/a_0$ | $\delta\mu/\mu_B$ | $s_{res}$ | $r_{bg}$ | $\zeta$ | Reference |
|---|---|---|---|---|---|---|---|---|---|---|---|
| $^6$Li | *ab* | *s* | *s* | 834.1 | −300 | −1405 | 2.0 | 59 | −47 | 1400 | Bartenstein *et al.*, 2005 |
| | *ac* | *s* | *s* | 690.4 | −122.3 | −1727 | 2.0 | 29 | −58 | 850 | Bartenstein *et al.*, 2005 |
| | *bc* | *s* | *s* | 811.2 | −222.3 | −1490 | 2.0 | 46 | −50 | 1200 | Bartenstein *et al.*, 2005 |
| | *ab* | *s* | *s* | 543.25 | 0.1 | 60 | 2.0 | 0.001 | 2.0 | 0.001 | Strecker *et al.*, 2003 |
| | *aa* | *p* | *p* | 159.14 | na | na | 2.0 | na | na | na | Zhang *et al.*, 2004; Schunck *et al.*, 2005 |
| | *ab* | *p* | *p* | 185.09 | na | na | 2.0 | na | na | na | Zhang *et al.*, 2004; Schunck *et al.*, 2005 |
| | *bb* | *p* | *p* | 214.94 | na | na | 2.0 | na | na | na | Zhang *et al.*, 2004; Schunck *et al.*, 2005 |
| $^7$Li | *aa* | *s* | *s* | 736.8 | −192.3 | −25 | 1.93 | 0.80 | −0.79 | 0.31 | Strecker *et al.*, 2002; Pollack *et al.*, 2009[a] |
| $^{23}$Na | *cc* | *s* | *s* | 1195 | −1.4 | 62 | −0.15 | 0.0050 | 1.4 | 0.004 | Inouye *et al.*, 1998; Stenger *et al.*, 1999[a] |
| | *aa* | *s* | *s* | 907 | 1 | 63 | 3.8 | 0.09 | 1.5 | 0.07 | Inouye *et al.*, 1998; Stenger *et al.*, 1999[a] |
| | *aa* | *s* | *s* | 853 | 0.0025 | 63 | 3.8 | 0.0002 | 1.5 | 0.0002 | Inouye *et al.*, 1998; Stenger *et al.*, 1999[a] |
| $^{39}$K | *aa* | *s* | *s* | 402.4 | −52 | −29 | 1.5 | 2.1 | −0.47 | 0.49 | D'Errico *et al.*, 2007 |
| $^{40}$K | *bb* | *p* | *p* | 198.4 | na | na | 0.134 | na | na | na | Regal *et al.*, 2003b; Ticknor *et al.*, 2004[a] |
| | *bb* | *p* | *p* | 198.8 | na | na | 0.134 | na | na | na | Regal *et al.*, 2003b; Ticknor *et al.*, 2004[a] |
| | *ab* | *s* | *s* | 202.1 | 8.0 | 174 | 1.68 | 2.2 | 2.8 | 3.1 | Regal *et al.*, 2004[a] |
| | *ac* | *s* | *s* | 224.2 | 9.7 | 174 | 1.68 | 2.7 | 2.8 | 3.8 | Regal and Jin, 2003[a] |
| $^{85}$Rb | *ee* | *s* | *s* | 155.04 | 10.7 | −443 | −2.33 | 28 | −5.6 | 80 | Claussen *et al.*, 2003 |
| $^{87}$Rb | *aa* | *s* | *s* | 1007.4 | 0.21 | 100 | 2.79 | 0.13 | 1.27 | 0.08 | Volz *et al.*, 2003; Dürr, Volz, and Rempe, 2004[a] |
| | *aa* | *s* | *s* | 911.7 | 0.0013 | 100 | 2.71 | 0.001 | 1.27 | 0.0006 | Marte *et al.*, 2002[a] |
| | *aa* | *s* | *s* | 685.4 | 0.006 | 100 | 1.34 | 0.006 | 1.27 | 0.004 | Marte *et al.*, 2002; Dürr, Volz, and Rempe, 2004[a] |
| | *aa* | *s* | *s* | 406.2 | 0.0004 | 100 | 2.01 | 0.0002 | 1.27 | 0.0001 | Marte *et al.*, 2002[a] |
| | *ae* | *s* | *s* | 9.13 | 0.015 | 99.8 | 2.00 | 0.008 | 1.27 | 0.005 | Widera *et al.*, 2004 |
| $^{133}$Cs | *aa* | *s* | *s* | −11.7 | 28.7 | 1720 | 2.30 | 560 | 17.8 | 5030 | Chin, Vuletić, *et al.*, 2004; Lange *et al.*, 2009[a] |
| | *aa* | *s* | *d* | 47.97 | 0.12 | 926 | 1.21 | 0.67 | 9.60 | 3.2 | Chin, Vuletić, *et al.*, 2004; Lange *et al.*, 2009[a] |
| | *aa* | *s* | *g* | 19.84 | 0.005 | 160 | 0.57 | 0.002 | 1.66 | 0.002 | Chin, Vuletić, *et al.*, 2004[a] |
| | *aa* | *s* | *g* | 53.5 | 0.0025 | 995 | 1.52 | 0.019 | 10.3 | 0.1 | Chin, Vuletić, *et al.*, 2004; Lange *et al.*, 2009[a] |
| | *aa* | *s* | *s* | 547 | 7.5 | 2500 | 1.79 | 170 | 26 | 2200 | [a] |
| | *aa* | *s* | *s* | 800 | 87.5 | 1940 | 1.75 | 1470 | 20 | 15000 | [a] |
| $^{52}$Cr | *aa* | *s* | *d* | 589.1 | 1.7 | 105 | 2.00 | 0.31 | 2.45 | 0.38 | Werner *et al.*, 2005[a] |
| | *aa* | *s* | *d* | 499.9 | 0.08 | 107 | 4.00 | 0.03 | 2.49 | 0.04 | Werner *et al.*, 2005[a] |
| $^6$Li $^{23}$Na | *aa* | *s* | *s* | 746 | 0.44 | 14.0 | | | | | Stan *et al.*, 2004; Gacesa *et al.*, 2008 |
| | *aa* | *s* | *s* | 795.6 | 2.177 | 13.0 | | | | | Stan *et al.*, 2004; Gacesa *et al.*, 2008 |
| $^6$Li $^{40}$K | *aa* | *s* | *s* | 157.6 | 0.25 | | | | | | Wille *et al.*, 2008 |
| | *aa* | *s* | *s* | 168.2 | 0.15 | | | | | | Wille *et al.*, 2008 |
| $^6$Li $^{87}$Rb | *aa* | *p* | *p* | 882 | na | na | | na | na | na | Deh *et al.*, 2008; Li *et al.*, 2008 |
| | *aa* | *s* | *s* | 1067 | 10.62 | | | | | | Deh *et al.*, 2008; Li *et al.*, 2008 |
| $^7$Li $^{87}$Rb | *aa* | *s* | *s* | 649 | −70 | −36 | | | | | Marzok *et al.*, 2009 |
| $^{39}$K $^{87}$Rb | *aa* | *s* | *s* | 317.9 | 7.6 | 34 | 2.0 | 0.74 | 0.50 | 0.18 | Simoni *et al.*, 2008 |
| $^{40}$K $^{87}$Rb | *aa* | *s* | *s* | 546.9 | −3.10 | −189 | 2.30 | 1.96 | −2.75 | 2.70 | Pashov *et al.*, 2007; Simoni *et al.*, 2008 |
| $^{41}$K $^{87}$Rb | *aa* | *s* | *s* | 39 | 37 | 284 | 1.65 | 25.8 | 4.11 | 53.0 | Simoni *et al.*, 2008; Thalhammer *et al.*, 2008 |
| $^{41}$K $^{87}$Rb | *aa* | *s* | *s* | 79 | 1.2 | 284 | 1.59 | 0.81 | 4.11 | 1.66 | Simoni *et al.*, 2008; Thalhammer *et al.*, 2008 |
| $^{85}$Rb $^{87}$Rb | *ec* | *s* | *s* | 265.4 | 5.8 | 213 | | | | | Papp and Wieman, 2006 |
| $^{85}$Rb $^{87}$Rb | *ec* | *s* | *s* | 372 | 1 | 213 | | | | | Papp and Wieman, 2006 |

[a]Table entries partially based on unpublished calculations by the authors.

lengths $a_{bg}$, their strengths $s_{res}$ (Sec. II.B.2), and the parameter $\zeta$ (Sec. II.C.5).

For atomic cesium, a resonance location is given with a negative magnetic field value. This is not an experimental value. Here $B_0$ is determined from a fit of Eq. (1) to the slowly varying scattering length as shown in Fig. 22. Vogels *et al.* (1998) gave the physical interpretation of a negative $B_0$, namely, taking $B<0$ corresponds to the case for $B>0$ with the spin projections of each atom reversed in sign. For the case of cesium, a negative magnetic field in the *aa* channel corresponds to a positive field in the *gg* channel.

Figure 49 shows the rich variety of Feshbach resonances in terms of their widths $\Delta$ and strengths $s_{res}$. Both parameters change over six orders of magnitude. Resonances with $\Delta>1$ G tend to be entrance channel dominated ($s_{res}>1$). A notable exception is the $^7$Li 737 G resonance mentioned in Sec. II.B.5.

## REFERENCES


Abo-Shaeer, J. R., D. E. Miller, J. K. Chin, K. Xu, T. Mukaiyama, and W. Ketterle, 2005, "Coherent molecular optics using ultracold sodium dimers," Phys. Rev. Lett. **94**, 040405.

Abraham, E. R. I., W. I. McAlexander, J. M. Gerton, R. G. Hulet, R. Côté, and A. Dalgarno, 1997, "Triplet *s*-wave resonance in $^6$Li collisions and scattering lengths of $^6$Li and $^7$Li," Phys. Rev. A **55**, R3299–R3002.

Altmeyer, A., S. Riedl, C. Kohstall, M. Wright, R. Geursen, M. Bartenstein, C. Chin, J. Hecker Denschlag, and R. Grimm, 2007, "Precision measurements of collective modes in the BEC-BCS crossover," Phys. Rev. Lett. **98**, 040401.

Anderson, M. H., J. R. Ensher, M. R. Matthews, C. E. Wieman, and E. A. Cornell, 1995, "Observation of Bose-Einstein condensation in dilute atomic vapor," Science **269**, 198–201.

Arimondo, E., W. D. Phillips, and F. Strumia, 1992, Eds., *Laser Manipulation of Atoms and Ions*, Proceedings of the International School of Physics "Enrico Fermi," Course CXVIII, Varenna, 1991 (North-Holland, Amsterdam).

Arndt, M., M. B. Dahan, D. Guéry-Odelin, M. W. Reynolds, and J. Dalibard, 1997, "Observation of a zero-energy resonance in Cs-Cs collisions," Phys. Rev. Lett. **79**, 625–628.

Avdeenkov, A. V., and J. L. Bohn, 2002, "Collisional dynamics of ultracold OH molecules in an electrostatic field," Phys. Rev. A **66**, 052718.

Balakrishnan, N., and A. Dalgarno, 2001, "Chemistry at ultracold temperatures," Chem. Phys. Lett. **341**, 652–656.

Balakrishnan, N., V. Kharchenko, R. Forrey, and A. Dalgarno, 1997, "Complex scattering lengths in multi-channel atom-molecule collisions," Chem. Phys. Lett. **280**, 5–9.

Bartenstein, M., A. Altmeyer, S. Riedl, R. Geursen, S. Jochim, C. Chin, J. Hecker Denschlag, R. Grimm, A. Simoni, E. Tiesinga, C. J. Williams, and P. S. Julienne, 2005, "Precise determination of $^6$Li cold collision parameters by radio-frequency spectroscopy on weakly bound molecules," Phys. Rev. Lett. **94**, 103201.

Bartenstein, M., A. Altmeyer, S. Riedl, S. Jochim, C. Chin, J. Hecker Denschlag, and R. Grimm, 2004a, "Collective excitations of a degenerate gas at the BEC-BCS crossover," Phys. Rev. Lett. **92**, 203201.

Bartenstein, M., A. Altmeyer, S. Riedl, S. Jochim, C. Chin, J. Hecker Denschlag, and R. Grimm, 2004b, "Crossover from a molecular Bose-Einstein condensate to a degenerate Fermi gas," Phys. Rev. Lett. **92**, 120401.

Beaufils, Q., A. Crubellier, T. Zanon, B. Laburthe-Tolra, E. Maréchal, L. Vernac, and O. Gorceix, 2009, "Feshbach resonance in *d*-wave collisions," Phys. Rev. A **79**, 032706.

Bedaque, P. F., E. Braaten, and H.-W. Hammer, 2000, "Three-body recombination in Bose gases with large scattering length," Phys. Rev. Lett. **85**, 908–911.

Bergeman, T., M. G. Moore, and M. Olshanii, 2003, "Atom-atom scattering under cylindrical harmonic confinement: Numerical and analytic studies of the confinement induced resonance," Phys. Rev. Lett. **91**, 163201.

Bergmann, K., H. Theuer, and B. W. Shore, 1998, "Coherent population transfer among quantum states of atoms and molecules," Rev. Mod. Phys. **70**, 1003–1025.

Bethe, H., 1935, "Theory of disintegration of nuclei by neutrons," Phys. Rev. **47**, 747–759.

Beutler, H., 1935, "Über Absorptionsserien von Argon, Krypton und Xenon zu Termen zwischen den beiden Ionisierungsgrenzen $^2P_3{}^{2/0}$ und $^2P_1{}^{2/0}$," Z. Phys. **93**, 177–196.

Bhattacharya, M., L. O. Baksmaty, S. B. Weiss, and N. P. Bigelow, 2004, "Feshbach resonances in $^{23}$Na-$^{87}$Rb," Eur. Phys. J. D **31**, 301–306.

Blatt, J. M., and V. F. Weisskopf, 1952, *Theoretical Nuclear Physics* (Wiley, New York).

Bloch, I., 2005, "Ultracold quantum gases in optical lattices," Nat. Phys. **1**, 23–30.

Bloch, I., J. Dalibard, and W. Zwerger, 2008, "Many-body physics with ultracold gases," Rev. Mod. Phys. **80**, 885–964.

Blume, D., and C. H. Greene, 2002, "Fermi pseudopotential approximation: Two particles under external confinement," Phys. Rev. A **65**, 043613.

Boesten, H. M. J. M., C. C. Tsai, J. R. Gardner, D. J. Heinzen, and B. J. Verhaar, 1997, "Observation of a shape resonance in the collision of two cold $^{87}$Rb atoms," Phys. Rev. A **55**, 636–640.

Boesten, H. M. J. M., C. C. Tsai, B. J. Verhaar, and D. J. Heinzen, 1996, "Observation of a shape resonance in cold-atom scattering by pulsed photoassociation," Phys. Rev. Lett. **77**, 5194–5197.

Boesten, H. M. J. M., J. M. Vogels, J. G. C. Tempelaars, and B. J. Verhaar, 1996, "Properties of cold collisions of $^{39}$K atoms and of $^{41}$K atoms in relation to Bose-Einstein condensation," Phys. Rev. A **54**, R3726–R3729.

Bohn, J., and P. S. Julienne, 1997, "Prospects for influencing scattering lengths with far-off-resonant light," Phys. Rev. A **56**, 1486–1491.

Bohn, J. L., A. V. Avdeenkov, and M. P. Deskevich, 2002, "Rotational Feshbach resonances in ultracold molecular collisions," Phys. Rev. Lett. **89**, 203202.

Bohn, J. L., J. P. Burke, C. H. Greene, H. Wang, P. L. Gould, and W. C. Stwalley, 1999, "Collisional properties of ultracold potassium: Consequences for degenerate Bose and Fermi gases," Phys. Rev. A **59**, 3660–3664.

Bohn, J. L., and P. S. Julienne, 1996, "Semianalytic treatment of two-color photoassociation spectroscopy and control of cold atoms," Phys. Rev. A **54**, R4637–R4640.

Bohn, J. L., and P. S. Julienne, 1999, "Semianalytic theory of laser-assisted resonant cold collisions," Phys. Rev. A **60**, 414–425.

Bolda, E. L., E. Tiesinga, and P. S. Julienne, 2002, "Effective-scattering-length model of ultracold atomic collisions and

Feshbach resonances in tight harmonic traps," Phys. Rev. A **66**, 013403.

Bolda, E. L., E. Tiesinga, and P. S. Julienne, 2003, "Pseudopotential model of ultracold atomic collisions in quasi-one- and two-dimensional traps," Phys. Rev. A **68**, 032702.

Bourdel, T., J. Cubizolles, L. Khaykovich, K. M. F. Magalhães, S. J. J. M. F. Kokkelmans, G. V. Shlyapnikov, and C. Salomon, 2003, "Measurement of the interaction energy near a Feshbach resonance in a $^6$Li Fermi gas," Phys. Rev. Lett. **91**, 020402.

Bourdel, T., L. Khaykovich, J. Cubizolles, J. Zhang, F. Chevy, M. Teichmann, L. Tarruell, S. J. J. M. F. Kokkelmans, and C. Salomon, 2004, "Experimental study of the BEC-BCS crossover region in lithium-6," Phys. Rev. Lett. **93**, 050401.

Braaten, E., and H.-W. Hammer, 2001, "Three-body recombination into deep bound states in a Bose gas with large scattering length," Phys. Rev. Lett. **87**, 160407.

Braaten, E., and H.-W. Hammer, 2006, "Universality in few-body systems with large scattering length," Phys. Rep. **428**, 259–390.

Braaten, E., and H.-W. Hammer, 2007, "Resonant dimer relaxation in cold atoms with a large scattering length," Phys. Rev. A **75**, 052710.

Braaten, E., H.-W. Hammer, D. Kang, and L. Platter, 2009, "Three-body recombination of $^6$Li atoms with large negative scattering lengths," Phys. Rev. Lett. **103**, 073202.

Bradley, C. C., C. A. Sacket, and R. G. Hulet, 1997, "Bose-Einstein condensation of lithium: Observation of limited condensate number," Phys. Rev. Lett. **78**, 985–989.

Bradley, C. C., C. A. Sackett, J. J. Tollett, and R. G. Hulet, 1995, "Evidence of Bose-Einstein condensation in an atomic gas with attractive interactions," Phys. Rev. Lett. **75**, 1687–1690.

Breit, G., and I. I. Rabi, 1931, "Measurement of nuclear spin," Phys. Rev. **38**, 2082–2083.

Breit, G., and E. Wigner, 1936, "Capture of slow neutrons," Phys. Rev. **49**, 519–531.

Bringas, F., M. T. Yamashita, and T. Frederico, 2004, "Triatomic continuum resonances for large negative scattering lengths," Phys. Rev. A **69**, 040702(R).

Bryant, H. C., B. D. Dieterle, J. Donahue, H. Sharifian, H. Tootoonchi, D. M. Wolfe, P. A. M. Gram, and M. A. Yates-Williams, 1977, "Observation of resonances near 11 eV in the photodetachment cross section of the $H^-$ ion," Phys. Rev. Lett. **38**, 228–230.

Büchler, H. P., E. Demler, M. Lukin, A. Micheli, N. Prokof'ev, G. Pupillo, and P. Zoller, 2007, "Strongly correlated 2D quantum phases with cold polar molecules: Controlling the shape of the interaction potential," Phys. Rev. Lett. **98**, 060404.

Buggle, C., J. Léonard, W. von Klitzing, and J. T. M. Walraven, 2004, "Interferometric determination of the *s*- and *d*-wave scattering amplitudes in $^{87}$Rb," Phys. Rev. Lett. **93**, 173202.

Burke, J. P., J. L. Bohn, B. D. Esry, and C. H. Greene, 1998, "Prospects for mixed-isotope Bose-Einstein condensates in rubidium," Phys. Rev. Lett. **80**, 2097–2100.

Busch, T., B.-G. Englert, K. Rzażewski, and M. Wilkens, 1998, "Two cold atoms in a harmonic trap," Found. Phys. **28**, 549–559.

Carusotto, I., L. Pitaevskii, S. Stringari, G. Modugno, and M. Inguscio, 2005, "Sensitive measurements of forces at the micron scale using Bloch oscillations of ultracold atoms," Phys. Rev. Lett. **95**, 093202.

Chen, Q., J. Stajic, S. Tan, and K. Levin, 2005, "BCS-BEC crossover: From high-temperature superconductors to ultracold superfluids," Phys. Rep. **412**, 1–88.

Chin, C., M. Bartenstein, A. Altmeyer, S. Riedl, S. Jochim, J. Hecker Denschlag, and R. Grimm, 2004, "Observation of the pairing gap in a strongly interacting Fermi gas," Science **305**, 1128–1130.

Chin, C., and R. Grimm, 2004, "Thermal equilibrium and efficient evaporation of an ultracold atom-molecule mixture," Phys. Rev. A **69**, 033612.

Chin, C., and P. S. Julienne, 2005, "Radio-frequency transitions on weakly bound ultracold molecules," Phys. Rev. A **71**, 012713.

Chin, C., A. J. Kerman, V. Vuletić, and S. Chu, 2003, "Sensitive detection of cold cesium molecules formed on Feshbach resonances," Phys. Rev. Lett. **90**, 033201.

Chin, C., T. Kraemer, M. Mark, J. Herbig, P. Waldburger, H.-C. Nägerl, and R. Grimm, 2005, "Observation of Feshbach-like resonances in collisions between ultracold molecules," Phys. Rev. Lett. **94**, 123201.

Chin, C., V. Vuletić, A. J. Kerman, and S. Chu, 2000, "High resolution Feshbach spectroscopy of cesium," Phys. Rev. Lett. **85**, 2717–2720.

Chin, C., V. Vuletić, A. J. Kerman, S. Chu, E. Tiesinga, P. J. Leo, and C. J. Williams, 2004, "Precision Feshbach spectroscopy of ultracold $Cs_2$," Phys. Rev. A **70**, 032701.

Chu, S., 1998, "Nobel Lecture: The manipulation of neutral particles," Rev. Mod. Phys. **70**, 685–706.

Ciuryło, R., E. Tiesinga, and P. S. Julienne, 2005, "Optical tuning of the scattering length of cold alkaline earth atoms," Phys. Rev. A **71**, 030701.

Claussen, N. R., S. J. J. M. F. Kokkelmans, S. T. Thompson, E. A. Donley, E. Hodby, and C. E. Wieman, 2003, "Very-high-precision bound-state spectroscopy near a $^{85}$Rb Feshbach resonance," Phys. Rev. A **67**, 060701(R).

Cohen-Tannoudji, C. N., 1998, "Nobel Lecture: Manipulating atoms with photons," Rev. Mod. Phys. **70**, 707–719.

Cornell, E. A., and C. E. Wieman, 2002, "Nobel Lecture: Bose-Einstein condensation in a dilute gas, the first 70 years and some recent experiments," Rev. Mod. Phys. **74**, 875–893.

Cornish, S. L., N. R. Claussen, J. L. Roberts, E. A. Cornell, and C. E. Wieman, 2000, "Stable $^{85}$Rb Bose-Einstein condensates with widely tunable interactions," Phys. Rev. Lett. **85**, 1795–1798.

Cornish, S. L., S. T. Thompson, and C. E. Wieman, 2006, "Formation of bright matter-wave solitions during the collapse of attractive Bose-Einstein condensates," Phys. Rev. Lett. **96**, 170401.

Courteille, P., R. S. Freeland, D. J. Heinzen, F. A. van Abeelen, and B. J. Verhaar, 1998, "Observation of a Feshbach resonance in cold atom scattering," Phys. Rev. Lett. **81**, 69–72.

Cubizolles, J., T. Bourdel, S. J. J. M. F. Kokkelmans, G. V. Shlyapnikov, and C. Salomon, 2003, "Production of long-lived ultracold $Li_2$ molecules from a Fermi gas," Phys. Rev. Lett. **91**, 240401.

Cvitas, M. T., P. Soldan, J. M. Hutson, P. Honvault, and J.-M. Launay, 2007, "Interactions and dynamics in Li+$Li_2$ ultracold collisions," J. Chem. Phys. **127**, 074302.

Dalfovo, F., S. Giorgini, L. P. Pitaevskii, and S. Stringari, 1999, "Theory of Bose-Einstein condensation in trapped gases," Rev. Mod. Phys. **71**, 463–512.

Danzl, J. G., E. Haller, M. Gustavsson, M. J. Mark, R. Hart, N. Bouloufa, O. Dulieu, H. Ritsch, and H.-C. Nägerl, 2008,

"Quantum gas of deeply bound ground state molecules," Science **321**, 1062–1066.
Davis, K. B., M. O. Mewes, M. R. Andrews, N. J. van Druten, D. S. Durfee, D. M. Kurn, and W. Ketterle, 1995, "Bose-Einstein condensation in a gas of sodium atoms," Phys. Rev. Lett. **75**, 3969–3973.
DeCarvalho, R., J. M. Doyle, B. Friedrich, T. Guillet, J. Kim, D. Patterson, and J. D. Weinstein, 1999, "Buffer-gas loaded magnetic traps for atoms and molecules: A primer," Eur. Phys. J. D **7**, 289–309.
Deh, B., C. Marzok, C. Zimmermann, and P. W. Courteille, 2008, "Feshbach resonances in mixtures of ultracold $^6$Li and $^{87}$Rb gases," Phys. Rev. A **77**, 010701(R).
DeMarco, B., J. L. Bohn, J. P. Burke, Jr., M. Holland, and D. S. Jin, 1999, "Measurement of *p*-wave threshold law using evaporatively cooled fermionic atoms," Phys. Rev. Lett. **82**, 4208–4211.
DeMille, D., 2002, "Quantum computation with trapped polar molecules," Phys. Rev. Lett. **88**, 067901.
Derevianko, A., W. R. Johnson, M. S. Safronova, and J. F. Babb, 1999, "High-precision calculations of dispersion coefficients, static dipole polarizabilities, and atom-wall interaction constants for alkali-metal atoms," Phys. Rev. Lett. **82**, 3589–3592.
D'Errico, C., M. Zaccanti, M. Fattori, G. Roati, M. Inguscio, G. Modugno, and A. Simoni, 2007, "Feshbach resonances in ultracold $^{39}$K," New J. Phys. **9**, 223.
Deuretzbacher, F., K. Plassmeier, D. Pfannkuche, F. Werner, C. Ospelkaus, S. Ospelkaus, K. Sengstock, and K. Bongs, 2008, "Heteronuclear molecules in an optical lattice: Theory and experiment," Phys. Rev. A **77**, 032726.
Dickerscheid, D. B. M., U. A. Khawaja, D. van Oosten, and H. T. C. Stoof, 2005, "Feshbach resonances in an optical lattice," Phys. Rev. A **71**, 043604.
Dickerscheid, D. B. M., and H. T. C. Stoof, 2005, "Feshbach molecules in a one-dimensional Fermi gas," Phys. Rev. A **72**, 053625.
Dieckmann, K., C. A. Stan, S. Gupta, Z. Hadzibabic, C. H. Schunck, and W. Ketterle, 2002, "Decay of an ultracold fermionic lithium gas near a Feshbach resonance," Phys. Rev. Lett. **89**, 203201.
D'Incao, J. P., and B. D. Esry, 2006, "Enhancing the observability of the Efimov effect in ultracold atomic gas mixtures," Phys. Rev. A **73**, 030703.
D'Incao, J. P., H. Suno, and B. D. Esry, 2004, "Limits on universality in ultracold three-boson recombination," Phys. Rev. Lett. **93**, 123201.
Donley, E. A., N. R. Claussen, S. L. Cornish, J. L. Roberts, E. A. Cornell, and C. E. Wieman, 2001, "Dynamics of collapsing and exploding Bose-Einstein condensates," Nature (London) **412**, 295–299.
Donley, E. A., N. R. Claussen, S. T. Thompson, and C. E. Wieman, 2002, "Atom-molecule coherence in a Bose-Einstein condensate," Nature (London) **417**, 529–533.
Doyle, J., B. Friedrich, R. V. Krems, and F. Masnou Seeuws, 2004, "Ultracold polar molecules: Formation and collision," Eur. Phys. J. D **31**, 149–446, special issue on polar molecules.
Du, X., L. Luo, B. Clancy, and J. E. Thomas, 2008, "Observation of anomalous spin segregation in a trapped Fermi gas," Phys. Rev. Lett. **101**, 150401.
Duine, R. A., and H. T. C. Stoof, 2003, "Microscopic many-body theory of atomic Bose gases near a Feshbach resonance," J. Opt. B: Quantum Semiclassical Opt. **5**, S212.
Duine, R. A., and H. T. C. Stoof, 2004, "Atom-molecule coherence in Bose gases," Phys. Rep. **396**, 115–195.
Dürr, S., T. Volz, A. Marte, and G. Rempe, 2004, "Observation of molecules produced from a Bose-Einstein condensate," Phys. Rev. Lett. **92**, 020406.
Dürr, S., T. Volz, and G. Rempe, 2004, "Dissociation of ultracold molecules with Feshbach resonances," Phys. Rev. A **70**, 031601(R).
Efimov, V., 1970, "Energy levels arising from resonant two-body forces in a three-body system," Phys. Lett. **33B**, 563–564.
Efimov, V., 1971, "Weakly-bound states of three resonantly-interacting particles," Sov. J. Nucl. Phys. **12**, 589–595.
Efimov, V., 1979, "Low-energy properties of three resonantly interacting particles," Sov. J. Nucl. Phys. **29**, 546–553.
Enomoto, K., K. Kasa, M. Kitagawa, and Y. Takahashi, 2008, "Optical Feshbach resonance using the intercombination transition," Phys. Rev. Lett. **101**, 203201.
Erhard, M., H. Schmaljohann, J. Kronjäger, K. Bongs, and K. Sengstock, 2004, "Measurement of a mixed-spin-channel Feshbach resonance in $^{87}$Rb," Phys. Rev. A **69**, 032705.
Esry, B. D., C. H. Greene, and J. P. Burke, 1999, "Recombination of three atoms in the ultracold limit," Phys. Rev. Lett. **83**, 1751–1754.
Esry, B. D., C. H. Greene, and H. Suno, 2001, "Threshold laws for three-body recombination," Phys. Rev. A **65**, 010705.
Fano, U., 1935, "Sullo spettro di assorbimento dei gas nobili presso il limite dello spettro d'arco," Nuovo Cimento **12**, 154–161.
Fano, U., 1961, "Effects of configuration interaction on intensities and phase shifts," Phys. Rev. **124**, 1866.
Fano, U., G. Pupillo, A. Zannoni, and C. W. Clark, 2005, "On the absorption spectrum of noble gases at the arc spectrum limit," J. Res. Natl. Inst. Stand. Technol. **110**, 583–587.
Fatemi, F. K., K. M. Jones, and P. D. Lett, 2000, "Observation of optically induced Feshbach resonances in collisions of cold atoms," Phys. Rev. Lett. **85**, 4462–4465.
Fattori, M., C. D'Errico, G. Roati, M. Zaccanti, M. Jona-Lasinio, M. Modugno, M. Inguscio, and G. Modugno, 2008, "Atom interferometry with a weakly-interacting Bose-Einstein condensate," Phys. Rev. Lett. **100**, 080405.
Fattori, M., G. Roati, B. Deissler, C. D'Errico, M. Zaccanti, M. Jona-Lasinio, L. Santos, M. Inguscio, and G. Modugno, 2008, "Magnetic dipolar interaction in a Bose-Einstein condensate atomic interferometer," Phys. Rev. Lett. **101**, 190405.
Fedichev, P. O., M. J. Bijlsma, and P. Zoller, 2004, "Extended molecules and geometric scattering resonances in optical lattices," Phys. Rev. Lett. **92**, 080401.
Fedichev, P. O., Y. Kagan, G. V. Shlyapnikov, and J. T. M. Walraven, 1996, "Influence of nearly resonant light on the scattering length in low-temperature atomic gases," Phys. Rev. Lett. **77**, 2913–2916.
Fedichev, P. O., M. W. Reynolds, and G. V. Shlyapnikov, 1996, "Three-body recombination of ultracold atoms to a weakly bound *s* level," Phys. Rev. Lett. **77**, 2921–2924.
Ferlaino, F., C. D'Errico, G. Roati, M. Zaccanti, M. Inguscio, G. Modugno, and A. Simoni, 2006, "Feshbach spectroscopy of a K-Rb atomic mixture," Phys. Rev. A **73**, 040702(R); **74**, 039903(E) (2006).
Ferlaino, F., S. Knoop, M. Mark, M. Berninger, H. Schöbel, H.-C. Nägerl, and R. Grimm, 2008, "Collisions between tunable halo dimers: Exploring an elementary four-body process with identical bosons," Phys. Rev. Lett. **101**, 023201.

Feshbach, H., 1958, "Unified theory of nuclear reactions," Ann. Phys. (N.Y.) **5**, 357–390.
Feshbach, H., 1962, "Unified theory of nuclear reactions II," Ann. Phys. (N.Y.) **19**, 287–313.
Flambaum, V. V., G. F. Gribakin, and C. Harabti, 1999, "Analytic calculation of cold-atom scattering," Phys. Rev. A **59**, 1998–2005.
Floerchinger, S., R. Schmidt, and C. Wetterich, 2009, "Three-body loss in lithium from functional renormalization," Phys. Rev. A **79**, 053633.
Forrey, R. C., N. Balakrishnan, V. Kharchenko, and A. Dalgarno, 1998, "Feshbach resonances in ultracold atom-diatom scattering," Phys. Rev. A **58**, R2645–R2647.
Fuchs, J., C. Ticknor, P. Dyke, G. Veeravalli, E. Kuhnle, W. Rowlands, P. Hannaford, and C. J. Vale, 2008, "Binding energies of $^6$Li $p$-wave Feshbach molecules," Phys. Rev. A **77**, 053616.
Gacesa, M., P. Pellegrini, and R. Côté, 2008, "Feshbach resonances in ultracold $^{6,7}$Li+$^{23}$Na atomic mixtures," Phys. Rev. A **78**, 010701(R).
Gaebler, J. P., J. T. Stewart, J. L. Bohn, and D. S. Jin, 2007, "$p$-wave Feshbach molecules," Phys. Rev. Lett. **98**, 200403.
Gao, B., 1996, "Theory of slow-atom collisions," Phys. Rev. A **54**, 2022–2039.
Gao, B., 1998a, "Quantum-defect theory of atomic collisions and molecular vibrational spectra," Phys. Rev. A **58**, 4222–4225.
Gao, B., 1998b, "Solutions of the Schrödinger equation for an attractive $1/r^6$ potential," Phys. Rev. A **58**, 1728–1734.
Gao, B., 2000, "Zero-energy bound or quasibound states and their implications for diatomic systems with an asymptotic van der Waals interaction," Phys. Rev. A **62**, 050702.
Gao, B., 2001, "Angular-momentum-insensitive quantum-defect theory for diatomic systems," Phys. Rev. A **64**, 010701.
Gao, B., 2004, "Binding energy and scattering length for diatomic systems," J. Phys. B **37**, 4273–4279.
Gauyacq, J. P., and A. Herzenberg, 1982, "Nuclear-excited Feshbach resonances in $e$+HCl scattering," Phys. Rev. A **25**, 2959–2967.
Giorgini, S., L. P. Pitaevskii, and S. Stringari, 2008, "Theory of ultracold Fermi gases," Rev. Mod. Phys. **80**, 1215–1274.
González-Martinez, M. L., and J. M. Hutson, 2007, "Ultracold atom-molecule collisions and bound states in magnetic fields: Tuning zero-energy Feshbach resonances in He-NH ($^3\Sigma^-$)," Phys. Rev. A **75**, 022702.
Góral, K., T. Köhler, S. A. Gardiner, E. Tiesinga, and P. S. Julienne, 2004, "Adiabatic association of ultracold molecules via magnetic-field tunable interactions," J. Phys. B **37**, 3457–3500.
Góral, K., K. Rzazewski, and T. Pfau, 2000, "Bose-Einstein condensation with magnetic dipole-dipole forces," Phys. Rev. A **61**, 051601.
Granger, B. E., and D. Blume, 2004, "Tuning the interactions of spin-polarized fermions using quasi-one-dimensional confinement," Phys. Rev. Lett. **92**, 133202.
Greiner, M., C. A. Regal, and D. S. Jin, 2003, "Emergence of a molecular Bose-Einstein condensate from a Fermi gas," Nature (London) **426**, 537–540.
Gribakin, G. F., and V. V. Flambaum, 1993, "Calculation of the scattering length in atomic collisions using the semiclassical approximation," Phys. Rev. A **48**, 546–553.
Griesmaier, A., J. Werner, S. Hensler, J. Stuhler, and T. Pfau, 2005, "Bose-Einstein condensation of chromium," Phys. Rev. Lett. **94**, 160401.
Grimm, R., M. Weidemüller, and Y. B. Ovchinnikov, 2000, "Optical dipole traps for neutral atoms," Adv. At., Mol., Opt. Phys. **42**, 95–170.
Gross, N., and L. Khaykovich, 2008, "All-optical production of $^7$Li Bose-Einstein condensation using Feshbach resonances," Phys. Rev. A **77**, 023604.
Grupp, M., R. Walser, W. P. Schleich, M. A., and M. Weitz, 2007, "Resonant Feshbach scattering of fermions in one-dimensional optical lattices," J. Phys. B **40**, 2703–2718.
Gubbels, K. B., D. B. M. Dickerscheid, and H. T. C. Stoof, 2006, "Dressed molecules in an optical lattice," New J. Phys. **8**, 151.
Günter, K., T. Stöferle, H. Moritz, M. Köhl, and T. Esslinger, 2005, "$p$-wave interactions in low-dimensional fermionic gases," Phys. Rev. Lett. **95**, 230401.
Gupta, S., K. Dieckmann, Z. Hadzibabic, and D. E. Pritchard, 2002, "Contrast interferometry using Bose-Einstein condensates to measure $h/m$ and $\alpha$," Phys. Rev. Lett. **89**, 140401.
Gupta, S., Z. Hadzibabic, M. W. Zwierlein, C. A. Stan, K. Dieckmann, C. H. Schunck, E. G. M. van Kempen, B. J. Verhaar, and W. Ketterle, 2003, "Radio-frequency spectroscopy of ultracold fermions," Science **300**, 1723–1726.
Gustavsson, M., E. Haller, M. J. Mark, J. G. Danzl, G. Rojas-Kopeinig, and H.-C. Nägerl, 2008, "Control of interaction-induced dephasing of Bloch oscillations," Phys. Rev. Lett. **100**, 080404.
Hammer, H.-W., and L. Platter, 2007, "Universal properties of the four-body system with large scattering length," Eur. Phys. J. A **32**, 113–120.
Hanna, T. M., T. Köhler, and K. Burnett, 2007, "Association of molecules using a resonantly modulated magnetic field," Phys. Rev. A **75**, 013606.
Herbig, J., T. Kraemer, M. Mark, T. Weber, C. Chin, H.-C. Nägerl, and R. Grimm, 2003, "Preparation of a pure molecular quantum gas," Science **301**, 1510–1513.
Hodby, E., S. T. Thompson, C. A. Regal, M. Greiner, A. C. Wilson, D. S. Jin, and E. A. Cornell, 2005, "Production efficiency of ultra-cold Feshbach molecules in bosonic and fermionic systems," Phys. Rev. Lett. **94**, 120402.
Houbiers, M., H. T. C. Stoof, W. I. McAlexander, and R. G. Hulet, 1998, "Elastic and inelastic collisions of $^6$Li atoms in magnetic and optical traps," Phys. Rev. A **57**, R1497–R1500.
Huang, K., and T. D. Lee, 1957, "Quantum mechanical many-body problem with hard sphere interaction," Phys. Rev. **105**, 767–775.
Huckans, J. H., J. R. Williams, E. L. Hazlett, R. W. Stites, and K. M. O'Hara, 2009, "Three-body recombination in a three-state Fermi gas with widely tunable interactions," Phys. Rev. Lett. **102**, 165302.
Hudson, E. R., N. B. Gilfoy, S. Kotochigova, J. M. Sage, and D. DeMille, 2008, "Inelastic collisions of ultracold heteronuclear molecules in an optical trap," Phys. Rev. Lett. **100**, 203201.
Hudson, E. R., C. Ticknor, B. C. Sawyer, C. A. Taatjes, H. J. Lewandowski, J. R. Bochinski, J. L. Bohn, and Y. Jun, 2006, "Production of cold formaldehyde molecules for study and control of chemical reaction dynamics with hydroxyl radicals," Phys. Rev. A **73**, 063404.
Hutson, J., and P. Soldán, 2006, "Molecule formation in ultracold atomic gases," Int. Rev. Phys. Chem. **25**, 497–526.
Hutson, J. M., 2007, "Feshbach resonances in the presence of inelastic scattering: Threshold behavior and suppression of

poles in scattering lengths," New J. Phys. **9**, 152.
Hutson, J. M., and P. Soldán, 2007, "Molecular collisions in ultracold atomic gases," Int. Rev. Phys. Chem. **26**, 1–28.
Hutson, J. M., E. Tiesinga, and P. S. Julienne, 2008, "Avoided crossings between bound states of ultracold cesium dimers," Phys. Rev. A **78**, 052703.
Inada, Y., M. Horikoshi, S. Nakajima, M. Kuwata-Gonokami, M. Ueda, and T. Mukaiyama, 2008, "Collisional properties of *p*-wave Feshbach molecules," Phys. Rev. Lett. **101**, 100401.
Inguscio, M., W. Ketterle, and C. Salomon, 2008, Eds., *Ultracold Fermi Gases*, Proceedings of the International School of Physics "Enrico Fermi," Course CLXIV, Varenna, 2006 (ISO, Amsterdam).
Inguscio, M., S. Stringari, and C. E. Wieman, 1999, Eds., *Bose-Einstein Condensation in Atomic Gases*, Proceedings of the International School of Physics "Enrico Fermi," Course CXL, Varenna, 1998 (IOS, Amsterdam).
Inouye, S., M. R., Andrews, J. Stenger, H.-J. Miesner, D. M. Stamper-Kurn, and W. Ketterle, 1998, "Observation of Feshbach resonances in a Bose-Einstein condensate," Nature (London) **392**, 151–154.
Inouye, S., J. Goldwin, M. L. Olsen, C. Ticknor, J. L. Bohn, and D. S. Jin, 2004, "Observation of heteronuclear Feshbach resonances in a mixture of bosons and fermions," Phys. Rev. Lett. **93**, 183201.
Jensen, A. S., K. Riisager, D. V. Fedorov, and E. Garrido, 2004, "Structure and reactions of quantum halos," Rev. Mod. Phys. **76**, 215–261.
Jochim, S., M. Bartenstein, A. Altmeyer, G. Hendl, C. Chin, J. Hecker Denschlag, and R. Grimm, 2003a, "Pure gas of optically trapped molecules created from fermionic atoms," Phys. Rev. Lett. **91**, 240402.
Jochim, S., M. Bartenstein, A. Altmeyer, G. Hendl, S. Riedl, C. Chin, J. Hecker Denschlag, and R. Grimm, 2003b, "Bose-Einstein condensation of molecules," Science **302**, 2101–2103.
Jochim, S., M. Bartenstein, G. Hendl, J. Hecker Denschlag, R. Grimm, A. Mosk, and W. Weidemüller, 2002, "Magnetic field control of elastic scattering in a cold gas of fermionic lithium atoms," Phys. Rev. Lett. **89**, 273202.
Jones, K. M., E. Tiesinga, P. D. Lett, and P. S. Julienne, 2006, "Photoassociation spectroscopy of ultracold atoms: Long-range molecules and atomic scattering," Rev. Mod. Phys. **78**, 483–535.
Julienne, P. S., and B. Gao, 2006, in *Atomic Physics 20*, edited by C. Roos, H. Häffner, and R. Blatt (AIP, Melville, NY), pp. 261–268.
Julienne, P. S., and F. H. Mies, 1989, "Collisions of ultracold trapped atoms," J. Opt. Soc. Am. B **6**, 2257–2269.
Julienne, P. S., E. Tiesinga, and T. Köhler, 2004, "Making cold molecules by time-dependent Feshbach resonances," J. Mod. Opt. **51**, 1787–1806.
Junker, M., D. Dries, C. Welford, J. Hitchcock, Y. P. Chen, and R. G. Hulet, 2008, "Photoassociation of a Bose-Einstein condensate near a Feshbach resonance," Phys. Rev. Lett. **101**, 060406.
Kagan, Y., B. V. Svistunov, and G. V. Shlyapnikov, 1985, "Effect of Bose condensation on inelastic processes in gases," Pis'ma Zh. Eksp. Teor. Fiz. **42**, 169–172 [JETP Lett. **42**, 209–212 (1985)].
Ketterle, W., 2002, "Nobel Lecture: When atoms behave as waves: Bose-Einstein condensation and the atom laser," Rev. Mod. Phys. **74**, 1131–1151.
Ketterle, W., and N. J. van Druten, 1997, "Evaporative cooling of trapped atoms," Adv. At., Mol., Opt. Phys. **37**, 181–236.
Khaykovich, L., F. Schreck, G. Ferrari, T. Bourdel, J. Cubizolles, L. D. Carr, Y. Castin, and C. Salomon, 2002, "Formation of a matter-wave bright soliton," Science **296**, 1290–1293.
Kinast, J., S. L. Hemmer, M. E. Gehm, A. Turlapov, and J. E. Thomas, 2004, "Evidence for superfluidity in a resonantly interacting Fermi gas," Phys. Rev. Lett. **92**, 150402.
Kishimoto, T., J. Kobayashi, K. Noda, K. Aikawa, M. Ueda, and S. Inouye, 2009, "Direct evaporative cooling of $^{41}$K into a Bose-Einstein condensate," Phys. Rev. A **79**, 031602.
Kitagawa, M., K. Enomoto, K. Kasa, Y. Takahashi, R. Ciurylo, P. Naidon, and P. S. Julienne, 2008, "Two-color photoassociation spectroscopy of ytterbium atoms and the precise determinations of *s*-wave scattering lengths," Phys. Rev. A **77**, 012719.
Klempt, C., T. Henninger, O. Topic, M. Scherer, L. Kattner, E. Tiemann, W. Ertmer, and J. J. Arlt, 2008, "Radio-frequency association of heteronuclear Feshbach molecules," Phys. Rev. A **78**, 061602(R).
Klempt, C., T. Henninger, O. Topic, J. Will, W. Ertmer, E. Tiemann, and J. Arlt, 2007, "$^{40}$K-$^{87}$Rb Feshbach resonances: Modeling the interatomic potential," Phys. Rev. A **76**, 020701(R).
Kleppner, D., 2004, "Professor Feshbach and his resonance," Phys. Today **57** (8), 12–13.
Knoop, S., F. Ferlaino, M. Mark, J. G. Danzl, T. Kraemer, H.-C. Nägerl, and R. Grimm, 2009, "Observation of an Efimov-like trimer resonance in ultracold atom-dimer scattering," Nat. Phys. **5**, 227–230.
Knoop, S., M. Mark, F. Ferlaino, J. G. Danzl, T. Kraemer, H.-C. Nägerl, and R. Grimm, 2008, "Metastable Feshbach molecules in high rotational states," Phys. Rev. Lett. **100**, 083002.
Koch, T., T. Lahaye, J. Metz, B. Fröhlich, A. Griesmaier, and T. Pfau, 2008, "Stabilization of a purely dipolar quantum gas against collapse," Nat. Phys. **4**, 218–212.
Köhler, T., K. Góral, and P. S. Julienne, 2006, "Production of cold molecules via magnetically tunable Feshbach resonances," Rev. Mod. Phys. **78**, 1311–1361.
Köhler, T., E. Tiesinga, and P. S. Julienne, 2005, "Spontaneous dissociation of long-range Feshbach molecules," Phys. Rev. Lett. **94**, 020402.
Kokkelmans, S. J. J. M. F., J. N. Milstein, M. L. Chiofalo, R. Walser, and M. J. Holland, 2002, "Resonance superfluidity: Renormalization of resonance scattering theory," Phys. Rev. A **65**, 053617.
Kokkelmans, S. J. J. M. F., G. V. Shlyapnikov, and C. Salomon, 2004, "Degenerate atom-molecule mixture in a cold Fermi gas," Phys. Rev. A **69**, 031602.
Kokkelmans, S. J. J. M. F., H. M. J. Vissers, and B. J. Verhaar, 2001, "Formation of a Bose condensate of stable molecules via a Feshbach resonance," Phys. Rev. A **63**, 031601(R).
Kotochigova, S., E. Tiesinga, and P. S. Julienne, 2000, "Relativistic *ab initio* treatment of the second-order spin-orbit splitting of the a $^3\Sigma_u^+$ potential of rubidium and cesium dimers," Phys. Rev. A **63**, 012517.
Kraemer, T., J. Herbig, M. Mark, T. Weber, C. Chin, H.-C. Nägerl, and R. Grimm, 2004, "Optimized production of a cesium Bose-Einstein condensate," Appl. Phys. B: Lasers Opt. **79**, 1013–1019.
Kraemer, T., M. Mark, P. Waldburger, J. G. Danzl, C. Chin, B. Engeser, A. D. Lange, K. Pilch, A. Jaakkola, H.-C. Nägerl, and R. Grimm, 2006, "Evidence for Efimov quantum states in

an ultracold gas of cesium atoms," Nature (London) **440**, 315–318.

Krems, R. V., 2005, "Molecules near absolute zero and external field control of atomic and molecular dynamics," Int. Rev. Phys. Chem. **24**, 99–118.

Lahaye, T., T. Koch, B. Fröhlich, M. Fattori, J. Metz, A. Griesmaier, S. Giovanazzi, and T. Pfau, 2007, "Strong dipolar effects in a quantum ferrofluid," Nature (London) **448**, 672–676.

Lahaye, T., J. Metz, B. Fröhlich, T. Koch, M. Meister, A. Griesmaier, T. Pfau, H. Saito, Y. Kawaguchi, and M. Ueda, 2008, "*d*-wave collapse and explosion of a dipolar Bose-Einstein condensate," Phys. Rev. Lett. **101**, 080401.

Lang, F., P. van der Straten, B. Brandstätter, G. Thalhammer, K. Winkler, P. S. Julienne, R. Grimm, and J. Hecker Denschlag, 2008, "Cruising through molecular bound state manifolds with radio frequency," Nat. Phys. **4**, 223–226.

Lang, F., K. Winkler, C. Strauss, R. Grimm, and J. Hecker Denschlag, 2008, "Ultracold triplet molecules in the rovibrational ground state," Phys. Rev. Lett. **101**, 133005.

Lange, A. D., K. Pilch, A. Prantner, F. Ferlaino, B. Engeser, H.-C. Nägerl, R. Grimm, and C. Chin, 2009, "Determination of atomic scattering lengths from measurements of molecular binding energies near Feshbach resonances," Phys. Rev. A **79**, 013622.

Lara, M., J. L. Bohn, D. E. Potter, P. Soldán, and J. M. Hutson, 2007, "Cold collisions between OH and Rb: The field-free case," Phys. Rev. A **75**, 012704.

Laue, T., E. Tiesinga, C. Samuelis, H. Knöckel, and E. Tiemann, 2002, "Magnetic-field imaging of weakly bound levels of the ground-state $Na_2$ dimer," Phys. Rev. A **65**, 023412.

Lee, M. D., T. Köhler, and P. S. Julienne, 2007, "Excited Thomas-Efimov levels in ultracold gases," Phys. Rev. A **76**, 012720.

Leo, P. J., C. J. Williams, and P. S. Julienne, 2000, "Collision properties of ultracold $^{133}$Cs atoms," Phys. Rev. Lett. **85**, 2721–2724.

Li, Z., S. Singh, T. V. Tscherbul, and K. W. Madison, 2008, "Feshbach resonances in ultracold $^{85}$Rb-$^{87}$Rb and $^{6}$Li-$^{87}$Rb mixtures," Phys. Rev. A **78**, 022710.

Loftus, T., C. A. Regal, C. Ticknor, J. L. Bohn, and D. S. Jin, 2002, "Resonant control of elastic collisions in an optically trapped Fermi gas of atoms," Phys. Rev. Lett. **88**, 173201.

Luu, T., and A. Schwenk, 2007, "Three-fermion problems in optical lattices," Phys. Rev. Lett. **98**, 103202.

MacArthur, D. W., K. B. Butterfield, D. A. Clark, J. B. Donahue, P. A. M. Gram, H. C. Bryant, C. J. Harvey, W. W. Smith, and G. Comtet, 1985, "Energy measurement of the lowest $^1P^0$ Feshbach resonance in $H^-$," Phys. Rev. A **32**, 1921–1923.

Madison, K. W., F. Chevy, W. Wohlleben, and J. Dalibard, 2000, "Vortex formation in a stirred Bose-Einstein condensate," Phys. Rev. Lett. **84**, 806–809.

Marcelis, B., E. G. M. van Kempen, B. J. Verhaar, and S. J. J. M. F. Kokkelmans, 2004, "Feshbach resonances with large background scattering length: Interplay with open-channel resonances," Phys. Rev. A **70**, 012701.

Marcelis, B., B. Verhaar, and S. Kokkelmans, 2008, "Total control over ultracold interactions via electric and magnetic fields," Phys. Rev. Lett. **100**, 153201.

Marinescu, M., and L. You, 1998, "Controlling atom-atom interaction at ultralow temperatures by dc electric fields," Phys. Rev. Lett. **81**, 4596–4599.

Marion, H., S. Bize, L. Cacciapuoti, D. Chambon, F. P. D. Santos, G. Santarelli, P. Wolf, A. Clairon, A. Luiten, M. Tobar, S. Kokkelmans, and C. Salomon, 2004, "First observation of Feshbach resonances at very low magnetic field in a $^{133}$Cs fountain," e-print arXiv:physics/0407064.

Mark, M., F. Ferlaino, S. Knoop, J. G. Danzl, T. Kraemer, C. Chin, H.-C. Nägerl, and R. Grimm, 2007, "Spectroscopy of ultracold, trapped cesium Feshbach molecules," Phys. Rev. A **76**, 042514.

Mark, M., T. Kraemer, J. Herbig, C. Chin, H.-C. Nägerl, and R. Grimm, 2005, "Efficient creation of molecules from a cesium Bose-Einstein condensate," Europhys. Lett. **69**, 706–712.

Mark, M., T. Kraemer, P. Waldburger, J. Herbig, C. Chin, H.-C. Nägerl, and R. Grimm, 2007, "Stückelberg interferometry with ultracold molecules," Phys. Rev. Lett. **99**, 113201.

Marte, A., T. Volz, J. Schuster, S. Dürr, G. Rempe, E. G. M. van Kempen, and B. J. Verhaar, 2002, "Feshbach resonances in rubidium 87: Precision measurement and analysis," Phys. Rev. Lett. **89**, 283202.

Marzok, C., B. Deh, C. Zimmermann, P. W. Courteille, E. Tiemann, Y. V. Vanne, and A. Saenz, 2009, "Feshbach resonances in an ultracold $^7$Li and $^{87}$Rb mixture," Phys. Rev. A **79**, 012717.

Massignan, P., and H. T. C. Stoof, 2008, "Efimov states near a Feshbach resonance," Phys. Rev. A **78**, 030701(R).

Menotti, C., M. Lewenstein, T. Lahaye, and T. Pfau, 2008, *Proceedings of the Workshop "Dynamics and Thermodynamics of Systems with Long Range Interactions,"* Assisi, 2007 (AIP, New York).

Messiah, A., 1966, *Quantum Mechanics* (Wiley, New York).

Metcalf, H. J., and P. van der Straten, 1999, *Laser Cooling and Trapping* (Springer, New York).

Micheli, A., G. K. Brennen, and P. Zoller, 2006, "A toolbox for lattice-spin models with polar molecules," Nat. Phys. **2**, 341–347.

Mies, F. H., and M. Raoult, 2000, "Analysis of threshold effects in ultracold atomic collisions," Phys. Rev. A **62**, 012708.

Mies, F. H., E. Tiesinga, and P. S. Julienne, 2000, "Manipulation of Feshbach resonances in ultracold atomic collisions using time-dependent magnetic fields," Phys. Rev. A **61**, 022721.

Moerdijk, A. J., and B. J. Verhaar, 1994, "Prospects for Bose-Einstein condensation in atomic $^7$Li and $^{23}$Na," Phys. Rev. Lett. **73**, 518–521.

Moerdijk, A. J., B. J. Verhaar, and A. Axelsson, 1995, "Resonances in ultracold collisions of $^6$Li, $^7$Li, and $^{23}$Na," Phys. Rev. A **51**, 4852–4861.

Monroe, C. R., E. A. Cornell, C. A. Sackett, C. J. Myatt, and C. E. Wieman, 1993, "Measurement of Cs-Cs elastic scattering at $T=30$ $\mu$K," Phys. Rev. Lett. **70**, 414–417.

Moritz, H., T. Stöferle, K. Günter, M. Köhl, and T. Esslinger, 2005, "Confinement induced molecules in a 1D Fermi gas," Phys. Rev. Lett. **94**, 210401.

Mott, N. F., and H. S. W. Massey, 1965, *Theory of Atomic Collisions*, 3rd ed. (Oxford University Press, London).

Mukaiyama, T., J. R. Abo-Shaeer, K. Xu, J. K. Chin, and W. Ketterle, 2004, "Dissociation and decay of ultracold sodium molecules," Phys. Rev. Lett. **92**, 180402.

Naidon, P., and P. S. Julienne, 2006, "Optical Feshbach resonances of alkaline-earth-metal atoms in a one- or two-dimensional optical lattice," Phys. Rev. A **74**, 062713.

Naidon, P., E. Tiesinga, W. F. Mitchell, and P. S. Julienne, 2007, "Effective-range description of a Bose gas under strong one- or two-dimensional confinement," New J. Phys. **9**, 19.

Naidon, P., and M. Ueda, 2009, "Possible Efimov trimer state in a three-hyperfine-component lithium-6 mixture," Phys. Rev. Lett. **103**, 073203.

Ni, K.-K., S. Ospelkaus, M. H. G. de Miranda, A. Pe'er, B. Neyenhuis, J. J. Zirbel, S. Kotochigova, P. S. Julienne, D. S. Jin, and J. Ye, 2008, "A high phase-space-density gas of polar molecules," Science **322**, 231–235.

Nieh, J.-C., and J. J. Valentini, 1990, "State-to-state dynamics of the $H+p\text{-}H_2 \rightarrow o,p\text{-}H_2+H$ reaction: Feshbach resonances and vibrational spectroscopy of the transition state," J. Chem. Phys. **92**, 1083–1097.

Nielsen, E., and J. H. Macek, 1999, "Low-energy recombination of identical bosons by three-body collisions," Phys. Rev. Lett. **83**, 1566–1569.

Nielsen, E., H. Suno, and B. D. Esry, 2002, "Efimov resonances in atom-diatom scattering," Phys. Rev. A **66**, 012705.

Nygaard, N., R. Piil, and K. Mølmer, 2008a, "Feshbach molecules in a one-dimensional optical lattice," Phys. Rev. A **77**, 021601(R).

Nygaard, N., R. Piil, and K. Mølmer, 2008b, "Two-channel Feshbach physics in a structured continuum," Phys. Rev. A **78**, 023617.

Nygaard, N., B. I. Schneider, and P. S. Julienne, 2006, "A two-channel R-matrix analysis of magnetic field induced Feshbach resonances," Phys. Rev. A **73**, 042705.

O'Hara, K., S. L. Hemmer, M. E. Gehm, S. R. Granade, and J. E. Thomas, 2002, "Observation of a strongly interacting degenerate Fermi gas," Science **298**, 2179–2182.

O'Hara, K. M., S. L. Hemmer, S. R. Granade, M. E. Gehm, J. E. Thomas, V. Venturi, E. Tiesinga, and C. J. Williams, 2002, "Measurement of the zero crossing in a Feshbach resonance of fermionic $^6$Li," Phys. Rev. A **66**, 041401.

Olshanii, M., 1998, "Atomic scattering in the presence of an external confinement and a gas of impenetrable bosons," Phys. Rev. Lett. **81**, 000938.

Orso, G., L. P. Pitaevskii, S. Stringari, and M. Wouters, 2005, "Formation of molecules near a Feshbach resonance in a 1D optical lattice," Phys. Rev. Lett. **95**, 060402.

Ospelkaus, C., S. Ospelkaus, L. Humbert, P. Ernst, K. Sengstock, and K. Bongs, 2006, "Ultracold heteronuclear molecules in a 3D optical lattice," Phys. Rev. Lett. **97**, 120402.

Ospelkaus, S., C. Ospelkaus, L. Humbert, K. Sengstock, and K. Bongs, 2006, "Tuning of heteronuclear interactions in a degenerate Fermi-Bose mixture," Phys. Rev. Lett. **97**, 120403.

Ospelkaus, S., A. Pe'er, K.-K. Ni, J. J. Zirbel, B. Neyenhuis, S. Kotochigova, P. S. Julienne, J. Ye, and D. S. Jin, 2008, "Efficient state transfer in an ultracold dense gas of heteronuclear molecules," Nat. Phys. **4**, 622–626.

Ottenstein, T. B., T. Lompe, M. Kohnen, A. N. Wenz, and S. Jochim, 2008, "Collisional stability of a three-component degenerate Fermi gas," Phys. Rev. Lett. **101**, 203202.

Papp, S. B., J. M. Pino, R. J. Wild, S. Ronen, C. E. Wieman, D. S. Jin, and E. A. Cornell, 2008, "Bragg spectroscopy of a strongly interacting $^{85}$Rb Bose-Einstein condensate," Phys. Rev. Lett. **101**, 135301.

Papp, S. B., and C. E. Wieman, 2006, "Observation of heteronuclear Feshbach molecules from a $^{85}$Rb-$^{87}$Rb gas," Phys. Rev. Lett. **97**, 180404.

Partridge, G. B., W. Li, R. I. Kamar, Y.-an Liao, and R. G. Hulet, 2006, "Pairing and phase separation in a polarized Fermi gas," Science **311**, 503–505.

Partridge, G. B., K. E. Strecker, R. I. Kamar, M. W. Jack, and R. G. Hulet, 2005, "Molecular probe of pairing in the BEC-BCS crossover," Phys. Rev. Lett. **95**, 020404.

Pashov, A., O. Docenko, M. Tamanis, R. Ferber, H. Knöckel, and E. Tiemann, 2005, "Potentials for modeling cold collisions between Na (3S) and Rb (5S) atoms," Phys. Rev. A **72**, 062505.

Pashov, A., O. Docenko, M. Tamanis, R. Ferber, H. Knöckel, and E. Tiemann, 2007, "Coupling of the $X\,^1\Sigma^+$ and $a\,^3\Sigma^+$ states of KRb," Phys. Rev. A **76**, 022511.

Pethick, C. J., and H. Smith, 2008, *Bose-Einstein Condensation in Dilute Gases* (Cambridge University Press, Cambridge).

Petrov, D. S., 2003, "Three-body problem in Fermi gases with short-range interparticle interaction," Phys. Rev. A **67**, 010703.

Petrov, D. S., 2004, "Three-boson problem near a narrow Feshbach resonance," Phys. Rev. Lett. **93**, 143201.

Petrov, D. S., G. E. Astrakharchik, D. J. Papoular, C. Salomon, and G. V. Shlyapnikov, 2007, "Crystalline phase of strongly interacting Fermi mixtures," Phys. Rev. Lett. **99**, 130407.

Petrov, D. S., M. Holzmann, and G. V. Shlyapnikov, 2000, "Bose-Einstein condensation in quasi-2D trapped gases," Phys. Rev. Lett. **84**, 2551–2554.

Petrov, D. S., C. Salomon, and G. V. Shlyapnikov, 2004, "Weakly bound molecules of fermionic atoms," Phys. Rev. Lett. **93**, 090404.

Petrov, D. S., and G. V. Shlyapnikov, 2001, "Interatomic collisions in a tightly confined Bose gas," Phys. Rev. A **64**, 012706.

Phillips, W. D., 1998, "Nobel Lecture: Laser cooling and trapping of neutral atoms," Rev. Mod. Phys. **70**, 721–741.

Pilch, K., A. D. Lange, A. Prantner, G. Kerner, F. Ferlaino, H.-C. Nägerl, and R. Grimm, 2009, "Observation of interspecies Feshbach resonances in an ultracold Rb-Cs mixture," Phys. Rev. A **79**, 042718.

Pollack, S. E., D. Dries, M. Junker, Y. P. Chen, T. A. Corcovilos, and R. G. Hulet, 2009, "Extreme tunability of interactions in a $^7$Li Bose-Einstein condensate," Phys. Rev. Lett. **102**, 090402.

Porsev, S. G., and A. Derevianko, 2002, "High-accuracy relativistic many-body calculations of van der Waals coefficients $C_6$ for alkaline-earth-metal atoms," Phys. Rev. A **65**, 020701(R).

Porsev, S. G., and A. Derevianko, 2006, "High-accuracy calculations of dipole, quadrupole, and octupole electric dynamic polarizabilities and van der Waals coefficients $C_6$, $C_8$, and $C_{10}$ for alkaline-earth dimers," JETP Lett. **102**, 195–205 [Pis'ma Zh. Eksp. Teor. Fiz. **129**, 227–238 (2006)].

Quéméner, G., P. Honvault, J.-M. Launay, P. Soldán, D. E. Potter, and J. M. Hutson, 2005, "Ultracold quantum dynamics: Spin-polarized $K+K_2$ collisions with three identical bosons or fermions," Phys. Rev. A **71**, 032722.

Raoult, M., and F. H. Mies, 2004, "Feshbach resonance in atomic binary collisions in the Wigner threshold law regime," Phys. Rev. A **70**, 012710.

Rau, A. R. P., 2005, "Historical notes on Feshbach resonances," Phys. Today **58** (2), 13–13.

Regal, C. A., M. Greiner, and D. S. Jin, 2004, "Observation of resonance condensation of fermionic atom pairs," Phys. Rev. Lett. **92**, 040403.

Regal, C. A., and D. S. Jin, 2003, "Measurement of positive and negative scattering lengths in a Fermi gas of atoms," Phys. Rev. Lett. **90**, 230404.

Regal, C. A., C. Ticknor, J. L. Bohn, and D. S. Jin, 2003a, "Creation of ultracold molecules from a Fermi gas of atoms," Nature (London) **424**, 47–50.

Regal, C. A., C. Ticknor, J. L. Bohn, and D. S. Jin, 2003b, "Tuning *p*-wave interactions in an ultracold Fermi gas of atoms," Phys. Rev. Lett. **90**, 053201.

Reynolds, M. W., I. Shinkoda, R. W. Cline, and W. N. Hardy, 1986, "Observation of inverse predissocation of spin-polarized atomic hydrogen at low temperatures," Phys. Rev. B **34**, 4912–4915.

Rice, O. K., 1933, "Predissociation and the crossing of molecular potential energy curves," J. Chem. Phys. **1**, 375–389.

Riisager, K., 1994, "Nuclear halo states," Rev. Mod. Phys. **66**, 1105–1116.

Roati, G., G. de Mirandes, F. Ferlaino, G. Modugno, and M. Inguscio, 2004, "Atom interferometry with trapped Fermi gases," Phys. Rev. Lett. **92**, 230402.

Roati, G., C. D'Errico, F. L, M. Fattori, C. Fort, M. Zaccanti, G. Modugno, M. Modugno, and M. Inguscio, 2008, "Anderson localization of a non-interacting Bose-Einstein condensate," Nature (London) **453**, 895–898.

Roati, G., M. Zaccanti, C. D'Errico, J. Catani, M. Modugno, A. Simoni, M. Inguscio, and G. Modugno, 2007, "$^{39}$K Bose-Einstein condensate with tunable interactions," Phys. Rev. Lett. **99**, 010403.

Roberts, J. L., N. R. Clausen, J. P. Burke, Jr., C. H. Greene, E. A. Cornell, and C. E. Wieman, 1998, "Resonant magnetic field control of elastic scattering in cold $^{85}$Rb," Phys. Rev. Lett. **81**, 5109–5112.

Roberts, J. L., N. R. Claussen, S. L. Cornish, E. A. Donley, E. A. Cornell, and C. E. Wieman, 2001, "Controlled collapse of a Bose-Einstein condensate," Phys. Rev. Lett. **86**, 4211–4214.

Roberts, J. L., N. R. Claussen, S. L. Cornish, and C. E. Wieman, 2000, "Magnetic field dependence of ultracold inelastic collisions near a Feshbach resonance," Phys. Rev. Lett. **85**, 728–731.

Rychtarik, D., B. Engeser, H.-C. Nägerl, and R. Grimm, 2004, "Two-dimensional Bose-Einstein condensate in an optical surface trap," Phys. Rev. Lett. **92**, 173003.

Sadeghpour, H., J. Bohn, M. Cavagnero, B. Esry, I. Fabrikant, J. Macek, and A. Rau, 2000, "Collisions near threshold in atomic and molecular physics," J. Phys. B **33**, R93–R140.

Samuelis, C., E. Tiesinga, T. Laue, M. Elbs, H. Knöckel, and E. Tiemann, 2000, "Cold atomic collisions studied by molecular spectroscopy," Phys. Rev. A **63**, 012710.

Santos, L., and T. Pfau, 2006, "Spin-3 chromium Bose-Einstein condensates," Phys. Rev. Lett. **96**, 190404.

Santos, L., G. V. Shlyapnikov, and M. Lewenstein, 2003, "Roton-maxon spectrum and stability of trapped dipolar Bose-Einstein condensates," Phys. Rev. Lett. **90**, 250403.

Schöllkopf, W., and J. Toennies, 1994, "Nondestructive mass selection of small van der Waals clusters," Science **266**, 1345–1348.

Schreck, F., L. Khaykovich, K. L. Corwin, G. Ferrari, T. Bourdel, J. Cubizolles, and C. Salomon, 2001, "Quasipure Bose-Einstein condensate immersed in a Fermi sea," Phys. Rev. Lett. **87**, 080403.

Schunck, C. H., Yong-il Shin, A. Schirotzek, and W. Ketterle, 2008, "Determination of the fermion pair size in a resonantly interacting superfluid," Nature (London) **454**, 739–744.

Schunck, C. H., M. W. Zwierlein, C. A. Stan, S. M. F. Raupach, W. Ketterle, A. Simoni, E. Tiesinga, C. J. Williams, and P. S. Julienne, 2005, "Feshbach resonances in fermionic $^{6}$Li," Phys. Rev. A **71**, 045601.

Seto, J. Y., R. J. LeRoy, J. Vergés, and C. Amiot, 2000, "Direct potential fit analysis of the $X\,^1\Sigma_g^+$ state of $Rb_2$: Nothing else will do!," J. Chem. Phys. **113**, 3067–3076.

Shin, Y., C. H. Schunck, A. Schirotzek, and W. Ketterle, 2008, "Phase diagram of a two-component Fermi gas with resonant interactions," Nature (London) **451**, 689–693.

Simoni, A., F. Ferlaino, G. Roati, G. Modugno, and M. Inguscio, 2003, "Magnetic control of the interaction in ultracold K-Rb mixtures," Phys. Rev. Lett. **90**, 163202.

Simoni, A., M. Zaccanti, C. D'Errico, M. Fattori, G. Roati, M. Inguscio, and G. Modugno, 2008, "Near-threshold model for ultracold KRb dimers from interisotope Feshbach spectroscopy," Phys. Rev. A **77**, 052705.

Simonucci, S., P. Pieri, and G. C. Strinati, 2005, "Broad vs. narrow Fano-Feshbach resonances in the BCS-BEC crossover with trapped Fermi atoms," Europhys. Lett. **69**, 713–718.

Smirne, G., R. M. Godun, D. Cassettari, V. Boyer, C. J. Foot, T. Volz, N. Syassen, S. Dürr, G. Rempe, M. D. Lee, K. Góral, and T. Köhler, 2007, "Collisional relaxation of Feshbach molecules and three-body recombination in $^{87}$Rb Bose-Einstein condensates," Phys. Rev. A **75**, 020702.

Spence, D., and T. Noguchi, 1975, "Feshbach resonances associated with Rydberg states of the hydrogen halides," J. Chem. Phys. **63**, 505–514.

Staanum, P., S. D. Kraft, J. Lange, R. Wester, and M. Weidemüller, 2006, "Experimental investigation of ultracold atom-molecule collisions," Phys. Rev. Lett. **96**, 023201.

Stan, C. A., M. W. Zwierlein, C. H. Schunck, S. M. F. Raupach, and W. Ketterle, 2004, "Observation of Feshbach resonances between two different atomic species," Phys. Rev. Lett. **93**, 143001.

Stenger, J., S. Inouye, M. R. Andrews, H.-J. Miesner, D. M. Stamper-Kurn, and W. Ketterle, 1999, "Strongly enhanced inelastic collisions in a Bose-Einstein condensate near Feshbach resonances," Phys. Rev. Lett. **82**, 2422–2425.

Stöferle, T., H. Moritz, K. Günter, M. Köhl, and T. Esslinger, 2006, "Molecules of fermionic atoms in an optical lattice," Phys. Rev. Lett. **96**, 030401.

Stoll, M., and T. Köhler, 2005, "Production of three-body Efimov molecules in an optical lattice," Phys. Rev. A **72**, 022714.

Stoof, H. T. C., A. M. L. Jansen, J. M. V. A. Koelman, and B. J. Verhaar, 1989, "Decay of spin-polarized atomic hydrogen in the presence of a Bose condensate," Phys. Rev. A **39**, 3157–3169.

Stoof, H. T. C., J. M. V. A. Koelman, and B. J. Verhaar, 1988, "Spin-exchange and dipole relaxation rates in atomic hydrogen: Rigorous and simplified calculations," Phys. Rev. B **38**, 4688–4697.

Strecker, K. E., G. B. Partridge, and R. G. Hulet, 2003, "Conversion of an atomic Fermi gas to a long-lived molecular Bose gas," Phys. Rev. Lett. **91**, 080406.

Strecker, K. E., G. B. Partridge, A. G. Truscott, and R. G. Hulet, 2002, "Formation and propagation of matter-wave soliton trains," Nature (London) **417**, 150–153.

Stringari, S., and L. Pitaevskii, 2003, *Bose-Einstein Condensation* (Oxford University, London).

Stuhler, J., A. Griesmaier, T. Koch, M. Fattori, T. Pfau, S. Giovanazzi, P. Pedri, and L. Santos, 2005, "Observation of dipole-dipole interaction in a degenerate quantum gas," Phys. Rev. Lett. **95**, 150406.

Stwalley, W. C., 1976, "Stability of spin-aligned hydrogen at low temperatures and high magnetic fields: New field-dependent scattering resonances and predissociations," Phys. Rev. Lett. **37**, 1628–1631.

Suno, H., B. D. Esry, and C. H. Greene, 2003, "Recombination of three ultracold fermionic atoms," Phys. Rev. Lett. **90**, 053202.

Syassen, N., D. M. Bauer, M. Lettner, D. Dietze, T. Volz, S. Dürr, and G. Rempe, 2007, "Atom-molecule Rabi oscillations in a Mott insulator," Phys. Rev. Lett. **99**, 033201.

Syassen, N., T. Volz, S. Teichmann, S. Dürr, and G. Rempe, 2006, "Collisional decay of $^{87}$Rb Feshbach molecules at 1005.8 G," Phys. Rev. A **74**, 062706.

Szymanska, M. H., K. Góral, T. Köhler, and K. Burnett, 2005, "Conventional character of the BCS-BEC crossover in ultracold gases of $^{40}$K," Phys. Rev. A **72**, 013610.

Taglieber, M., A.-C. Voigt, T. Aoki, T. W. Hänsch, and K. Dieckmann, 2008, "Quantum degenerate two-species Fermi-Fermi mixture coexisting with a Bose-Einstein condensate," Phys. Rev. Lett. **100**, 010401.

Tang, K. T., J. M. Norbeck, and P. R. Certain, 1976, "Upper and lower bounds of two- and three-body dipole, quadrupole, and octupole van der Waals coefficients for hydrogen, noble gas, and alkali atom interactions," J. Chem. Phys. **64**, 3063–3074.

Taylor, J. R., 1972, *Scattering Theory* (Wiley, New York).

Thalhammer, G., G. Barontini, L. D. Sarlo, J. Catani, F. Minardi, and M. Inguscio, 2008, "Double species Bose-Einstein condensate with tunable interspecies interactions," Phys. Rev. Lett. **100**, 210402.

Thalhammer, G., M. Theis, K. Winkler, R. Grimm, and J. Hecker Denschlag, 2005, "Inducing an optical Feshbach resonance via stimulated Raman coupling," Phys. Rev. A **71**, 033403.

Thalhammer, G., K. Winkler, F. Lang, S. Schmid, R. Grimm, and J. Hecker Denschlag, 2006, "Long-lived Feshbach molecules in a 3D optical lattice," Phys. Rev. Lett. **96**, 050402.

Theis, M., G. Thalhammer, K. Winkler, M. Hellwig, G. Ruff, R. Grimm, and J. Hecker Denschlag, 2004, "Tuning the scattering length with an optically induced Feshbach resonance," Phys. Rev. Lett. **93**, 123001.

Thomas, N. R., N. Kjærgaard, P. S. Julienne, and A. C. Wilson, 2004, "Imaging of *s* and *d* partial-wave interference in quantum scattering of identical bosonic atoms," Phys. Rev. Lett. **93**, 173201.

Thompson, S. T., E. Hodby, and C. E. Wieman, 2005a, "Spontaneous dissociation of $^{85}$Rb Feshbach molecules," Phys. Rev. Lett. **94**, 020401.

Thompson, S. T., E. Hodby, and C. E. Wieman, 2005b, "Ultracold molecule production via a resonant oscillating magnetic field," Phys. Rev. Lett. **95**, 190404.

Ticknor, C., C. A. Regal, D. S. Jin, and J. L. Bohn, 2004, "Multiplet structure of Feshbach resonances in non-zero partial waves," Phys. Rev. A **69**, 042712.

Tiesinga, E., B. J. Verhaar, and H. T. C. Stoof, 1993, "Threshold and resonance phenomena in ultracold ground-state collisions," Phys. Rev. A **47**, 4114–4122.

Tiesinga, E., C. J. Williams, F. H. Mies, and P. S. Julienne, 2000, "Interacting atoms under strong quantum confinement," Phys. Rev. A **61**, 063416.

Timmermans, E., P. Tommasini, M. Hussein, and A. Kerman, 1999, "Feshbach resonances in atomic Bose-Einstein condensates," Phys. Rep. **315**, 199–230.

Tojo, S., M. Kitagawa, K. Enomoto, Y. Kato, Y. Takasu, M. Kumakura, and Y. Takahashi, 2006, "High-resolution photoassociation spectroscopy of ultracold ytterbium atoms by using the intercombination transition," Phys. Rev. Lett. **96**, 153201.

Truscott, A. G., K. E. Strecker, W. I. McAlexander, G. B. Partridge, and R. G. Hulet, 2001, "Observation of Fermi pressure in a gas of trapped atoms," Science **291**, 2570–2572.

Tsai, C. C., R. S. Freeland, J. M. Vogels, H. M. J. M. Boesten, B. J. Verhaar, and D. J. Heinzen, 1997, "Two-color photoassociation spectroscopy of ground State $Rb_2$," Phys. Rev. Lett. **79**, 1245–1248.

Tscherbul, T. V., and R. V. Krems, 2008, "Quantum theory of chemical reactions in the presence of electromagnetic fields," J. Chem. Phys. **129**, 034112.

van Abeelen, F. A., D. J. Heinzen, and B. J. Verhaar, 1998, "Photoassociation as a probe of Feshbach resonances in cold-atom scattering," Phys. Rev. A **57**, R4102–R4105.

van Abeelen, F. A., and B. J. Verhaar, 1999a, "Determination of collisional properties of cold Na atoms from analysis of bound-state photoassociation and Feshbach resonance field data," Phys. Rev. A **59**, 578–584.

van Abeelen, F. A., and B. J. Verhaar, 1999b, "Time-dependent Feshbach resonance scattering and anomalous decay of a Na Bose-Einstein condensate," Phys. Rev. Lett. **83**, 1550–1553.

van de Meerakker, S. Y. T., N. Vanhaecke, and G. Meijer, 2006, "Stark deceleration and trapping of OH radicals," Annu. Rev. Phys. Chem. **57**, 159–190.

van Kempen, E. G. M., S. J. J. M. F. Kokkelmans, D. J. Heinzen, and B. J. Verhaar, 2002, "Interisotope determination of ultracold rubidium interactions from three high-precision experiments," Phys. Rev. Lett. **88**, 093201.

van Kempen, E. G. M., B. Marcelis, and S. J. J. M. F. Kokkelmans, 2004, "Formation of fermionic molecules via interisotope Feshbach resonances," Phys. Rev. A **70**, 050701.

Vogels, J. M., R. S. Freeland, C. C. Tsai, B. J. Verhaar, and D. J. Heinzen, 2000, "Coupled singlet-triplet analysis of two-color cold-atom photoassociation spectra," Phys. Rev. A **61**, 043407.

Vogels, J. M., C. C. Tsai, R. S. Freeland, S. J. J. M. F. Kokkelmans, B. J. Verhaar, and D. J. Heinzen, 1997, "Prediction of Feshbach resonances in collisions of ultracold rubidium atoms," Phys. Rev. A **56**, R1067–R1070.

Vogels, J. M., B. J. Verhaar, and R. H. Blok, 1998, "Diabatic models for weakly bound states and cold collisions of ground-state alkali-metal atoms," Phys. Rev. A **57**, 4049–4052.

Voigt, A.-C., M. Taglieber, L. Costa, T. Aoki, W. Wieser, T. W. Hänsch, and K. Dieckmann, 2008, "Ultracold heteronuclear Fermi-Fermi molecules," Phys. Rev. Lett. **102**, 020405.

Volz, T., S. Dürr, S. Ernst, A. Marte, and G. Rempe, 2003, "Characterization of electic scattering near a Feshbach resonance in $^{87}$Rb," Phys. Rev. A **68**, 010702.

Volz, T., S. Dürr, N. Syassen, G. Rempe, E. van Kempen, and S. Kokkelmans, 2005, "Feshbach spectroscopy of a shape resonance," Phys. Rev. A **72**, 010704.

Volz, T., N. Syassen, D. Bauer, E. Hansis, S. Dürr, and G. Rempe, 2006, "Preparation of a quantum state with one molecule at each site of an optical lattice," Nat. Phys. **2**, 692–695.

von Stecher, J., J. P. D'Incao, and C. H. Greene, 2009, "Signatures of universal four-body phenomena and their relation to the Efimov effect," Nat. Phys. **5**, 417–421.

Vuletić, V., A. J. Kerman, C. Chin, and S. Chu, 1999, "Observation of low-field Feshbach resonances in collsions of cesium atoms," Phys. Rev. Lett. **82**, 1406.

Wang, Y., and B. D. Esry, 2009, "Efimov trimer formation via ultracold four-body recombination," Phys. Rev. Lett. **102**, 133201.

Weber, C., G. Barontini, J. Catani, G. Thalhammer, M. Inguscio, and F. Minardi, 2008, "Association of ultracold double-species bosonic molecules," Phys. Rev. A **78**, 061601(R).

Weber, J. M., E. Leber, M.-W. Ruf, and H. Hotop, 1999, "Nuclear-excited Feshbach resonances in electron attachment to molecular clusters," Phys. Rev. Lett. **82**, 516–519.

Weber, T., J. Herbig, M. Mark, H.-C. Nägerl, and R. Grimm, 2003a, "Bose-Einstein condensation of cesium," Science **299**, 232–235.

Weber, T., J. Herbig, M. Mark, H.-C. Nägerl, and R. Grimm, 2003b, "Three-body recombination at large scattering lengths in an ultracold atomic gas," Phys. Rev. Lett. **91**, 123201.

Weck, P. F., and N. Balakrishnan, 2005, "Quantum dynamics of the Li+HF→H+LiF reaction at ultralow temperatures," J. Chem. Phys. **122**, 154309.

Werner, J., A. Griesmaier, S. Hensler, J. Stuhler, T. Pfau, A. Simoni, and E. Tiesinga, 2005, "Observation of Feshbach resonances in an ultracold gas of $^{52}$Cr," Phys. Rev. Lett. **94**, 183201.

Widera, A., O. Mandel, M. Greiner, S. Kreim, T. W. Hänsch, and I. Bloch, 2004, "Entanglement interferometry for precision measurement of atomic scattering properties," Phys. Rev. Lett. **92**, 160406.

Wille, E., F. M. Spiegelhalder, G. Kerner, D. Naik, A. Trenkwalder, G. Hendl, F. Schreck, R. Grimm, T. G. Tiecke, J. T. M. Walraven, S. J. J. M. F. Kokkelmans, E. Tiesinga, and P. S. Julienne, 2008, "Exploring an ultracold Fermi-Fermi mixture: Interspecies Feshbach resonances and scattering properties of $^6$Li and $^{40}$K," Phys. Rev. Lett. **100**, 053201.

Winkler, K., F. Lang, G. Thalhammer, P. van der Straten, R. Grimm, and J. Hecker Denschlag, 2007, "Coherent optical transfer of Feshbach molecules to a lower vibrational state," Phys. Rev. Lett. **98**, 043201.

Winkler, K., G. Thalhammer, F. Lang, R. Grimm, J. Hecker Denschlag, A. J. Daley, A. Kantian, H. P. Büchler, and P. Zoller, 2006, "Repulsively bound atom pairs in an optical lattice," Nature (London) **441**, 853–856.

Wynar, R., R. S. Freeland, D. J. Han, C. Ryu, and D. J. Heinzen, 2000, "Molecules in a Bose-Einstein condensate," Science **287**, 1016–1019.

Xu, K., T. Mukaiyama, J. Abo-Shaeer, J. Chin, D. Miller, and W. Ketterle, 2003, "Formation of quantum-degenerate sodium molecules," Phys. Rev. Lett. **91**, 210402.

Yan, Z.-C., J. F. Babb, A. Dalgarno, and G. W. F. Drake, 1996, "Variational calculations of dispersion coefficients for interactions among H, He, and Li atoms," Phys. Rev. A **54**, 2824–2833.

Yi, S., and L. You, 2002, "Probing dipolar effects with condensate shape oscillation," Phys. Rev. A **66**, 013607.

Yurovsky, V. A., M. Olshanii, and D. S. Weiss, 2008, "Collisions, correlations, and integrability in atom wave guides," Adv. At., Mol., Opt. Phys. **55**, 61–138.

Zaccanti, M., C. D'Errico, F. Ferlaino, G. Roati, M. Inguscio, and G. Modugno, 2006, "Control of the interaction in a Fermi-Bose mixture," Phys. Rev. A **41**, 041605(R).

Zaccanti, M., G. Modugno, C. D'Errico, M. Fattori, G. Roati, and M. Inguscio, 2008, Talk at DAMOP-2008, State College, PA, 2008 (unpublished).

Zahzam, N., T. Vogt, M. Mudrich, D. Comparat, and P. Pillet, 2006, "Atom-molecule collisions in an optically trapped gas," Phys. Rev. Lett. **96**, 023202.

Zelevinsky, T., M. M. Boyd, A. D. Ludlow, T. Ido, J. Ye, R. Ciurylo, P. Naidon, and P. S. Julienne, 2006, "Narrow line photoassociation in an optical lattice," Phys. Rev. Lett. **96**, 203201.

Zhang, J., E. G. M. van Kempen, T. Bourdel, L. Khaykovich, J. Cubizolles, F. Chevy, M. Teichmann, L. Tarruell, S. J. J. M. F. Kokkelmans, and C. Salomon, 2004, "*p*-wave Feshbach resonances of ultracold $^6$Li," Phys. Rev. A **70**, 030702(R).

Zhang, J., E. G. M. van Kempen, T. Bourdel, L. Khaykovich, J. Cubizolles, F. Chevy, M. Teichmann, L. Tarruell, S. J. J. M. F. Kokkelmans, and C. Salomon, 2005, in *Atomic Physics 19, Proceedings of the 19th International Conference on Atomic Physics*, edited by L. Marcassa, V. Bagnato, and K. Helmerson, AIP Conf. Proc. No. 770 (AIP, New York).

Zirbel, J. J., K.-K. Ni, S. Ospelkaus, J. P. D'Incao, C. E. Wieman, J. Ye, and D. S. Jin, 2008, "Collisional stability of fermionic Feshbach molecules," Phys. Rev. Lett. **100**, 143201.

Zirbel, J. J., K.-K. Ni, S. Ospelkaus, T. L. Nicholson, M. L. Olsen, C. E. Wieman, J. Ye, D. S. Jin, and P. S. Julienne, 2008, "Heteronuclear molecules in an optical dipole trap," Phys. Rev. A **78**, 013416.

Zwierlein, M. W., J. R. Abo-Shaeer, A. Schirotzek, C. H. Schunck, and W. Ketterle, 2005, "Vortices and superfluidity in a strongly interacting Fermi gas," Nature (London) **435**, 1047–1051.

Zwierlein, M. W., A. Schirotzek, C. H. Schunck, and W. Ketterle, 2006, "Fermionic superfluidity with imbalanced spin populations," Science **311**, 492–496.

Zwierlein, M. W., C. A. Stan, C. H. Schunck, S. M. F. Raupach, S. Gupta, Z. Hadzibabic, and W. Ketterle, 2003, "Observation of Bose-Einstein condensation of molecules," Phys. Rev. Lett. **91**, 250401.

Zwierlein, M. W., C. A. Stan, C. H. Schunck, S. M. F. Raupach, A. J. Kerman, and W. Ketterle, 2004, "Condensation of pairs of fermionic atoms near a Feshbach resonance," Phys. Rev. Lett. **92**, 120403.